FUNCTIONAL ANALYSIS OF NEUROGENESIS IN THE ZEBRAFISH HYPOTHALAMUS

by

Adam Donovan McPherson

A dissertation submitted to the faculty of
The University of Utah
in partial fulfillment of the requirements for the degree of

Doctor of Philosophy

in

Neuroscience

Interdepartmental Program in Neuroscience

The University of Utah

December 2015

The University of Utah Graduate School

STATEMENT OF DISSERTATION APPROVAL

The dissertation of **Adam Donovan McPherson**

has been approved by the following supervisory committee members:

Richard Dorsky	, Chair	**5/14/2015** Date Approved
Scott Rogers	, Member	**5/14/2015** Date Approved
Sabine Fuhrmann	, Member	**5/14/2015** Date Approved
Amnon Schlegel	, Member	**5/14/2015** Date Approved
William Crowley	, Member	**5/14/2015** Date Approved

and by **Richard Dorsky**, Chair/Dean of the Department/College/School of **Interdepartmental Program in Neuroscience**

and by David B. Kieda, Dean of The Graduate School.

ABSTRACT

The occurrence of postembryonic neurogenesis in the vertebrate brain is now a widely accepted belief. Observations of adult neurogenesis have been made in multiple regions of the brain across numerous species. However, why some regions continue to make neurons while others do not is not completely clear. The functional significance of continual neurogenesis is also not well understood and remains a highly investigated topic. Determining why the brain continues to make new neurons under normal physiologic and pathophysiologic conditions will allow us to better understand how it functions overall. Additionally, a greater understanding of postembryonic neurogenesis will provide valuable therapeutic benefits to human life in terms of treating brain injury and neurodegenerative disease.

One of the more recently identified regions to undergo continual neurogenesis is the hypothalamus—the homeostatic control center of the brain. It responds to both physiological and external environmental cues in order to regulate conditions in the body, such as body temperature, heart rate, sleep/wake cycles, and energy balance. Previous studies in Dr. Richard Dorsky's lab identified a population of neural precursors that express *dlx* transcription factors and continue to generate new neurons throughout adulthood in the hypothalamus of zebrafish. When I began my studies in this lab, I wanted to

understand the functional significance of continual neurogenesis of this cell population. In this dissertation, I present findings that further our understanding of the factors regulating postembryonic neurogenesis of these neural precursors and the functional role these cells play. I developed reagents that aided in determining that the *dlx*+ cells were regulated by Wnt signaling. I also developed reagents that lead to the identification and characterization of a neurogenic radial glia-like population of cells, called tanycytes, residing in the caudal hypothalamus, which our lab went on to show was a stem cell population capable of giving rise to many cell types postembryonically. Furthermore, I determined that the *dlx*+ neural precursors generated tyrosine hydroxylase 2 (*th2)*-positive dopaminergic neurons that modulate swimming behavior. Finally, I went on to show that these *th2*+ neurons are capable of functional recovery. This discovery has potential therapeutic significance in future studies of neurodegenerative disease, such as Parkinson's disease. Overall, my investigations have lead to significant advances in our understanding of postembryonic neurogenesis.

Dedicated in loving memory to my parents.

TABLE OF CONTENTS

ACKNOWLEDGEMENTS

I would like to thank the Neuroscience Program first for accepting me and second for everything they have done to support me throughout graduate school. The faculty, staff, and students that make up this program are remarkable and I will miss working and hanging out with all of you.

I also want to thank everyone in the Neurobiology and Anatomy Department. This has been a wonderful department of which to be a part. People have been so helpful throughout my career in giving and sharing reagents and knowledge. You have made my work better and I thank you all.

I would not have been successful without all the guidance that I received from my graduate mentor, Rich Dorsky. He has provided an incredible environment for graduate students to flourish. He pushed me to become a better scientist. Furthermore, in addition to sharing his vast scientific knowledge, he also gave great life advice. I thank him for all of it.

I have dedicated my work to my mom and dad. They sacrificed more than most to provide me an education and great life. I miss them every day.

Finally, I would like to thank all of friends and family for all of their amazing encouragement and support, not just during my time in grad school, but also throughout my entire educational career. If I named all of you here, it would be an environmental tragedy to print this thesis. So I will just say thanks to all of you for being in my life and enriching it thoroughly.

CHAPTER 1

INTRODUCTION

It was a long-held belief that the vertebrate brain was incapable of producing new neurons postembryonically. However, with advances in both labeling and imaging techniques, this argument has been put to rest and it is now well accepted that several regions of the vertebrate brain are capable of continually making neurons. The questions now become: what areas of the brain are capable of postembryonic neurogenesis and why?

Continual neurogenesis in the vertebrate brain: a brief overview

Neurogenesis is a highly intricate process in which multipotent stem cells transition to become mature neurons. During vertebrate embryogenesis, it is no surprise that neurogenesis is rapid and widespread as the brain develops. However, the rate of proliferation quickly decreases and is restricted to certain regions of the brain, which are capable of continual neurogenesis following development and throughout life (Chapouton et al., 2007; Gould, 2007). There has been a long vetting process for each new region claimed to be neurogenic, and since the first discovery of the adult brain's neurogenic potential in the 1960s, the field has been heavily contested. The first regions identified as capable of continual neurogenesis were the hippocampus, olfactory bulb, and neocortex (Gould, 2007). However, due to the poor reproducibility of these findings, they were generally ignored. This all began to change with advances in imaging techniques (such as confocal microscopy) and the development of more sophisticated labeling for dividing cells (such as PCNA, BrdU and related thymidine analogs, and transgenics to label immature and mature neurons). Now, it is well accepted that the dentate gyrus of the hippocampus and

subventricular zone (SVZ) and rostral migratory stream (RMS), which feeds new neurons to the olfactory bulb, are bona fide sites of continual neurogenesis. These areas are now the most extensively studied and well-documented regions of postembryonic neurogenesis in part because they have the highest levels of proliferation in the brain, which probably enabled their identification as neurogenic regions in the first place. Now, thanks to new advances that have taken place in the field, many other regions of the brain have been identified as neurogenic niches, such as the amygdala (Bernier et al., 2002), striatum (Dayer et al., 2005), substantia nigra (Zhao et al., 2003), piriform cortex (Yuan et al., 2014), neocortex (Gould, 1999), and as I will discuss in greater detail, the hypothalamus (Fowler et al., 2005; Fowler, 2002; Huang, 1998; Kokoeva, 2005; Lee et al., 2012; Pierce and Xu, 2010; Xu et al., 2005).

Currently, it remains unknown why the entire vertebrate brain is unable to produce new neurons throughout life and why some areas proliferate at higher levels than others. However, a question that has been emerging is whether production of new neurons is a necessary process for the proper function of a given structure.

Functional significance of continual neurogenesis

Many studies have been performed to determine why specific regions of the vertebrate brain are capable of generating new neurons following embryogenesis. Many studies in the hippocampus and olfactory bulb show that continual neurogenesis is responsive to many different types of cues, which I will discuss in the following sections.

Function in the hippocampus

Numerous studies on the mammalian hippocampus have revealed that new neurons are necessary for both learning and memory tasks (Cameron and Glover, 2015; Deng et al., 2010; Gould et al., 1999b; Welberg, 2014). In addition, it has been shown that the amount of neurogenesis can be regulated by factors such as stress (Gould and Tanapat, 1999; Mahar et al., 2014), exercise (Speisman et al., 2013a), the environment (Speisman et al., 2013b), aging (F.H., 2005), and learning (Dranovsky et al., 2011; Gould et al., 1999a). In summary, extensive work shows that the hippocampus alters the rate of neurogenesis in response to multiple cues and this appears necessary for proper functional output.

Function in the olfactory bulb

In the olfactory bulb, it is less clear why neurogenesis occurs at such a high rate in the adult, but there are many theories emerging. This is confounded by the fact that while the rate of neurogenesis is far greater than in the hippocampus, the olfactory bulb never gets larger in size (Biebl, 2000; Petreanu, 2002). It is possible that neuronal cell death and birth occur at a continual rate, and therefore, the new neurons are necessary for reorganization and/or maintaining a homeostatic level of neurons (Imayoshi et al., 2008). In addition, evidence indicates that new neurons will not completely integrate into the circuit, but rather die off, unless provided the appropriate sensory input (Baker, 2001; Petreanu, 2002). This observation has led to the proposal that neurogenesis in the olfactory bulb not only allows the maintenance of the tissue but also is used

for specific functions like novel odorant detection (Gheusi, 2000). Much like the hippocampus, neurogenesis in the olfactory bulb can be affected by environmental conditions like odor-associated learning and memory tasks (Alonso et al., 2006), and odor and pheromone detection (Mak et al., 2007; Rochefort, 2002) This suggests that homeostatic maintenance may not be the sole reason for continued neurogenesis.

Studies on the hippocampus and olfactory bulb show us that postembryonic neurogenesis is necessary for numerous processes and is highly regulated. These structures respond to many cues intrinsically and extrinsically, from morphogen and neurotransmitter signaling to changes in physiologic state or the external environment. More recently, the hypothalamus was identified as a region of the vertebrate brain that undergoes postembryonic neurogenesis. In hindsight, this should not be surprising as the hypothalamus is also a structure of the brain that is necessary for quickly responding to the internal and external environments and subsequently signaling to regulate homeostatic conditions in the body (see below). Our lab and others have shown that the hypothalamus of zebrafish exhibits high levels of proliferation throughout life (Lee et al., 2006; Wang et al., 2012). The questions I sought to answer were: what kinds of cells are being continually generated and what is the function of postembryonic neurogenesis that we see in the zebrafish hypothalamus? Also, given that the hippocampus and olfactory bulb exhibit similarities and differences in the regulation of neurogenesis, I wanted to know: what modes of regulation are necessary for continual proliferation in the hypothalamus?

What is the hypothalamus?

The hypothalamus is one of the most ancient regions of the vertebrate brain. In mammals, it occupies a very small region of the ventral diencephalon. In humans, for example, it makes up only about 0.3% of the total brain volume (Hofman, 1992). However, in the zebrafish, it appears to occupy a much larger percentage of the brain. Zebrafish do not possess a cortex or many of the subcortical structures seen in mammals, such as the hippocampus, basal ganglia, and amygdala. It is unclear but an intriguing question as to whether their larger hypothalamus is a result of increased function that has evolutionarily been promoted to highly specialized brain structures in "higher vertebrates."

Much of the function of the hypothalamus has been deduced in the mammalian brain. The hypothalamus is responsible for regulating all of the homeostatic conditions throughout the body by linking the nervous system with the endocrine system. To do so, it constantly responds to intrinsic and extrinsic cues and then signals with neurotransmitters and releasing hormones to the pituitary, which subsequently releases hormones into the blood stream that regulate or modulate physiological parameters, such as a change in heart rate, body temperature, circadian rhythms, or energy metabolism.

In order for the hypothalamus to be able to regulate so many complex processes, it is divided into several cellular and molecularly distinct nuclei, several of which I will discuss further below. Each nucleus is specialized and responsible for regulating just a subset of homeostatic conditions. For simplicity purposes, a nucleus' function is generally referred to in broad strokes; however, it

is important to note that there are connections between different nuclei, and projections to other areas of the brain besides the pituitary. Therefore, which process a given nucleus is involved in is not so clearly defined.

The hypothalamus is a novel neurogenic niche

Much like in the hippocampus and olfactory bulb, neurogenesis in the mammalian hypothalamus was dismissed for a long time. Furthermore, even after the hippocampus and olfactory bulb began to be accepted as true neurogenic niches, the hypothalamus remained viewed as incapable of postembryonic neurogenesis. It is apparent now that this was due to the lower levels of neurogenesis in the hypothalamus. Just as with the hippocampus and olfactory bulb, optimization and sophistication of labeling techniques revealed that the hypothalamus was in fact neurogenic (Gould, 2007; Yuan, 2011). This observation has now been made across multiple species (Chapouton et al., 2007), including primates and humans. Currently, continual neurogenesis in the mammalian hypothalamus appears to be restricted to the nuclei that line the 3rd ventricle and the paraventricular region (Cheng, 2013). However, it will be interesting to see whether more areas within the hypothalamus emerge as neurogenic as the field advances. My research on neurogenesis in the zebrafish aimed to determine what types of cells are being continually made in the caudal hypothalamus and for what purpose.

Function of hypothalamic neurogenesis

Fewer studies investigating the roles of hypothalamic neurogenesis exist compared to the large literature on the hippocampus and olfactory bulb that has accumulated over the last 50-plus years. Regardless, many studies have linked postembryonic neurogenesis in the hypothalamus to behavioral and physiological changes, and some of the very first showed that not only did neurogenesis occur in multiple species, but that environmental cues also had an effect on the number of newly born cells. For instance, it was found that the photoperiod affected the number of newly born neurons in the golden hamster (Huang, 1998). Studies in the prairie vole identified low levels of neurogenesis in the hypothalamus that was affected by social environment versus isolation (Fowler, 2002). Furthermore, a later study by this group found that both prairie and meadow voles varied rates of neurogenesis in response to estrogen manipulation (Fowler et al., 2005).

The ventricular zones where neurogenesis is found have long been considered as the main feeding regulatory centers within the hypothalamus – namely, the arcuate nucleus, ventromedial nucleus, and lateral nucleus. Hence, many of the pioneering researchers began with the hypothesis that continual neurogenesis was involved in feeding behavior and energy metabolism, which proved to be true (Sousa-Ferreira et al., 2014). One early study showed that injecting the neurotrophic factor CNTF into the 3rd ventricle of mice resulted in increased cell proliferation (Kokoeva, 2005). Additionally, this study reported that this increase led to reduced feeding and body weight. Conversely, blocking proliferation by injecting AraC into the 3rd ventricle resulted in increased feeding

and body weight. Another study showed that blocking proliferation specifically in the median eminence led to changes in metabolism (Lee et al., 2012). These studies linked hypothalamic cell proliferation, though not necessarily neurogenesis, with physiological changes in the body.

Agouti-related protein (AgRP) and proopiomelanocortin (POMC) neurons are two well-studied neuronal populations that influence feeding and energy balance. They reside in the arcuate nucleus, which straddles the 3rd ventricle and are known to have opposing roles to one another in feeding and metabolism. AgRP neurons are orexigenic (promote feeding), whereas POMC neurons are anorexigenic (promote satiety). When AgRP neurons are acutely ablated, it leads to a major reduction in feeding and body weight. Interestingly, one study showed that inducing progressive neurodegeneration of AgRP neurons in the arcuate nucleus led to an increase in proliferation of cells that took on an AgRP and POMC identity (Pierce and Xu, 2010). This provided evidence that the hypothalamus could selectively make new neurons. The authors further showed that newborn neurons could regain functionality, and that blocking proliferation prevented restoration of normal feeding and body weight. This observation indicates that one function of hypothalamic neurogenesis may be to respond to injury and degeneration. Shortly after these results, another study showed that transplanting immature wild-type hypothalamic neurons into *db/db* mice rescued their obesity phenotype (Czupryn et al., 2011). Moreover, a high fat diet can induce neurodegeneration in the hypothalamus through IKKβ/NF-κB activation which leads to obesity and pre-diabetes (Li et al., 2012). Conversely, inhibition of

IKKβ/NF-κB leads to increased neurogenesis in the hypothalamus. These studies demonstrate that the hypothalamus is capable of neurogenesis, permissive to functional integration of newborn neurons, and that neurogenesis is necessary for proper functioning of the feeding circuitry. What remains unclear is whether the continually proliferating cells in the zebrafish caudal hypothalamus, which appears analogous to the 3rd ventricle and paraventricular region, are also necessary for feeding and metabolism regulation or any other processes.

Neurogenesis in the zebrafish hypothalamus

We are currently using zebrafish as a model to study hypothalamic neurogenesis. The main advantage is that the zebrafish displays much higher levels of postembryonic neurogenesis compared to mammals, and therefore, they may provide new information as to what makes the mature brain permissive to continual neurogenesis. Also, despite differences in relative size and organization, their hypothalamus is quite similar molecularly and cellularly to mammals. Postembryonic neurogenesis also appears highly concentrated around the 3rd ventricle and paraventricular organ just as it has been observed in mammals (Chapouton et al., 2007; Marz et al., 2010). Zebrafish are born externally and are amenable to genetic manipulation by injecting DNA and RNA at the one-cell stage. They also develop rapidly allowing studies of postembryonic neurogenesis within 5 days of birth. Zebrafish are small and their brains remain optically clear enough for us to image the entire intact hypothalamus up to 4 weeks post-fertilization. These attributes make zebrafish a strong model for studying postembryonic hypothalamic neurogenesis.

Before discussing neurogenesis in the zebrafish hypothalamus, it is important to note that much research has first been performed to characterize adult neural stem cells in the zebrafish brain. This mainly grew out of a necessity to answer important questions arising from the differences in biology between zebrafish and mammals, namely that fish can grow for its entire life and that it possesses an amazing regenerative capacity. This includes the brain, which has been shown to undergo a proliferative response after injury (Kizil et al., 2012; Kroehne et al., 2011). These properties led to the important question whether postembryonic neurogenesis in zebrafish was really adult neurogenesis like that seen in mammals, or was merely attributed to growth and regeneration. Several groups have now shown that like mammals during postembryonic neurogenesis, the zebrafish recapitulates many mechanisms from embryogenesis during postembryonic neurogenesis (Chapouton et al., 2007; Kizil et al., 2012). However, processes unique from embryonic neurogenesis have also been reported (Marz et al., 2010). Another study showed that neural stem cells in the adult zebrafish brain transition from a fast to a slow proliferation mode (Chapouton et al., 2006; Rothenaigner et al., 2011). These data suggest a transition in states of neurogenesis in the postembryonic fish that sets it apart from embryogenesis and suggests an alternative function.

What can this tell us about continual neurogenesis in the zebrafish hypothalamus? In studies looking at the whole brain, it was observed that the adult hypothalamus in zebrafish maintains very high levels of neurogenesis (Adolf et al., 2006). While the majority of studies characterizing the different

mechanisms of embryonic versus adult neurogenesis have focused on the telencephalon, some have looked at multiple areas of the brain (Chapouton et al., 2011). The hypothalamus was found to exhibit the same transitions in neurogenesis states as the ones observed in the telencephalon. However, which cells undergo postembryonic neurogenesis and what function this serves was still unclear when I began my thesis. I have made several findings addressing these questions in Chapter 4.

dlx **genes mark a GABAergic and dopaminergic neural precursor population in the hypothalamus**

dlx genes are a family of transcription factors expressed in neural precursors throughout the mammalian brain and are necessary for producing GABAergic and tyrosine hydroxylase (TH)-positive neurons (Brill et al., 2008; Stühmer, 2002; Wang et al., 2010). These genes have also been identified in neural precursors undergoing adult neurogenesis. In the mouse olfactory bulb, the *dlx* genes are expressed in the neural precursors of the rostral migratory stream that differentiate into new GABAergic and TH-positive neurons (Brill et al., 2008). Also, the mouse hypothalamus was shown to express *dlx* genes during embryogenesis in a population of cells in the arcuate nucleus that also make GABAergic and TH-positive neurons (Yee et al., 2009). What remains unclear is whether this molecular program also exists postnatally. Previous studies by graduate students Ji Eun Lee and Xu Wang in our lab have investigated a similar population of cells in the paraventricular organ of zebrafish hypothalamus, a region with molecular similarities to the arcuate, ventromedial, and lateral nuclei

of the mammalian hypothalamus. First, Ji Eun showed that *dlx* genes are also expressed in the zebrafish hypothalamus (Lee et al., 2006). Xu's ensuing study (Wang et al., 2012) to which I contributed (Chapter 2) used *dlx5/6* transgenes to show that GABAergic neurons, but surprisingly not TH neurons, arise from this lineage. We further showed that a *dlx5/6* transgene was continually expressed in the hypothalamus throughout life, suggesting that neural precursors were present and neurogenesis was ongoing in this region. Considering that cells expressing *Dlx* give rise to TH neurons in the mouse but apparently not in fish, it was unclear whether these cells similar to those found in the mouse brain. One unique feature in all nonmammalian brains is that they possess two TH genes (*th1* and *th2*), and not one like in mammals (Ren et al., 2013; Yamamoto et al., 2010). A *th2* probe showed expression by RNA *in situ* hybridization in paraventricular organ. However, this technique never provided enough cellular resolution to determine whether there were distinct *th1* and *th2* populations and whether there was coexpression with our *dlx5/6* transgenes. Two important advances have been made since the time of Xu Wang's study. One group recently developed an antibody that recognizes both TH1 and TH2 proteins. Its use in combination with a TH1 antibody allowed the detection of two distinct populations in the zebrafish hypothalamus (Semenova, 2014). In addition, in Chapter 4, I present a study I performed in collaboration with Dr. Adam Douglass' lab, who recently cloned the first *th2* enhancer/promoter sequence. This provided us with, for the first time ever, genetic accessibility to these cells. We were able to show that the *dlx5/6* population developed into *th2* neurons. Thus, our studies revealed for the first

time that the *dlx5/6* cell population in the zebrafish hypothalamus gives rise to both GABAergic and tyrosine hydroxylase expressing cells, similar to the mouse hypothalamus. A previous study presented evidence that the *th2* cells in the zebrafish hypothalamus may not actually be dopaminergic, but rather serotonergic (Ren et al., 2013). This, however, was based on the fact that TH2 could make serotonin *in vitro*. My study answers this question once and for all, showing that *in vivo*, these cells are dopaminergic and not serotonergic.

Role of dopamine in the hypothalamus

Our genetic accessibility to *th2* neurons allowed us to investigate the function of these continually generated neurons. Dopamine signaling in the brain has been extensively studied for many years. Dopamine signaling is associated with numerous physiological and behavioral functions, including locomotion, learning, reward and motivation, mood, arousal, and cognition (Ikemoto et al., 2015; Salamone and Correa, 2012; Schultz, 2007; Wise, 2004). Furthermore, defects in dopaminergic signaling are also associated with diseases like Parkinson's, schizophrenia, and addiction. There are multiple structures in the vertebrate brain that contain dopamine-expressing neurons, which project from these centers toward numerous other brain regions (Beaulieu and Gainetdinov, 2011). Furthermore, it has been shown that not all dopaminergic cells are molecularly the same (Bjorklund and Dunnett, 2007). Therefore, there is much diversity among dopaminergic neurons in the brain. No doubt this speaks to the many functions in which they are involved. My investigation of the function of continual neurogenesis led me to ask: what function do *th2* neurons serve in the

zebrafish brain? One study suggested that dopaminergic neurons in the caudal hypothalamus are involved in modulating a cross modal startle response through the Mauthner neurons in zebrafish (Mu et al., 2012). However, this study did not have genetic access to the *th2* neurons and instead, they used targeted laser ablation of cells expressing VMAT, *th2* morpholino knockdown, and dopamine pharmacology to deduce that dopaminergic cells were involved in modulating the startle response. While all together this study provided an intriguing argument, the findings implicating *th2* neurons were still indirect. Indeed, dopamine agonists and antagonists applied to the Mauthner neurons implicate dopaminergic modulation of the startle response. However, VMAT labels several monoaminergic populations in the caudal hypothalamus and morpholino knockdown in zebrafish has been highly contested throughout the years due to knockdown efficacy, off target cell death, and a high incident of null mutant data not aligning with the morpholino data (Kok et al., 2015; Schulte-Merker and Stainier, 2014). Therefore, I took advantage of our new *th2* enhancer/promoter to genetically ablate and optogenetically activate these neurons and directly test their function *in vivo* (Chapter 4). Here I present data that *th2* cells derived from the *dlx5/6* lineage are involved in modulating locomotor activity in the zebrafish.

The caudal hypothalamus where the *dlx5/6* and *th2* cells reside in zebrafish is similar in identity to the mammalian feeding circuit; therefore, I originally hypothesized that the function of these cells may be to regulate feeding and/or energy metabolism. As mentioned earlier, neurogenesis affects these outputs and vice versa. Therefore, I investigated whether feeding versus fasting

was capable of affecting the rate of neurogenesis in the hypothalamus. I present preliminary results in the Appendix suggesting that fasting alters the cell proliferation cycle in the hypothalamus. This initial work may provide inroads for future studies in the lab.

References

Adolf, B., Chapouton, P., Lam, C.S., Topp, S., Tannhauser, B., Strahle, U., Gotz, M., and Bally-Cuif, L. (2006). Conserved and acquired features of adult neurogenesis in the zebrafish telencephalon. Developmental Biology *295*, 278-293.

Alonso, M., Viollet, C., Gabellec, M.M., Meas-Yedid, V., Olivo-Marin, J.C., and Lledo, P.M. (2006). Olfactory discrimination learning increases the survival of adult-born neurons in the olfactory bulb. The Journal of Neuroscience *26*, 10508-10513.

Baker, H.L., N.; Chun, H.S.; Saino, S.; Berlin, R.; Volpe, B.; Son, J.H. (2001). Phenotypic Differentiation during Migration of Dopaminergic Progenitor Cells to the Olfactory Bulb. Journal of Neuroscience *21*, 8505-8513.

Beaulieu, J.M., and Gainetdinov, R.R. (2011). The physiology, signaling, and pharmacology of dopamine receptors. Pharmacological Reviews *63*, 182-217.

Bernier, P.J., Bedard, A., Vinet, J., Levesque, M., and Parent, A. (2002). Newly generated neurons in the amygdala and adjoining cortex of adult primates. Proceedings of the National Academy of Sciences of the United States of America *99*, 11464-11469.

Biebl, M.C., C.M.; Winkler, J.; Kuhn, H.G. (2000). Analysis of neurogenesis and programmed cell death reveals a selfrenewing capacity in the adult rat brain. Neuroscience Letters *291*, 17-20.

Bjorklund, A., and Dunnett, S.B. (2007). Dopamine neuron systems in the brain: an update. Trends in Neurosciences *30*, 194-202.

Brill, M.S., Snapyan, M., Wohlfrom, H., Ninkovic, J., Jawerka, M., Mastick, G.S., Ashery-Padan, R., Saghatelyan, A., Berninger, B., and Gotz, M. (2008). A dlx2- and pax6-dependent transcriptional code for periglomerular neuron specification in the adult olfactory bulb. The Journal of Neuroscience *28*, 6439-6452.

Cameron, H.A., and Glover, L.R. (2015). Adult neurogenesis: beyond learning and memory. Annual Review of Psychology *66*, 53-81.

Chapouton, P., Adolf, B., Leucht, C., Tannhauser, B., Ryu, S., Driever, W., and Bally-Cuif, L. (2006). her5 expression reveals a pool of neural stem cells in the adult zebrafish midbrain. Development *133*, 4293-4303.

Chapouton, P., Jagasia, R., and Bally-Cuif, L. (2007). Adult neurogenesis in non-

mammalian vertebrates. BioEssays : News and Reviews in Molecular, Cellular and Developmental Biology *29*, 745-757.

Chapouton, P., Webb, K.J., Stigloher, C., Alunni, A., Adolf, B., Hesl, B., Topp, S., Kremmer, E., and Bally-Cuif, L. (2011). Expression of hairy/enhancer of split genes in neural progenitors and neurogenesis domains of the adult zebrafish brain. The Journal of Comparative Neurology *519*, 1748-1769.

Cheng, M.F. (2013). Hypothalamic neurogenesis in the adult brain. Frontiers in Neuroendocrinology *34*, 167-178.

Czupryn, A., Zhou, Y.D., Chen, X., McNay, D., Anderson, M.P., Flier, J.S., and Macklis, J.D. (2011). Transplanted hypothalamic neurons restore leptin signaling and ameliorate obesity in db/db mice. Science *334*, 1133-1137.

Dayer, A.G., Cleaver, K.M., Abouantoun, T., and Cameron, H.A. (2005). New GABAergic interneurons in the adult neocortex and striatum are generated from different precursors. The Journal of Cell Biology *168*, 415-427.

Deng, W., Aimone, J.B., and Gage, F.H. (2010). New neurons and new memories: how does adult hippocampal neurogenesis affect learning and memory? Nature Reviews Neuroscience *11*, 339-350.

Dranovsky, A., Picchini, A.M., Moadel, T., Sisti, A.C., Yamada, A., Kimura, S., Leonardo, E.D., and Hen, R. (2011). Experience dictates stem cell fate in the adult hippocampus. Neuron *70*, 908-923.

F.H., v.P.H.S.T.Z.C.G. (2005). Exercise enhances learning and hippocampal neurogenesis in aged mice. Journal of Neuroscience *25*, 8680–8685.

Fowler, C.D., Johnson, F., and Wang, Z. (2005). Estrogen regulation of cell proliferation and distribution of estrogen receptor-alpha in the brains of adult female prairie and meadow voles. The Journal of Comparative Neurology *489*, 166-179.

Fowler, C.D.L., Y.; Ouimet, C.; Wang, Z. (2002). The effects of social environment on adult neurogenesis in the female prairie vole. Journal of Neurobiology *51*, 115-128.

Gheusi, G.C., H.; McLean, H.; Chazal, G.; Vincent, J.D.; Lledo, P.M. (2000). Importance of newly generated neurons in the adult olfactory bulb for odor discrimination. Proceedings of the National Academy of Sciences of the United States of America *97*, 1823-1828.

Gould, E. (2007). How widespread is adult neurogenesis in mammals? Nature Reviews Neuroscience *8*, 481-488.

Gould, E., Beylin, A., Tanapat, P., Reeves, A., and Shors, T.J. (1999a). Learning enhances adult neurogenesis in the hippocampal formation. Nature Neuroscience *2*, 260-265.

Gould, E., and Tanapat, P. (1999). Stress and hippocampal neurogenesis. Biological Psychiatry *46*, 1472-1479.

Gould, E., Tanapat, P., Hastings, N.B., and Shors, T.J. (1999b). Neurogenesis in adulthood: a possible role in learning. Trends in Cognitive Sciences *3*, 186-192.

Gould, E.R., A.J.; Graziano, M.S.A; Gross, C.G. (1999). Neurogenesis in the neocortex of adult primates. Science *286*, 548-552.

Hofman, M.A.S., D.F. (1992). The human hypothalamus: comparative morphometry and photoperiodic influences. Prog Brain Research *93*, 133-149.

Huang, L.D., G.J.; Bittman, E.L. (1998). Photoperiod regulates neuronal bromodeoxyuridine labeling in the brain of a seasonally breeding mammal. Journal of Neurobiology *36*, 410-420.

Ikemoto, S., Yang, C., and Tan, A. (2015). Basal ganglia circuit loops, dopamine and motivation: A review and enquiry. Behavioural Brain Research *290*, 17-31.

Imayoshi, I., Sakamoto, M., Ohtsuka, T., Takao, K., Miyakawa, T., Yamaguchi, M., Mori, K., Ikeda, T., Itohara, S., and Kageyama, R. (2008). Roles of continuous neurogenesis in the structural and functional integrity of the adult forebrain. Nature Neuroscience *11*, 1153-1161.

Kizil, C., Kaslin, J., Kroehne, V., and Brand, M. (2012). Adult neurogenesis and brain regeneration in zebrafish. Developmental Neurobiology *72*, 429-461.

Kokoeva, M.V.Y., H.; Flier, J.S. (2005). Neurogenesis in the hypothalamus of adult mice-potential role in energy balance. Science *310*, 679-683.

Kroehne, V., Freudenreich, D., Hans, S., Kaslin, J., and Brand, M. (2011). Regeneration of the adult zebrafish brain from neurogenic radial glia-type progenitors. Development *138*, 4831-4841.

Lee, D.A., Bedont, J.L., Pak, T., Wang, H., Song, J., Miranda-Angulo, A., Takiar, V., Charubhumi, V., Balordi, F., Takebayashi, H*., et al.* (2012). Tanycytes of the hypothalamic median eminence form a diet-responsive neurogenic niche. Nature Neuroscience *15*, 700-702.

Lee, J.E., Wu, S.F., Goering, L.M., and Dorsky, R.I. (2006). Canonical Wnt signaling through Lef1 is required for hypothalamic neurogenesis. Development *133*, 4451-4461.

Li, J., Tang, Y., and Cai, D. (2012). IKKbeta/NF-kappaB disrupts adult hypothalamic neural stem cells to mediate a neurodegenerative mechanism of dietary obesity and pre-diabetes. Nature Cell Biology *14*, 999-1012.

Mahar, I., Bambico, F.R., Mechawar, N., and Nobrega, J.N. (2014). Stress, serotonin, and hippocampal neurogenesis in relation to depression and antidepressant effects. Neuroscience and Biobehavioral Reviews *38*, 173-192.

Mak, G.K., Enwere, E.K., Gregg, C., Pakarainen, T., Poutanen, M., Huhtaniemi, I., and Weiss, S. (2007). Male pheromone-stimulated neurogenesis in the adult female brain: possible role in mating behavior. Nature Neuroscience *10*, 1003-1011.

Marz, M., Chapouton, P., Diotel, N., Vaillant, C., Hesl, B., Takamiya, M., Lam, C.S., Kah, O., Bally-Cuif, L., and Strahle, U. (2010). Heterogeneity in progenitor cell subtypes in the ventricular zone of the zebrafish adult telencephalon. Glia *58*, 870-888.

Mu, Y., Li, X.Q., Zhang, B., and Du, J.L. (2012). Visual input modulates audiomotor function via hypothalamic dopaminergic neurons through a cooperative mechanism. Neuron *75*, 688-699.

Petreanu, L.A.-B., A. (2002). Maturation and death of adult-born olfactory bulb granule neurons-role of olfaction. Journal of Neuroscience *22*, 6106-6113.

Pierce, A.A., and Xu, A.W. (2010). De novo neurogenesis in adult hypothalamus as a compensatory mechanism to regulate energy balance. The Journal of Neuroscience *30*, 723-730.

Ren, G., Li, S., Zhong, H., and Lin, S. (2013). Zebrafish tyrosine hydroxylase 2 gene encodes tryptophan hydroxylase. The Journal of Biological Chemistry *288*, 22451-22459.

Rochefort, C.G., G.; Vincent, J.D.; Lledo, P.M. (2002). Enriched odor exposure increases the number of newborn neurons in the adult olfactory bulb and improves odor memory. Journal of Neuroscience *22*, 2679-2689.

Rothenaigner, I., Krecsmarik, M., Hayes, J.A., Bahn, B., Lepier, A., Fortin, G., Gotz, M., Jagasia, R., and Bally-Cuif, L. (2011). Clonal analysis by distinct viral vectors identifies bona fide neural stem cells in the adult zebrafish

telencephalon and characterizes their division properties and fate. Development *138*, 1459-1469.

Salamone, J.D., and Correa, M. (2012). The mysterious motivational functions of mesolimbic dopamine. Neuron *76*, 470-485.

Schultz, W. (2007). Multiple dopamine functions at different time courses. Annual Review of Neuroscience *30*, 259-288.

Semenova, S.A.C., Y.C.; Zhao, X.; Rauvala, H.; Panula, P. (2014). The tyrosine hydroxylase 2 (TH2) system in zebrafish brain and stress activation of hypothalamic cells. Histochemical Cell Biology *142*, 619-633.

Sousa-Ferreira, L., de Almeida, L.P., and Cavadas, C. (2014). Role of hypothalamic neurogenesis in feeding regulation. Trends in Endocrinology and Metabolism: TEM *25*, 80-88.

Speisman, R.B., Kumar, A., Rani, A., Foster, T.C., and Ormerod, B.K. (2013a). Daily exercise improves memory, stimulates hippocampal neurogenesis and modulates immune and neuroimmune cytokines in aging rats. Brain, Behavior, and Immunity *28*, 25-43.

Speisman, R.B., Kumar, A., Rani, A., Pastoriza, J.M., Severance, J.E., Foster, T.C., and Ormerod, B.K. (2013b). Environmental enrichment restores neurogenesis and rapid acquisition in aged rats. Neurobiology of Aging *34*, 263-274.

Stühmer, T.A., S.A.; Ekker, M.; Rubenstein, J.L. (2002). Ectopic expression of the Dlx genes induces glutamic acid decarboxylase and Dlx expression. Development *129*, 245-252

Wang, X., Kopinke, D., Lin, J., McPherson, A.D., Duncan, R.N., Otsuna, H., Moro, E., Hoshijima, K., Grunwald, D.J., Argenton, F.*, et al.* (2012). Wnt signaling regulates postembryonic hypothalamic progenitor differentiation. Developmental Cell *23*, 624-636.

Wang, Y., Dye, C.A., Sohal, V., Long, J.E., Estrada, R.C., Roztocil, T., Lufkin, T., Deisseroth, K., Baraban, S.C., and Rubenstein, J.L. (2010). Dlx5 and Dlx6 regulate the development of parvalbumin-expressing cortical interneurons. The Journal of Neuroscience *30*, 5334-5345.

Welberg, L. (2014). Learning and memory: Neurogenesis erases existing memories. Nature Reviews Neuroscience *15*, 428.

Wise, R.A. (2004). Dopamine, learning and motivation. Nature Reviews Neuroscience *5*, 483-494.

Xu, Y., Tamamaki, N., Noda, T., Kimura, K., Itokazu, Y., Matsumoto, N., Dezawa, M., and Ide, C. (2005). Neurogenesis in the ependymal layer of the adult rat 3rd ventricle. Experimental Neurology *192*, 251-264.

Yamamoto, K., Ruuskanen, J.O., Wullimann, M.F., and Vernier, P. (2010). Two tyrosine hydroxylase genes in vertebrates-new dopaminergic territories revealed in the zebrafish brain. Molecular and Cellular Neurosciences *43*, 394-402.

Yee, C.L., Wang, Y., Anderson, S., Ekker, M., and Rubenstein, J.L. (2009). Arcuate nucleus expression of NKX2.1 and DLX and lineages expressing these transcription factors in neuropeptide Y(+), proopiomelanocortin(+), and tyrosine hydroxylase(+) neurons in neonatal and adult mice. The Journal of Comparative Neurology *517*, 37-50.

Yuan, T.F., Liang, Y.X., and So, K.F. (2014). Occurrence of new neurons in the piriform cortex. Frontiers in Neuroanatomy *8*, 167.

Yuan, T.F.A.-C., O. (2011). Adult neurogenesis in the hypothalamus-evidence, functions and implications. CNS Neurological Disorder Drug Targets *10*, 433-439.

Zhao, M., Momma, S., Delfani, K., Carlen, M., Cassidy, R.M., Johansson, C.B., Brismar, H., Shupliakov, O., Frisen, J., and Janson, A.M. (2003). Evidence for neurogenesis in the adult mammalian substantia nigra. Proceedings of the National Academy of Sciences of the United States of America *100*, 7925-7930.

CHAPTER 2

WNT SIGNALING REGULATES POSTEMBRYONIC HYPOTHALAMIC PROGENITOR DIFFERENTIATION

Reprint of : Wang, X., Kopinke, D., Lin, J., McPherson, A.D., Duncan, R.N., Otsuna, H., Moro, E., Hoshijima, K., Grunwald, D.J., Argenton, F.*, et al.* (2012). Wnt signaling regulates postembryonic hypothalamic progenitor differentiation. Developmental Cell *23*, 624-636.

Introduction

I am including this chapter because I made significant contributions to the work. When I began my project, my fellow lab member Xu Wang was in the midst of investigating the role of Wnt signaling in hypothalamic progenitor differentiation. I was going to investigate the identity and function of these cells and began developing reagents to do so. In my initial work, I developed transgenic zebrafish lines that also proved valuable to Xu's study. First off, I made a DNA construct and transgenic line that drove mCherry expression in *dlx5/6+* cells that Xu was able to use in many of his coexpression analyses (Fig. 1, Fig. 4, Fig. S2, Fig. S3, and Table 1). I also characterized a Gal4 enhancer trap line from a screen conducted by Dr. Hideo Otsuna in Dr. Chi-Bin Chien's lab. I was searching for lines that expressed in the hypothalamus and came across a candidate *Et(Gal4VP16; myl7:gfp)*^{zc1066a}. By crossing this line to *Tg(UAS-E1b:nfsB-mCherry)*^{jh17} to drive expression of mCherry and NTR, I determined that this double transgenic line labels radial glia-like cells called tanycytes. I also determined that Wnt responsive cells were Gal4+ (data not shown). I then assisted Xu in showing that Wnt signaling inhibits this cell population by crossing the double transgenic, *Et(Gal4VP16; myl7:gfp)*^{zc1066a}; *Tg(UAS-E1b:nfsB-mCherry)*^{jh17} to either *hs:dkk* (inhibits Wnt signaling) or *hs:wnt8a* (increases Wnt signaling) (Fig. 3, Fig. 4, Fig. S2). All this helped further our understanding of the processes regulating hypothalamic neurogenesis.

Developmental Cell
Article

Wnt Signaling Regulates Postembryonic Hypothalamic Progenitor Differentiation

Xu Wang,[1] Daniel Kopinke,[2] Junji Lin,[1] Adam D. McPherson,[1] Robert N. Duncan,[1] Hideo Otsuna,[1] Enrico Moro,[3] Kazuyuki Hoshijima,[2] David J. Grunwald,[2] Francesco Argenton,[4] Chi-Bin Chien,[1] L. Charles Murtaugh,[2] and Richard I. Dorsky[1,*]
[1]Department of Neurobiology and Anatomy
[2]Department of Human Genetics
University of Utah, Salt Lake City, Utah 84112, USA
[3]Department of Biomedical Science
[4]Department of Biology
University of Padua, Padua 35351, Italy
*Correspondence: richard.dorsky@neuro.utah.edu
http://dx.doi.org/10.1016/j.devcel.2012.07.012

SUMMARY

Previous studies have raised the possibility that Wnt signaling may regulate both neural progenitor maintenance and neuronal differentiation within a single population. Here we investigate the role of Wnt/β-catenin activity in the zebrafish hypothalamus and find that the pathway is first required for the proliferation of unspecified hypothalamic progenitors in the embryo. At later stages, including adulthood, sequential activation and inhibition of Wnt activity is required for the differentiation of neural progenitors and negatively regulates radial glia differentiation. The presence of Wnt activity is conserved in hypothalamic progenitors of the adult mouse, where it plays a conserved role in inhibiting the differentiation of radial glia. This study establishes the vertebrate hypothalamus as a model for Wnt-regulated postembryonic neural progenitor differentiation and defines specific roles for Wnt signaling in neurogenesis.

INTRODUCTION

Although neurogenesis was originally defined as a phenomenon exclusive to developing brains, it has now been identified in the adult CNS of mammals (Ming and Song, 2011) and non-mammalian vertebrates (Kizil et al., 2012). The regulation of postembryonic neurogenesis is thus a critical modulator of CNS homeostasis and plasticity, and the molecular mechanisms underlying this process are of obvious intense interest. One of the best-characterized signaling pathways involved in developmental neurogenesis is the regulation of target gene transcription by Wnt/β-catenin signaling. For example, the hippocampus of null mutants for *Wnt3a* (Lee et al., 2000), *LRP6* (Zhou et al., 2004), and *Lef1* (Galceran et al., 2000), contains a smaller dentate gyrus, with reduced production of granule neurons and abnormalities in radial glial scaffolding due to proliferation and patterning defects. These results suggest that Wnt activity may be required for the proliferation and normal differentiation of embryonic neural progenitors at early stages.

Recently, several studies with conditional approaches have revealed new aspects of Wnt signaling in postembryonic neurogenesis. One prevailing model suggests that Wnt activity is required to keep neural progenitors undifferentiated (Machon et al., 2007; Mutch et al., 2010). However, other data indicate that ectopic Wnt activity can both inhibit and promote neuronal differentiation (Tang et al., 2010). Consistent with these conflicting outcomes, hippocampal progenitors persist as GFAP$^+$ radial stem-like cells when Wnt function is lost (Kuwabara et al., 2009), whereas activation of the pathway in the rostral migratory stream, by *Apc* deletion, results in developmental arrest of *Ascl1*$^+$ transit amplifying cells (Imura et al., 2010). Together, all these studies suggest an untested unifying model in which Wnt activity is required for an early step of the neurogenesis pathway, but must be inactivated for differentiation to proceed.

We have previously shown that Wnt signaling through Lef1 is required for neurogenesis in the embryonic zebrafish hypothalamus (Lee et al., 2006). Subsequently, we found that both Wnt signaling and neurogenesis continue in the zebrafish hypothalamus through adult stages (Wang et al., 2009). Compared with other forebrain regions, the hypothalamus is relatively unstudied as a model of postembryonic neurogenesis. Although the hypothalamus has been identified as a region with proliferation and neurogenesis in adult mammals (Kokoeva et al., 2007; Lee et al., 2012; Migaud et al., 2010; Pérez-Martín et al., 2010a), the regulation and function of this regional activity are poorly understood. Hypothalamic neurogenesis could be significant in the regulation of multiple autonomic and endocrine pathways, as already demonstrated with feeding behavior (Kokoeva et al., 2005). The presence and gene expression profiles of specific neuronal lineages, such as Dlx$^+$ GABAergic precursors, are similar to those of other brain regions (Yee et al., 2009). In addition, the hypothalamus contains persistent radial glial tanycytes that are essential for endocrine function and can also serve as a neural progenitor population (Lee et al., 2012; Rodríguez et al., 2005). However, the regulation of tanycyte differentiation has remained uncharacterized.

Here we identify Wnt-responsive cells in the embryonic and postembryonic zebrafish hypothalamus, and find evidence for

pathway activation first in unspecified progenitors, and again later in postmitotic neural progenitors. Consistent with the profile of pathway activity, we find that Wnt signaling is first required for proliferative expansion of unspecified progenitors in the embryo and later regulates the differentiation of GABAergic and serotonergic lineages. Significantly, our data indicate that Wnt signaling must be inactivated in order for neuronal differentiation to occur. In contrast, Wnt activity is not required for the differentiation of radial glia, and ectopic pathway activation disrupts the generation of these cells. Finally, we show that Wnt activity is present in ventricular and parenchymal cells of the adult mouse mediobasal hypothalamus that express neural progenitor markers. In this system, we find that the role of Wnt signaling in radial glial development is evolutionarily conserved. Together, these data lead to a general model for Wnt function in postembryonic hypothalamic progenitor differentiation.

RESULTS

Wnt Activity Is Present in Unspecified Hypothalamic Progenitors at Early Embryonic Stages

We previously showed that Wnt signaling and the transcriptional mediator Lef1 regulate embryonic hypothalamic neurogenesis (Lee et al., 2006). In subsequent work, we found that Wnt pathway activity is present in the hypothalamus throughout the life of the animal (Wang et al., 2009). To more completely characterize Wnt-responsive cells in the zebrafish hypothalamus, here we employed a combination of transcriptional reporter lines. We used both *TOP:GFP*, a Wnt reporter containing 4 TCF binding sites upstream of a destabilized *GFP* transgene (Dorsky et al., 2002) as well as *TCFSiam:GFP*, a Wnt reporter containing the *Xenopus siamois* promoter upstream of *eGFP* (Moro et al., 2012), to label Wnt-responsive cells and their progeny. At 32 hr postfertilization (hpf), we found that Wnt-responsive cells were present in the presumptive lateral and posterior recess regions (Figure 1A). At this embryonic stage, almost all *TCFSiam:GFP*$^+$ and *TOP:GFP*$^+$ cells were PCNA$^+$ (Figure 1B; Table 1). In contrast, few *TCFSiam:GFP*$^+$ and *TOP:GFP*$^+$ cells expressed Sox3 (Figure 1B; Table 1), a marker and direct activator of neural progenitor gene expression (Bergsland et al., 2011), and colocalization of both reporters with the neuronal marker HuC/D was very low (Figure 1B; Table 1). Together, these data show that the majority of Wnt-responsive cells and their progeny in the 32 hpf zebrafish hypothalamus are proliferating unspecified progenitors.

Wnt Signaling Is Active in Hypothalamic Neural Progenitors at Postembryonic Stages

At 4 days postfertilization (dpf), the third ventricle and its associated posterior recess serve as reliable hypothalamic landmarks. At this stage expression of *TCFSiam:GFP* and *TOP:GFP* suggested that most Wnt-responsive cells are located in the posterior recess (red oval in Figure 1C). At this stage, we found that Wnt-responsive cells were primarily PCNA$^+$/Sox3$^+$ neural progenitors, although a few were PCNA$^+$/Sox3$^+$, indicating a transition through cell cycle exit (Figure 1D; Table 1). BrdU labeling also showed that the majority of 4 dpf Wnt-responsive cells were not proliferating (Figure S1 available online).

At 4 dpf, we used GFP perdurance in the two reporter lines to determine which lineages derive from the Wnt-responsive cells. To confirm the difference in reporter responsiveness, we expressed the *hs:dkk1* transgene (Stoick-Cooper et al., 2007) to conditionally inhibit canonical Wnt signaling in both reporter lines and monitored the decrease in GFP expression following heat shock. We found that it took 24 hr to achieve an 80% reduction in *TCFSiam:GFP*$^+$ cells, compared to only 8 hr for *TOP:GFP* (Figure S1). Both Wnt reporters were coexpressed with the pan-neuronal marker HuC/D, the GABAergic lineage markers *dlx5/6:mCherry* and GABA, and serotonin. However, coexpression was much higher in cells expressing the stable reporter *TCFSiam:GFP* (Figures 1D and 1E; Table 1), and relatively low in cells expressing the destabilized reporter *TOP:GFP* (Figure S2; Table 1). Because we did not observe any overlap between markers for the GABAergic and serotonergic lineages (Figure S2; Table 1), these experiments suggest that Wnt-responsive cells generate at least two different neuronal lineages. Furthermore, the different compositions of the destabilized and stable GFP reporter populations suggest that Wnt activity is rapidly silenced as neuronal differentiation proceeds.

In the adult hypothalamus, analysis of *TCFSiam:GFP* and *TOP:GFP* expression confirmed a similar distribution of Wnt-responsive cells in the posterior recess region. We previously reported that *TOP:GFP*$^+$ cells in the adult hypothalamic lateral recess did not express the proliferation marker PCNA, the postmitotic neuronal marker HuC/D, or GFAP (Wang et al., 2009). To determine the identity of GFP$^+$ cells in the posterior recess, we performed whole-mount sagittal analysis of this region using 150 μm confocal projections taken from the midline. We found that Sox3 continues to be expressed in the majority of Wnt-responsive cells in the posterior recess (Figure 1G; Table 1). The expression of neuronal markers still distinguished the destabilized and stable reporters, as many *TCFSiam:GFP*$^+$ cells, but very few *TOP:GFP*$^+$ cells, coexpressed HuC/D (Figures 1G and S2; Table 1). In addition, we found that adult hypothalamic Wnt-responsive cells continue to contribute to the GABAergic and serotonergic lineages identified in 4 dpf hypothalamus (Figure 1G; Table 1).

Together, these analyses show that in the posterior recess region of the 4 dpf and adult zebrafish hypothalamus, Wnt activity is present in Sox3$^+$ GABAergic and serotonergic progenitors as they become postmitotic, but is then lost as they undergo further differentiation.

lef1 Is Required for Postembryonic Hypothalamic Neurogenesis

By analyzing the expression of multiple pathway components, we found that along with the Wnt8b ligand, the two transcriptional mediators Lef1 and Tcf7 were the best candidates to mediate Wnt signaling in the posterior hypothalamus. In particular, expression of Lef1 protein and of a *tcf7:GFP* reporter (Nagayoshi et al., 2008) mirrored that of *TCFSiam:GFP* (Figure S3; Table 1). Although Lef1 and *tcf7:GFP* were coexpressed in some cells (Figure S3), nonoverlapping expression in other cells suggested nonredundant roles in the hypothalamus.

Identified mutations in individual zebrafish *Tcf* genes produce relatively minor defects (Muncan et al., 2007; Nagayoshi et al., 2008), allowing us to investigate the role of Wnt activity in

Developmental Cell
Wnt Regulation of Hypothalamic Progenitors

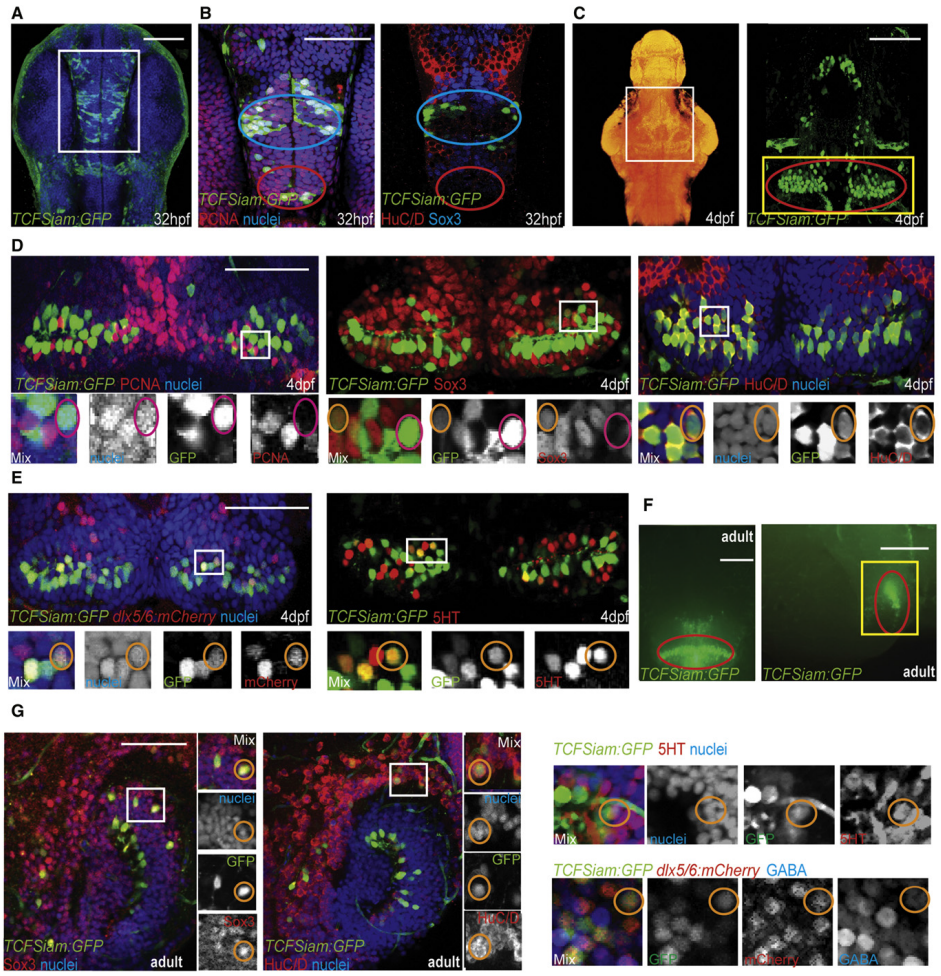

Figure 1. Identification of Wnt-Responsive Cells in the Zebrafish Hypothalamus

(A) Ventral view of *TCFSiam:GFP*.

(B) Costaining with PCNA, Sox3, and Hu. Blue ovals label the presumptive lateral recess, and red ovals label the presumptive posterior recess. White box in (A) marks the area shown.

(C) Maximum intensity confocal Z-projection of *TCFSiam:GFP* at 4 dpf. In nuclear stained ventral view of brain on left, white box marks hypothalamic area shown on right. Red oval marks the posterior recess.

(D) Costaining of *TCFSiam:GFP* with PCNA, Sox3, and HuC/D. Yellow box in (C) marks the area shown.

(E) Costaining of *TCFSiam:GFP* with *dlx5/6:gfp* and serotonin. Yellow box in (C) marks the area shown.

(F) Dissecting microscope ventral and sagittal views of *TCFSiam:GFP* in the adult hypothalamus. Red oval labels the presumptive posterior recess.

(G) Costaining of *TCFSiam:GFP* with Sox3, Hu, 5HT, *dlx5/6:mCherry*, and GABA in the adult posterior hypothalamus. Yellow box in (F) marks the area shown. Single optical sections from ventral views are shown in all panels, unless otherwise indicated. Small orange circles label cells with colocalization, and small magenta circles label cells without colocalization. Scale bars represent 80 μm (A–E,G), and 250 μm (F).

See also Figure S1.

Table 1. Coexpression Percentage of Cell Type Markers with Reporters

	PCNA	Sox3	HuC/D	*dlx5/6:mCherry*	GABA	5HT
32 hpf						
TOP:GFP	97.3 ± 1.5	13.1 ± 3.5	1.3 ± 0.5	–	–	–
TCFsiam:GFP	96.2 ± 1.2	7.2 ± 2.3	2.1 ± 0.8	–	–	–
4 dpf						
TOP:GFP	5.2 ± 1.3	89.2 ± 7.1	5.2 ± 2.1	7.1 ± 3.2	1.7 ± 1.1	2.9 ± 0.5
TCFsiam:GFP	9.3 ± 1.7	40.3 ± 9.9	78.2 ± 9.3	48.1 ± 9.9	31.2 ± 5.0	17.2 ± 4.3
tcf7:GFP	4.3 ± 2.3	68.1 ± 11.7	81.2 ± 6.8	26.1 ± 7.2	16.1 ± 4.1	30.1 ± 3.2
dlx5/6:GFP	9.2 ± 1.2	39.2 ± 7.1	61.3 ± 5.4	–	73.1 ± 6.1	0
Adult						
TOP:GFP	<1	98.1 ± 1.1	3.1 ± 2.4	<1	<1	1.1 ± 0.7
TCFsiam:GFP	<1	47.3 ± 3.4	66.3 ± 5.3	37.0 ± 4.9	7.1 ± 1.8	5.2 ± 1.5
tcf7:GFP	<1	59.1 ± 4.2	73.1 ± 4.1	–	9.1 ± 1.6	7.3 ± 2.5

Cells were counted from maximum intensity confocal Z projections of at least three individual brains for each set of markers. The entire hypothalamus (32 hpf) or posterior recess of whole (4 dpf) and half (adult) brains, defined by anatomical landmarks, was counted. Error = ±SD. dpf, days postfertilization; hpf, hours postfertilization. See also Figure S2.

neurogenesis in the context of grossly normal morphology. We chose to focus on *lef1* for several reasons. First, zebrafish *tcf7* null mutants are viable and fertile, suggesting a minor required function in development (Nagayoshi et al., 2008). Second, mouse *Lef1* mutants exhibit a smaller dentate gyrus with neurogenesis defects in the hippocampus (Galceran et al., 2000; Zhou et al., 2004), but hypothalamic phenotypes have not been explored. Finally, in zebrafish *lef1* morpholino knockdown produces neurogenesis defects in the hypothalamic GABAergic lineage (Lee et al., 2006).

To explore the later functions of *lef1* in the hypothalamus, we generated a *lef1* mutant using zinc finger nuclease-mediated gene targeting (Meng et al., 2008). Genomic (Figure 2A) and immunohistochemical (not shown) analyses indicated that this allele is a functional null, and we observed similar phenotypes to two other *lef1* null alleles generated by ENU mutagenesis (McGraw et al., 2011; Valdivia et al., 2011). At 15 dpf, *lef1* mutants can be identified by their smaller fins. Although mutant fish exhibit similar body mass and brain size as their wild-type siblings (Figures 2B and 2C), we observed a significant decrease in the size of the posterior hypothalamus. Using confocal volume reconstruction, we found the mutant posterior hypothalamus is 50% of wild-type size (Figures 2C and 2E), suggesting a specific proliferation defect in this tissue.

At 1 month postfertilization (mpf), the *lef1* mutant posterior hypothalamus is only 40% of wild-type size (Figure 2E), and 1 week BrdU tracing showed few proliferating cells in this region, with most of the remaining BrdU$^+$ cells located near the midline (Figure 2D). In addition, the HuC/D$^+$ neuronal population in the paraventricular posterior recess region is almost completely absent in *lef1* mutants (Figure 2D). Although the Sox3$^+$ neural progenitor pool is also smaller, BrdU labeling suggested that the remaining proliferating cells are arrested in the Sox3$^+$ state and unable to progress into HuC/D$^+$ neurons of either the GABAergic or serotonergic lineages (Figures 2D and 2F).

Although our previous data suggested a more significant role for *lef1* in early hypothalamic development, morpholino-based studies can be subject to off-target effects or targeting of maternally deposited pre-mRNA. Our analysis of zygotic mutants suggests that at postembryonic stages through adulthood, cells in the *lef1* mutant hypothalamus fail to proliferate or differentiate normally and are arrested as Sox3$^+$ neural progenitors.

Wnt Signaling Is Required for Hypothalamic Neurogenesis throughout Life

The phenotype of *lef1* mutants suggested a continuous requirement for Wnt signaling in hypothalamic neurogenesis, but the lack of conditional mutagenesis approaches in zebrafish precluded us from fully testing this hypothesis. We therefore used transgenic lines to perform conditional gain- and loss-of-function assays at early embryonic (24–32 hpf), later embryonic (3–4 dpf), and adult (6 mpf) stages. We used three different heat-shock lines to manipulate Wnt/β-catenin signaling: *hs:wnt8a* to activate the pathway (Weidinger et al., 2005), and *hs:dkk1* (Stoick-Cooper et al., 2007) and *hs:axin1* to inhibit the pathway. Neither heat shock alone nor transgene expression caused significant apoptosis, except for a small elevation following *hs:axin1* expression from 3–4 dpf (Figure S4). In addition, activation and inhibition of Wnt signaling caused the predicted effects on the target gene *axin2*, as assayed by in situ hybridization and RT-PCR (Figure S4).

Because our data suggested a role for Wnt signaling in unspecified proliferating progenitors at 32 hpf, we first analyzed the effects on proliferation following heat shock. A 2 hr BrdU pulse was performed at 22 hpf, followed by heat shock at 24 hpf, and fixation at 32 hpf. We found that the number of pH3$^+$ cells in the hypothalamic region was significantly increased following Wnt activation and decreased following Wnt inhibition (Figures 3A and S4), suggesting that Wnt signaling regulates overall proliferation levels. Following Wnt activation the hypothalamus was also noticeably larger with a folded ventricle and pH3$^+$ cells outside the midline (Figure S4). We found similar effects on the number of BrdU$^+$/Sox3$^+$ neural progenitors (Figure 3A), suggesting canonical Wnt signaling is also necessary and sufficient for the expansion of this population. In contrast, we did not observe any precocious expression of neuronal

Developmental Cell
Wnt Regulation of Hypothalamic Progenitors

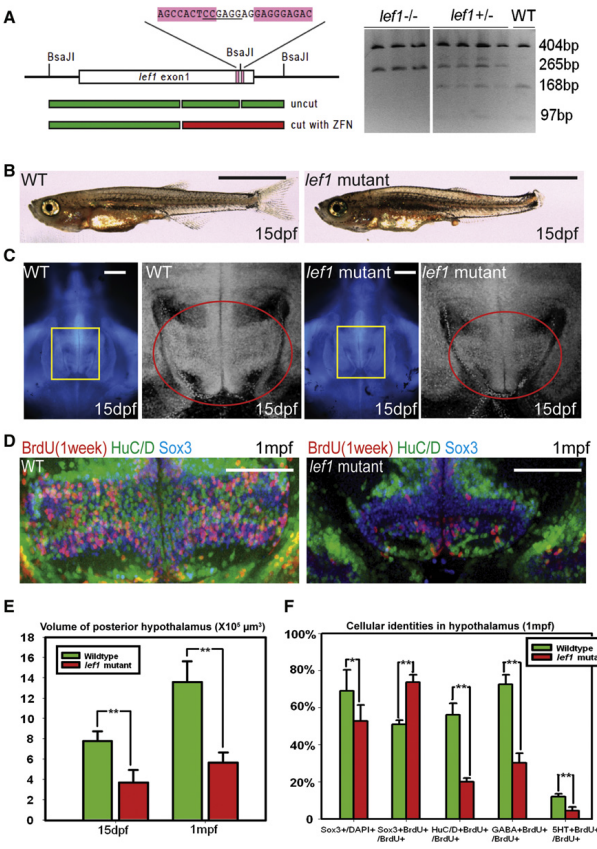

Figure 2. *lef1* Is Required for Proliferation and Neurogenesis in the Postembryonic Hypothalamus

(A) *lef1* ZFN target region and genotyping.

(B and C) Whole fish (B) and brain size (C) comparisons of *lef1* mutant to wild-type at 15 dpf. Boxed region in left panel is enlarged on right, posterior recess is circled.

(D) Expression of HuC/D, Sox3, and 7-day BrdU labeling in posterior recess of wild-type and *lef1* mutant hypothalamus.

(E) Quantification of posterior hypothalamus size.

(F) Tracing of proliferating cells. *lef1* mutants have a smaller Sox3$^+$ progenitor pool, but a higher percentage of BrdU$^+$ cells express Sox3 and fewer produce HuC/D$^+$, GABA$^+$, or 5HT$^+$ neurons. Single optical sections from ventral views are shown in (C) and (D). Scale bars represent 2 mm (B), 200 µm (C), and 100 µm (D). Brain volumes were calculated using Amira software. Cell counts were collected from maximum intensity Z projections through the posterior recess of three individual samples for each genotype and calculated using Volocity software. *$p < 0.05$, **$p < 0.005$. Error = ±SD.

See also Figure S3.

differentiation markers such as *Dlx* genes or HuC/D following heat shock (not shown). These data are consistent with existing models of Wnt as a mitogen in progenitor cells (Megason and McMahon, 2002).

Our analysis of Wnt activity at 4 dpf suggested a potential role for the pathway in neuronal differentiation. We therefore analyzed the effects on proliferation and differentiation following heat shock at this stage. A 2 hr BrdU pulse was performed at 70 hpf, followed by multiple heat shocks every 8 hr, and fixation at 96 hpf. In control embryos, we found that the number of BrdU$^+$ cells in the posterior recess increased ~3-fold over 24 hr, but we observed no statistically significant changes in overall BrdU labeling following expression of *hs:wnt8a*, *hs:dkk1*, or *hs:axin1* (Figure 3B). We then analyzed the BrdU$^+$ population to determine whether Wnt signaling was necessary or sufficient to promote differentiation of neural progenitors. Surprisingly, we found that both activation and inhibition of Wnt signaling caused a higher percentage of BrdU$^+$ cells to remain as undifferentiated Sox3$^+$ progenitors, and a lower percentage to differentiate into GABAergic and serotonergic progeny (Figures 3C and S4). The proportion of BrdU$^+$/Sox3$^+$ cells that were still mitotic (PCNA$^+$) at 4 dpf was increased following Wnt activation and decreased following Wnt inhibition (Figure 3C), indicating a continuing role for the pathway in maintaining the mitotic state. However, a decrease in overall *dlx5/6:gfp* expression (Figure S4) following Wnt activation, coupled with the lack of an overall increase in BrdU$^+$ cells (most of which are Sox3$^+$), strongly suggest a specific effect on differentiation. We therefore conclude that both activation and inhibition of Wnt signaling lead to a significant failure of progenitors to differentiate, independent from any effect on cell cycle exit.

Considering our observation of Wnt activity only prior to differentiation, these data suggested that Wnt signaling is required for progenitors to commit to neurogenesis but must be inhibited for the process to continue. We therefore tested whether progenitors would eventually differentiate following transient Wnt activation. The same experimental paradigm described above was used, except BrdU$^+$ cells were followed for two additional days. In this case, we found that the block in differentiation was indeed temporary, as by 6 dpf the number of BrdU$^+$ GABAergic precursors had recovered to control levels (Figure 3D).

To test whether the function of Wnt signaling in neurogenesis was conserved at adult stages, we analyzed 6 mpf zebrafish using *hs:wnt8a* and *hs:dkk1*. Because of the slower rate of proliferation at this stage, fish were incubated in BrdU for

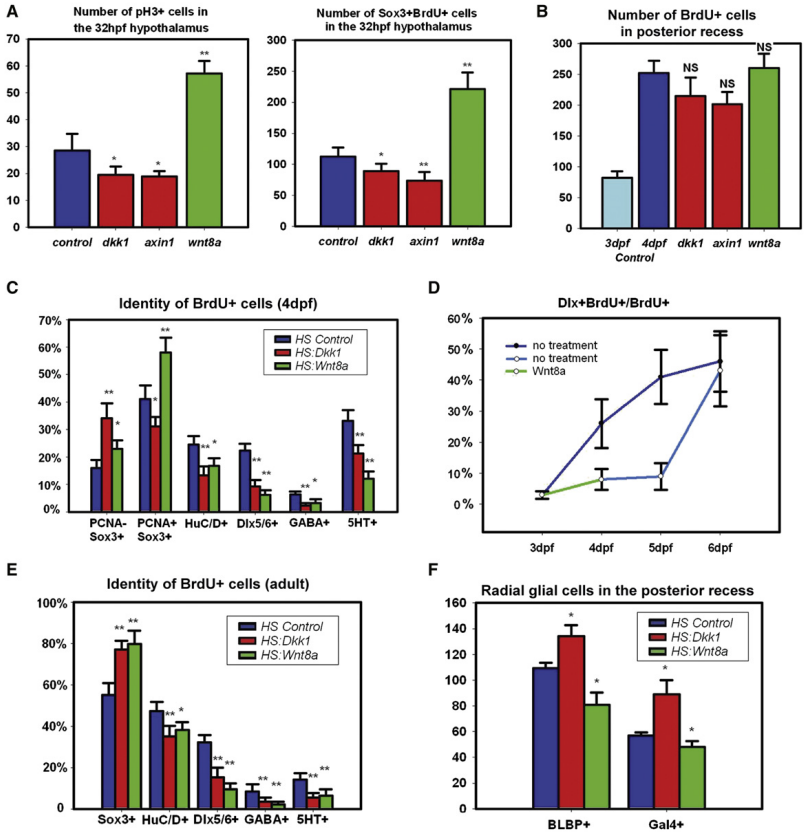

Figure 3. Wnt Signaling Regulates Hypothalamic Progenitor Proliferation and Differentiation

(A) pH3$^+$ and BrdU$^+$/Sox3$^+$ cell numbers in the 32hpf hypothalamus following 2 hr labeling and Wnt pathway inhibition or activation at 24 hpf.

(B) BrdU$^+$ cell numbers in the 4 dpf posterior recess following 2 hr labeling and Wnt pathway inhibition or activation at 3 dpf.

(C) BrdU$^+$ cell fates in the 4 dpf hypothalamus following labeling and Wnt pathway inhibition or activation at 3 dpf.

(D) Percentage of BrdU$^+$ cells expressing *dlx5/6:gfp* following Wnt pathway activation at 3 dpf.

(E) BrdU$^+$ cell fates in the adult hypothalamus following 2-day labeling and Wnt pathway inhibition or activation for 15 days.

(F) Number of Gal4$^+$ and BLBP+ cells in the 4 dpf posterior recess following Wnt pathway inhibition or activation at 3 dpf. All cell counts were collected from ventral maximum intensity confocal Z projections through five individual brains. The entire hypothalamus was counted at 32 hpf, the entire posterior recess was counted at 4 dpf, and a hemisphere of the posterior recess was counted in adults. * $p < 0.05$, ** $p < 0.005$. Error = ±SD.

See also Figure S4.

2 days, followed by 15 daily heat-shocks. We then traced the BrdU$^+$ cells in the posterior recess region and found that as at 4 dpf, an increased percentage remained as Sox3$^+$ neural progenitors, and fewer differentiated into mature neurons following both Wnt activation and inhibition (Figures 3E and S4). These data suggest a constant postembryonic requirement for sequential activation and inhibition of Wnt signaling in the differentiation of hypothalamic neural progenitors.

Wnt Signaling Inhibits Hypothalamic Radial Gliogenesis

Previous reports have implicated negative regulation of Wnt signaling in the maintenance of radial glia (Wang et al., 2011), a cell type that has been identified as a potential neural progenitor in the hypothalamus (Lee et al., 2012; Xu et al., 2005). We therefore asked whether the Wnt pathway was active and functional in this cell population in zebrafish. Although we did not observe any expression of GFAP in the posterior recess (not

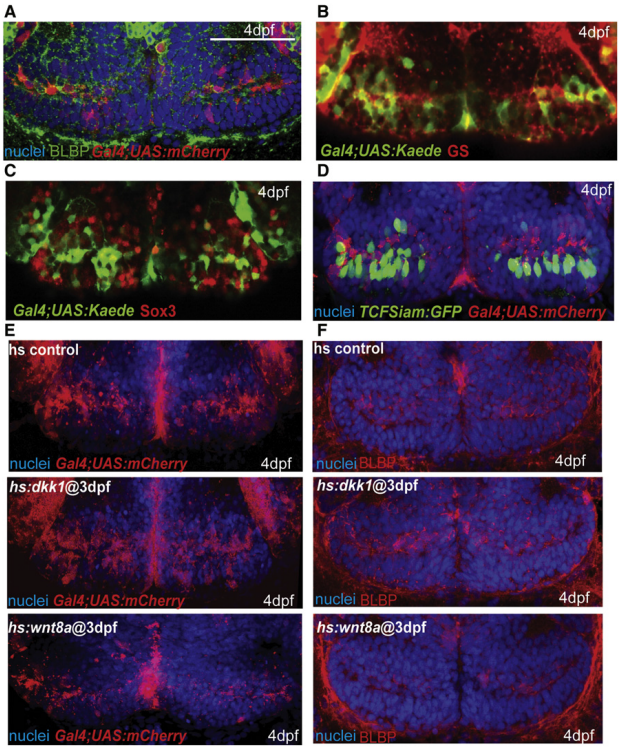

Figure 4. Wnt Signaling Inhibits the Formation of Radial Glia in the Posterior Recess at 4 dpf

(A) Coexpression of mCherry driven by the Gal4 *zc1066a* insertion with the radial glial marker BLBP.

(B) Coexpression of Gal4-driven Kaede with the radial glial marker glutamine synthetase.

(C) Costaining for Sox3 and Gal4-driven Kaede. Most Gal4$^+$ cells have low or absent Sox3 expression.

(D) Costaining for *TCFSiam:GFP* and Gal4-driven mCherry. Few Gal4$^+$ cells show Wnt reporter activity.

(E and F) Gal4 *zc1066a*-driven mCherry (E) and BLBP (F) expression in the posterior recess of 4 dpf embryos following Wnt pathway inhibition or activation at 3 dpf. Single ventral confocal optical sections are shown in all panels. Scale bar represents 80 μm.

shown), we took advantage of a Gal4 insertion that labels radial glia expressing Brain lipid-binding protein (BLBP) and glutamine synthetase, (GS) (Figures 4A and 4B). The level of Sox3 immunoreactivity in labeled cells was variable (Figure 4C), suggesting that a subset of them might be neural progenitors. However, few Gal4$^+$ cells showed evidence of Wnt reporter expression at 4 dpf (Figure 4D).

To test the role of Wnt signaling in radial glial development, we performed functional assays using *hs:dkk1* and *hs:wnt8a*. We heat shocked 3 dpf embryos every 8 hr and fixed at 4 dpf. We observed a higher number of Gal4$^+$ and BLBP$^+$ cells following Wnt inhibition and a lower number following Wnt activation (Figures 3F, 4E, and 4F), suggesting that Wnt activity is not required for the formation of radial glia, and ectopic Wnt activity results in a loss of this cell type.

Wnt Activity Is Present in the Adult Mouse Hypothalamus

In contrast to zebrafish, which have widespread proliferation throughout the adult CNS (Chapouton et al., 2007), adult neurogenesis is much more limited in mammals. However, proliferating progenitors have been identified in the rodent hypothalamus, where adult neurogenesis can influence feeding behavior (Kokoeva et al., 2005; Lee et al., 2012; Pierce and Xu, 2010). To determine whether the presence of Wnt signaling is conserved in the adult mouse hypothalamus, we used the reporter *BAT-LacZ* (Maretto et al., 2003) to identify Wnt-responsive cells. From sagittal sections, we observed abundant β-gal$^+$ cells in the adult cerebral cortex, hippocampus, olfactory epithelium, and cerebellum, as well as the posterior hypothalamus (Figure 5A). From coronal sections through the hypothalamus, we determined that the paraventricular and arcuate nuclei have the highest density of Wnt-responsive cells in this region (Figure 5B).

To determine the identity of hypothalamic Wnt-responsive cells we performed double immunohistochemistry for β-galactosidase and markers of either progenitors or differentiated cell types. We found that β-gal$^+$ cells exist in the ventricular and parenchymal zones of the mediobasal hypothalamus (Figure 5C). In the ventricular zone, β-gal$^+$ cells were primarily Sox2$^+$ ependymal cells and Sox2$^+$, Sox3$^+$, and GFAP$^+$ subependymal cells (Figures 5C–5E). Although the majority of β-gal$^+$ cells in the parenchymal zone were HuC/D$^+$ and NeuN$^+$ (Figures 5C–5E), some expressed Doublecortin, a marker of differentiating neurons, and many expressed the GABAergic precursor marker Dlx2 (Figures 5C–5E). Together, these results suggest that neural progenitors in the adult mammalian hypothalamus could be Wnt-responsive, as in zebrafish.

β-Catenin Negatively Regulates the Production of Ventricular Hypothalamic Tanycytes in the Mouse

To determine the function of Wnt signaling in adult mouse hypothalamic progenitors, we took a conditional genetic

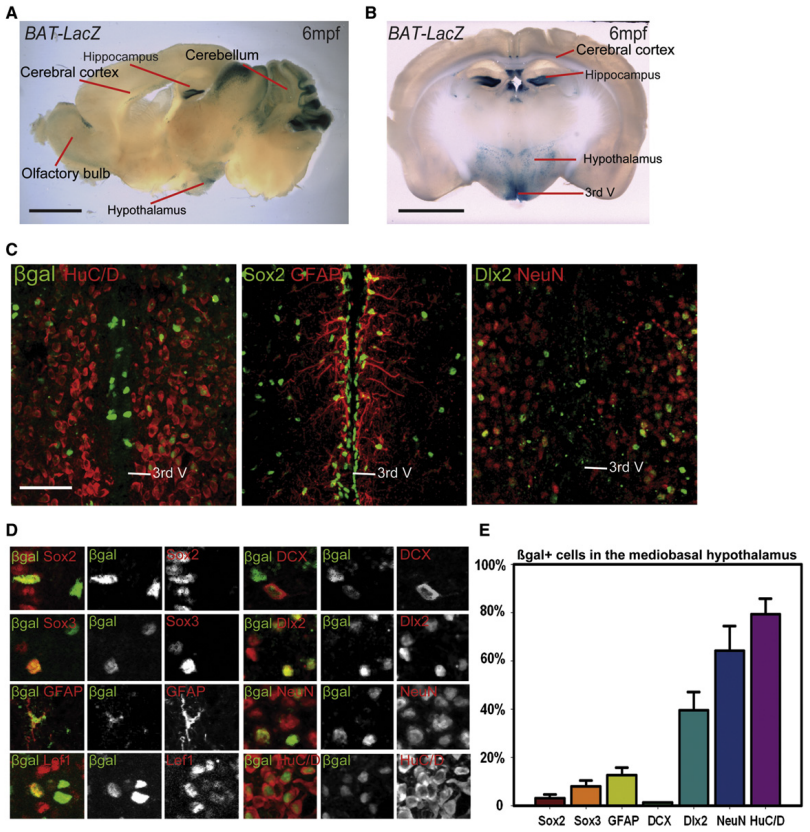

Figure 5. The Adult Mouse Hypothalamus Has a Wnt-Responsive Cell Population

(A and B) Sagittal (A) and coronal (B) sections of adult *Bat-LacZ* mouse brains.

(C) β-gal$^+$ cells are distributed in both the ventricular zone (where Sox2$^+$ and GFAP$^+$ cells reside) and the parenchymal zone (where Sox2, HuC/D$^+$, NeuN$^+$, and Dlx2$^+$ cells reside) Coronal 40μm cryosections are shown.

(D) Colocalization of β-gal with specific markers in the hypothalamus.

(E) Percentage of marker coexpression within the β-gal$^+$ population. Single confocal optical sections are shown in (C) and (D). Scale bars represent 2 mm (A and B), and 80 μm (C). Cell counts were collected from the mediobasal hypothalamus, using six 40μm cryosections each from three mice. Error = ±SD.

approach to remove and hyperactivate β-catenin. Because the expression of Notch pathway effectors has been observed in both the adult zebrafish and mouse hypothalamic ventricular zones (Chapouton et al., 2011; Lee et al., 2012), we chose to trace and manipulate cells expressing the Notch effector gene *Hes1*. We observed that knock-in mice expressing tamoxifen (TM)-dependent CreERT2 recombinase from the *Hes1* locus (*Hes1*^{C2}) (Kopinke et al., 2011) drive efficient and inducible recombination in hypothalamic ventricular progenitors (Figures 6A and 6B). Lineage tracing experiments with *R26R*^{LacZ} reporter mice (Soriano, 1999) showed that *Hes1*$^+$ cells are present in the ventricular zone of the adult hypothalamus 5 days after tamoxifen administration (Figure 6A), followed by expansion into the parenchymal zone 9 months posttamoxifen (Figure 6B).

To further characterize the Hes1-expressing population, we utilized the *R26R*^{EYFP} reporter (Srinivas et al., 2001) in mice that received tamoxifen at P60. The majority of EYFP$^+$ cells after a 5-day chase were located at the ventricular surface, having a cellular morphology without radial processes

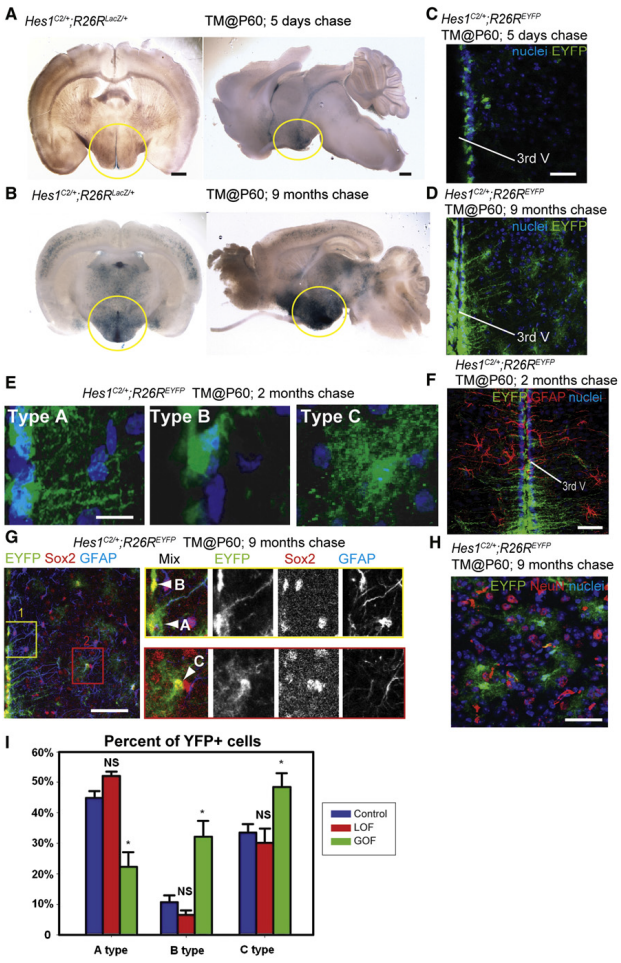

Figure 6. Wnt Signaling Inhibits the Production of Tanycytes from Adult *Hes1*$^{+}$ Progenitors

(A and B) Coronal and sagittal sections of adult *Hes1*$^{C2/+}$; *R26R*$^{LacZ/+}$ mouse brains, 5 days and 9 months after TM administration at P60.

(C and D) Coronal cryosections through the hypothalamus of adult *Hes1*$^{C2/+}$; *R26R*$^{EYFP/+}$ mouse brains, 5 days and 9 months after TM administration at P60.

(E) The three types of EYFP^{+} cells observed at 2 months post-TM.

(F) Expression of EYFP and GFAP in *Hes1*$^{C2/+}$; *R26R*$^{EYFP/+}$ mice 2 months post-TM.

(G and H) Marker analysis of *Hes1*$^{C2/+}$; *R26R*$^{EYFP/+}$ mice 9 months post-TM. Boxes in (G) show enlarged ventricular (yellow) and parenchymal (red) zones in which cell types are indicated by arrowheads. All EYFP^{+} cells are Sox2^{+}, and some ventricular Type A cells are also GFAP^{+}. (H) Expression of EYFP and NeuN^{+} in the parenchymal zone, where no colabeled cells are observed.

(I) Percentage of Type A, B, and C EYFP^{+} cells 2 months following β-catenin inactivation or activation. Single confocal optical sections are shown in (C–H). Scale bars represent 1 mm (A and B), 80 μm (C, D, F, G, and H), and 10 μm (E). Cell counts were collected from the mediobasal hypothalamus, using six 40 μm sections from three mice for each genotype. *$p < 0.05$. Error = ±SD.

(Figure 6C). After a 2-month or 9-month chase, EYFP^{+} cells comprised three classes. The most predominant class ("Type A") was located at the ventricular surface and had long radial processes (Figures 6D and 6E). All of these cells were Sox2^{+} (Figure 6G) and BLBP^{+} (not shown), but only the most dorsal were GFAP^{+} (Figures 6F and 6G). This combination of morphology and marker expression closely matches a profile previously described for radial glial tanycytes (Lee et al., 2012; Pérez-Martín et al., 2010b; Rodríguez et al., 2005). A second class ("Type B") was similar to the ventricular cells observed after a 5-day chase, lacking radial processes (Figures 6E and 6G). These cells were all Sox2^{+} (Figure 6G), BLBP^{+} (not shown), and GFAP (Figure 6G). A third class ("Type C") was located in the parenchymal zone, and was Sox2^{+} with stellate morphology (Figures 6E and 6G). Based on these characteristics, we conclude that Type C cells are most likely astrocytes. Notably, we never observed any Sox10 (not shown) HuC/D (not shown) or NeuN (Figure 6H) expression in Type C cells, or in the entire *Hes1* lineage. Together, these data indicate that *Hes1*$^{+}$ progenitors do not produce neurons in the adult mouse hypothalamus, but do produce multiple classes of glia.

To investigate the role of Wnt/β-catenin signaling in the differentiation of *Hes1*$^{+}$ progenitors, we crossed the *Hes1*^{C2} line with *Catnb*$^{lox(ex2-6)}$ (Brault et al., 2001) and *Catnb*$^{lox(ex3)}$ (Harada et al., 1999) mice allowing for β-catenin loss- and gain-of-function experiments, respectively. In addition, all mice carried one copy of the *R26R*^{EYFP} reporter allele, enabling us to determine the fate of recombined *Hes1*$^{+}$ cells. All mice were genotyped and treated with 2 mg TM at P60, and EYFP-expressing cells in the mediobasal hypothalamus were analyzed 2 months later. This dose of TM was used to avoid lethal effects of recombination in the intestinal *Hes1*$^{+}$ lineage (Kopinke et al., 2011).

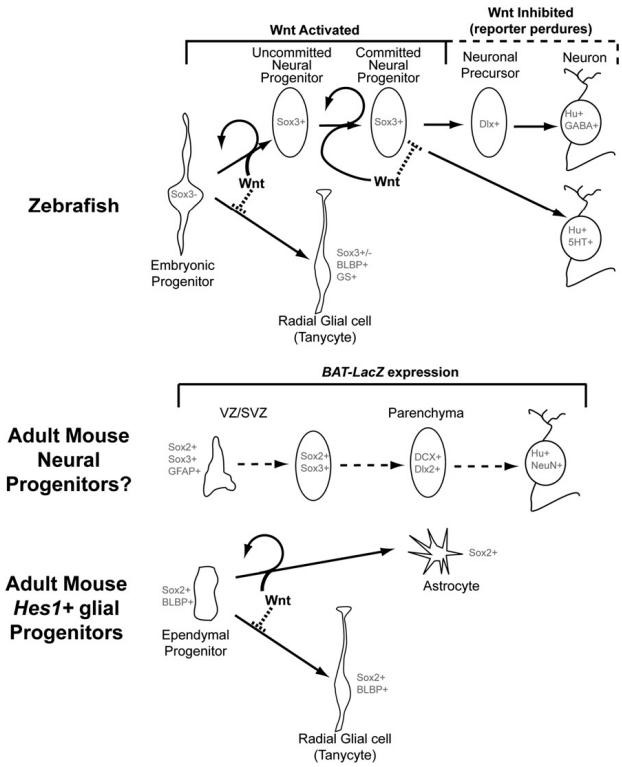

Figure 7. Model for the Role of Wnt Signaling in Hypothalamic Progenitor Differentiation

In zebrafish (top), Wnt signaling is active in unspecified embryonic progenitors and a neural progenitors, but is lost as these cells undergo neurogenesis. Wnt signaling promotes mitotic activity in progenitors, and is also required for their ability to undergo neuronal differentiation, which underlies the transition from an "uncommitted" to a "committed" progenitor state. Finally, Wnt signaling must be inhibited for differentiation to proceed. In contrast the formation of radial glia is inhibited by Wnt activity. In the adult mouse (bottom), Wnt signaling is active in ventricular/subventricular zone cells (VZ/SVZ) that express neural progenitor markers, and in parenchymal zone cells that express neuronal and neuronal precursor markers. Ventricular *Hes1*$^+$ progenitors do not require Wnt activity to make radial glial tanycytes, and ectopic pathway activity inhibits radial glial formation at the expense of other fates.

Following both gain and loss of β-catenin function, we observed numerous EYFP$^+$ cells in the ventricular and parenchymal zones, as in controls. Analysis of HuC/D and NeuN expression indicated that no EYFP$^+$ cells of any genotype were neurons (data not shown). Because we used a low TM dose, recombination was mosaic and each animal had a variable number of EYFP$^+$ cells, thus we were unable to statistically analyze the size of the lineage. Despite this, we did not observe a qualitative difference in number of EYFP$^+$ cells between different genotypes, suggesting there was no major effect on proliferation during the 2-month period. When we analyzed the proportion of Type A, B, and C EYFP$^+$ cells, we found that β-catenin activity was not required for radial glial differentiation (Figure 6I). In contrast, β-catenin activation led to a significant decrease in the proportion of radial glia, with a corresponding increase in the proportion of Type B ventricular cells without processes, and Type C astrocyte-like parenchymal cells (Figure 6I). These results suggest that Wnt/β-catenin activity negatively regulates the production of mouse ventricular hypothalamic tanycytes, consistent with our findings in zebrafish.

DISCUSSION

Wnt Signaling Regulates Hypothalamic Progenitor Differentiation in Zebrafish and Mouse

In this study, we have shown that both the postembryonic zebrafish and adult mouse hypothalamus contain Wnt-responsive cells (Figure 7). In zebrafish, hypothalamic Wnt-responsive cells are unspecified progenitors at early embryonic stages and Sox3$^+$ neural progenitors at postembryonic stages, contributing to GABAergic and serotonergic neuronal lineages. In the adult mouse, both ventricular and parenchymal cells expressing neural progenitor and GABAergic precursor markers also exhibit Wnt activity. In addition, we have identified radial glial tanycyte lineages in both species, marked by a Gal4 transgene in zebrafish and by *Hes1* in mouse. Our functional analyses demonstrate that Wnt/β-catenin signaling regulates progenitor proliferation in the early zebrafish embryo, but primarily regulates neuronal differentiation at postembryonic stages. In contrast, in both zebrafish and mouse Wnt signaling is not required for the formation of radial glia, and ectopic Wnt activity disrupts the formation of these cells. Together, this work suggests a conserved role for Wnt signaling in postembryonic hypothalamic progenitor differentiation in vertebrates.

Sequential Activation and Inhibition of Wnt Signaling Is Required for GABAergic Neurogenesis

Surprisingly, we found that both activation and inhibition of Wnt signaling led to arrest in the Sox3$^+$ progenitor state, and failure of further differentiation. Our data support a model proposed previously in retinal development (Agathocleous et al., 2009), in which Wnt signaling must be active in order for

Developmental Cell
Wnt Regulation of Hypothalamic Progenitors

uncommitted progenitors to acquire the competence to differentiate (Figure 7), but must then be inhibited for cells to complete the differentiation process. Consistent with this model, we find that Wnt signaling is active in postmitotic progenitors before they express *Dlx* genes, but is absent as they differentiate (Figure 7). A recent study examining constitutive activation of Wnt signaling in adult neural stem cells also supports this model (Imura et al., 2010). In our study, BrdU tracing only allowed us to follow proliferating cells, leaving open the possibility that once committed progenitors have already received the necessary Wnt signal, pathway inhibition will promote their differentiation.

Consistent with other work suggesting that Wnts generally act as mitogens (Megason and McMahon, 2002), we found that Wnt activity is associated with progenitor proliferation at embryonic and postembryonic stages. However, we also showed a clear role for Wnt activity in postmitotic neural progenitors, as Sox3+/PCNA− cells still fail to differentiate following Wnt pathway inhibition (Figure 3C). Even following Wnt pathway activation, our data support a specific effect on neuronal differentiation in addition to any proliferative expansion (Figure S4). Within a single cell population, the function of Wnt signaling may thus change over time in a context-dependent manner. Our data suggest that although Wnt activation promotes the mitotic expansion of progenitors, it also acts to hold cells in the progenitor state once they have become specified. In different cell populations, the specified state may or may not be proliferative, leading to seemingly conflicting phenotypes.

Hes1^{+} Ventricular Zone Progenitors Do Not Produce Neurons in the Adult Mouse Hypothalamus

Ventricular zones have been identified as the primary adult neural stem cell niches in the vertebrate brain (García-Verdugo et al., 2002). Using *Hes1*^{C2} lineage tracing, we observed a significant number of cells expanding outside the ventricular zone, but these cells did not become neurons. Adult hypothalamic neurogenesis in mammals has only been characterized relatively recently (Yuan and Arias-Carrión, 2011), partly because very few neurons are produced at any time. Consistent with the idea that the mammalian hypothalamus contains a functionally significant level of adult neurogenesis during normal homeostasis (Lee et al., 2012; Yuan and Arias-Carrión, 2011), we observed numerous Dlx2^{+} cells in the parenchymal zone. Although recent work has identified ventricular *Nestin*$^{+}$ tanycytes of the hypothalamic medial eminence as neural progenitors in the postnatal mouse (Lee et al., 2012), it is not clear whether they contribute to homeostatic adult neurogenesis as the lineage was only analyzed until P75. Furthermore, this study described additional neurogenesis that did not arise from *Nestin*$^{+}$ cells. It is possible, therefore, that a progenitor niche separate from the ventricular zone contributes to neurogenesis, or that *Nestin* /*Hes1* neural progenitors exist in the ventricular zone and subsequently migrate to the parenchyma (Migaud et al., 2010). To test the specific role of Wnt signaling in adult mouse hypothalamic neurogenesis, it will be necessary to employ conditional approaches using markers identified by our *BAT-LacZ* analysis, such as *Sox2*, *GFAP*, and *Dlx2*, in addition to *Nestin*.

The Role of Wnt Signaling in Hypothalamic Radial Glia

Our data show that tanycyte formation and maintenance does not require Wnt signaling. In contrast, we find that Wnt pathway activation leads to decreased tanycyte numbers at the expense of neurons in zebrafish, and other glial cell types in mouse. Other work has revealed a similar role for β-catenin in Bergmann glia, which are transformed into astrocyte-like cells following *Apc* mutation (Wang et al., 2011). Interestingly, zebrafish do not contain true astrocytes but instead have radial astroglial-like cells throughout their brain (Grupp et al., 2010). Combined with the known neurogenic capacity of radial glia in the adult zebrafish brain (Kroehne et al., 2011), this raises the interesting possibility that the alternative fates promoted by Wnt signaling differ between zebrafish and mouse due to the different developmental potential of glial progenitors.

In summary, this work resolves some of the seemingly conflicting conclusions regarding the role of Wnt signaling in neurogenesis, from studies in different systems using different manipulations. We believe that many of these results can be explained by a dual role for the pathway, first in expansion of unspecified progenitors, then later as a required inducer of neuronal differentiation that must subsequently be inhibited for neurogenesis to occur. Furthermore, we have established the vertebrate hypothalamus as a model system for Wnt function in postembryonic progenitor differentiation, and opened the field to future studies examining the role of this process in animal behavior.

EXPERIMENTAL PROCEDURES

All animal procedures were approved by the Institutional Animal Care and Use Committee of the University of Utah.

Zebrafish

Zebrafish embryos were obtained from natural spawning of wild-type (AB*), transgenic, and mutant adult fish. A detailed description of the strains used can be found in the Supplemental Experimental Procedures. Adult brains were dissected from anesthetized fish fixed in 4% paraformaldehyde for 2 days. Fish received BrdU pulses by immersion in E3 media with 10 mM BrdU, and received heat shock by immersion in prewarmed E3 media.

Mice

A detailed listing of mouse strains used can be found in the Supplemental Experimental Procedures. Tamoxifen (Sigma T-5648) was dissolved in corn oil and administered by oral gavage at doses of 10 mg (Hes1 lineage) or 2 mg (β-catenin loss and gain of function experiments) per mouse between 6–8 weeks of age.

X-gal Staining, In Situ Hybridization, and Immunohistochemistry

For X-gal staining in mice, fixed whole brains were sliced at 500 μm thickness, and staining was performed as described previously (Seymour et al., 2004) followed by clearing in 100% glycerol. Mouse immunostaining and analysis were performed on 40 μm cryosections as described previously (Kopinke et al., 2011). Zebrafish in situ hybridization and immunohistochemistry were performed as described previously (Oxtoby and Jowett, 1993), except that whole mount brains were first dissected (4 dpf and adult) and sliced longitudinally (adult), followed by collagenase treatment. All mRNA probes have been described previously (Lee et al., 2006; Wang et al., 2009). A detailed list of antibodies used can be found in the Supplemental Experimental Procedures.

Cryosectioning and Microscopy

Cryosections were cut at a thickness of 12 μm for embryonic zebrafish and 40 μm for adult mouse brains. All analysis of zebrafish brains was performed on whole-mount samples, except for Lef1 immunohistochemistry. Fluorescent

images of whole mount zebrafish brains were taken using an Olympus FV1000 confocal microscope and an Olympus SZX12 fluorescent dissecting microscope. Maximum intensity Z projections were used for all quantitative analyses. Bright field images were obtained using an Olympus BX51WI compound microscope.

Data Analysis

Colocalization analysis, volume measurements, statistical calculations, and graphs were generated with Image J, Volocity5.4, Amira 5.3.3, Microsoft Excel, and Sigma Plot 10.0. All analyses in zebrafish were performed on whole-mount brains. For analysis at 32 hpf, the entire hypothalamus was counted using the third ventricle and nuclear staining as landmarks. For analysis at 4 dpf–1 mpf, a rectangle defining the entire posterior recess was counted, using the ventricle and nuclear staining as landmarks. For analysis of adults, a rectangle defining the posterior recess in a midsagittal view was counted, using the ventricle and nuclear staining as landmarks. All analyses in mouse were performed on cryosections using morphological landmarks to define the mediobasal hypothalamus. Error bars represent SDs from at least three samples (N is listed in each figure legend), and comparisons of data sets were performed with one-tailed homoscedastic or heteroscedastic t tests.

Quantitative RT-PCR

Total RNA was isolated using an RNeasy extraction kit (QIAGEN) followed by DNase treatment. cDNA was synthesized by SuperScript II reverse transcriptase (Invitrogen). mRNA levels were normalized to an average of *beta-actin*. Quantitative realtime PCR using the Sybr Green reagent was performed with an ABI7900, using primers listed below:

axin2: F: TGAAGCGGGAACAGGAAAC; R: AGGAGCAAAGGCAGAGAA,
beta-actin: F: AGGATGCGGAAACTGGAAAG; R: GAGGAGGGCAAAGTG GTAAA.

Isolation of *lef1* Mutants using Engineered Zinc-Finger Nuclease

To introduce mutations in the *lef1* gene, a target site was chosen within the exon 1 using ZiFiT (http://zifit.partners.org/ZiFiT/). ZFNs were prepared using a detailed protocol posted elsewhere (http://wiki.zfin.org/), in which three-finger array libraries were constructed using OPEN pools (Maeder et al., 2009), but modified to be selectable in bacterial one-hybrid (B1H) system (Maeder et al., 2008). Selected three-finger array sequences were converted to ZFNs by fusion with the FokI nuclease domain. Synthetic mRNAs encoding the ZFNs were injected into one-cell stage zebrafish embryos. Mutations were identified by loss of BsaJI restriction sequence located in the target site. Genomic DNA was extracted from the individual 24 hpf embryos and amplified with the following primers: F: TTGGAGGTGTGCTACTCACG; R: CACTCTCT CCAGCCCAACAT. To isolate germ-line transmitted *lef1* mutations, ZFN-injected embryos were raised to adulthood and progeny were analyzed using PCR and BsaJI digestion.

SUPPLEMENTAL INFORMATION

Supplemental Information includes four figures and Supplemental Experimental Procedures and can be found with this article online at http://dx.doi.org/10.1016/j.devcel.2012.07.012.

ACKNOWLEDGMENTS

We thank Michael Klymkowsky (University of Colorado at Boulder) for sharing the Sox3 antibody, Jan Kaslin (Monash University, Australia) for sharing unpublished data, and Sabine Fuhrmann and Gabrielle Kardon (University of Utah) for providing *BAT-LacZ* mice. F.A. is supported by EU grant ZF-HEALTH CT-2010-242048. R.I.D. was supported by NIH (NINDS) R21NS055138.

Received: October 26, 2011
Revised: May 15, 2012
Accepted: July 17, 2012
Published online: September 10, 2012

REFERENCES

Agathocleous, M., Iordanova, I., Willardsen, M.I., Xue, X.Y., Vetter, M.L., Harris, W.A., and Moore, K.B. (2009). A directional Wnt/beta-catenin-Sox2-proneural pathway regulates the transition from proliferation to differentiation in the Xenopus retina. Development *136*, 3289–3299.

Bergsland, M., Ramsköld, D., Zaouter, C., Klum, S., Sandberg, R., and Muhr, J. (2011). Sequentially acting Sox transcription factors in neural lineage development. Genes Dev. *25*, 2453–2464.

Brault, V., Moore, R., Kutsch, S., Ishibashi, M., Rowitch, D.H., McMahon, A.P., Sommer, L., Boussadia, O., and Kemler, R. (2001). Inactivation of the beta-catenin gene by Wnt1-Cre-mediated deletion results in dramatic brain malformation and failure of craniofacial development. Development *128*, 1253–1264.

Chapouton, P., Jagasia, R., and Bally-Cuif, L. (2007). Adult neurogenesis in non-mammalian vertebrates. Bioessays *29*, 745–757.

Chapouton, P., Webb, K.J., Stigloher, C., Alunni, A., Adolf, B., Hesl, B., Topp, S., Kremmer, E., and Bally-Cuif, L. (2011). Expression of hairy/enhancer of split genes in neural progenitors and neurogenesis domains of the adult zebrafish brain. J. Comp. Neurol. *519*, 1748–1769.

Dorsky, R.I., Sheldahl, L.C., and Moon, R.T. (2002). A transgenic Lef1/beta-catenin-dependent reporter is expressed in spatially restricted domains throughout zebrafish development. Dev. Biol. *241*, 229–237.

Galceran, J., Miyashita-Lin, E.M., Devaney, E., Rubenstein, J.L., and Grosschedl, R. (2000). Hippocampus development and generation of dentate gyrus granule cells is regulated by LEF1. Development *127*, 469–482.

García-Verdugo, J.M., Ferrón, S., Flames, N., Collado, L., Desfilis, E., and Font, E. (2002). The proliferative ventricular zone in adult vertebrates: a comparative study using reptiles, birds, and mammals. Brain Res. Bull. *57*, 765–775.

Grupp, L., Wolburg, H., and Mack, A.F. (2010). Astroglial structures in the zebrafish brain. J. Comp. Neurol. *518*, 4277–4287.

Harada, N., Tamai, Y., Ishikawa, T., Sauer, B., Takaku, K., Oshima, M., and Taketo, M.M. (1999). Intestinal polyposis in mice with a dominant stable mutation of the beta-catenin gene. EMBO J. *18*, 5931–5942.

Imura, T., Wang, X., Noda, T., Sofroniew, M.V., and Fushiki, S. (2010). Adenomatous polyposis coli is essential for both neuronal differentiation and maintenance of adult neural stem cells in subventricular zone and hippocampus. Stem Cells *28*, 2053–2064.

Kizil, C., Kaslin, J., Kroehne, V., and Brand, M. (2012). Adult neurogenesis and brain regeneration in zebrafish. Dev. Neurobiol. *72*, 429–461.

Kokoeva, M.V., Yin, H., and Flier, J.S. (2005). Neurogenesis in the hypothalamus of adult mice: potential role in energy balance. Science *310*, 679–683.

Kokoeva, M.V., Yin, H., and Flier, J.S. (2007). Evidence for constitutive neural cell proliferation in the adult murine hypothalamus. J. Comp. Neurol. *505*, 209–220.

Kopinke, D., Brailsford, M., Shea, J.E., Leavitt, R., Scaife, C.L., and Murtaugh, L.C. (2011). Lineage tracing reveals the dynamic contribution of Hes1+ cells to the developing and adult pancreas. Development *138*, 431–441.

Kroehne, V., Freudenreich, D., Hans, S., Kaslin, J., and Brand, M. (2011). Regeneration of the adult zebrafish brain from neurogenic radial glia-type progenitors. Development *138*, 4831–4841.

Kuwabara, T., Hsieh, J., Muotri, A., Yeo, G., Warashina, M., Lie, D.C., Moore, L., Nakashima, K., Asashima, M., and Gage, F.H. (2009). Wnt-mediated activation of NeuroD1 and retro-elements during adult neurogenesis. Nat. Neurosci. *12*, 1097–1105.

Lee, D.A., Bedont, J.L., Pak, T., Wang, H., Song, J., Miranda-Angulo, A., Takiar, V., Charubhumi, V., Balordi, F., Takebayashi, H., et al. (2012). Tanycytes of the hypothalamic median eminence form a diet-responsive neurogenic niche. Nat. Neurosci. *15*, 700–702.

Lee, J.E., Wu, S.F., Goering, L.M., and Dorsky, R.I. (2006). Canonical Wnt signaling through Lef1 is required for hypothalamic neurogenesis. Development *133*, 4451–4461.

Lee, S.M., Tole, S., Grove, E., and McMahon, A.P. (2000). A local Wnt-3a signal is required for development of the mammalian hippocampus. Development *127*, 457–467.

Machon, O., Backman, M., Machonova, O., Kozmik, Z., Vacik, T., Andersen, L., and Krauss, S. (2007). A dynamic gradient of Wnt signaling controls initiation of neurogenesis in the mammalian cortex and cellular specification in the hippocampus. Dev. Biol. *311*, 223–237.

Maeder, M.L., Thibodeau-Beganny, S., Osiak, A., Wright, D.A., Anthony, R.M., Eichtinger, M., Jiang, T., Foley, J.E., Winfrey, R.J., Townsend, J.A., et al. (2008). Rapid "open-source" engineering of customized zinc-finger nucleases for highly efficient gene modification. Mol. Cell *31*, 294–301.

Maeder, M.L., Thibodeau-Beganny, S., Sander, J.D., Voytas, D.F., and Joung, J.K. (2009). Oligomerized pool engineering (OPEN): an 'open-source' protocol for making customized zinc-finger arrays. Nat. Protoc. *4*, 1471–1501.

Maretto, S., Cordenonsi, M., Dupont, S., Braghetta, P., Broccoli, V., Hassan, A.B., Volpin, D., Bressan, G.M., and Piccolo, S. (2003). Mapping Wnt/beta-catenin signaling during mouse development and in colorectal tumors. Proc. Natl. Acad. Sci. USA *100*, 3299–3304.

McGraw, H.F., Drerup, C.M., Culbertson, M.D., Linbo, T., Raible, D.W., and Nechiporuk, A.V. (2011). Lef1 is required for progenitor cell identity in the zebrafish lateral line primordium. Development *138*, 3921–3930.

Megason, S.G., and McMahon, A.P. (2002). A mitogen gradient of dorsal midline Wnts organizes growth in the CNS. Development *129*, 2087–2098.

Meng, X., Noyes, M.B., Zhu, L.J., Lawson, N.D., and Wolfe, S.A. (2008). Targeted gene inactivation in zebrafish using engineered zinc-finger nucleases. Nat. Biotechnol. *26*, 695–701.

Migaud, M., Batailler, M., Segura, S., Duittoz, A., Franceschini, I., and Pillon, D. (2010). Emerging new sites for adult neurogenesis in the mammalian brain: a comparative study between the hypothalamus and the classical neurogenic zones. Eur. J. Neurosci. *32*, 2042–2052.

Ming, G.L., and Song, H. (2011). Adult neurogenesis in the mammalian brain: significant answers and significant questions. Neuron *70*, 687–702.

Moro, E., Ozhan-Kizil, G., Mongera, A., Beis, D., Wierzbicki, C., Young, R.M., Bournele, D., Domenichini, A., Valdivia, L.E., Lum, L., et al. (2012). In vivo Wnt signaling tracing through a transgenic biosensor fish reveals novel activity domains. Dev. Biol. *366*, 327–340.

Muncan, V., Faro, A., Haramis, A.P., Hurlstone, A.F., Wienholds, E., van Es, J., Korving, J., Begthel, H., Zivkovic, D., and Clevers, H. (2007). T-cell factor 4 (Tcf7l2) maintains proliferative compartments in zebrafish intestine. EMBO Rep. *8*, 966–973.

Mutch, C.A., Schulte, J.D., Olson, E., and Chenn, A. (2010). Beta-catenin signaling negatively regulates intermediate progenitor population numbers in the developing cortex. PLoS ONE *5*, e12376.

Nagayoshi, S., Hayashi, E., Abe, G., Osato, N., Asakawa, K., Urasaki, A., Horikawa, K., Ikeo, K., Takeda, H., and Kawakami, K. (2008). Insertional mutagenesis by the Tol2 transposon-mediated enhancer trap approach generated mutations in two developmental genes: tcf7 and synembryn-like. Development *135*, 159–169.

Oxtoby, E., and Jowett, T. (1993). Cloning of the zebrafish krox-20 gene (krx-20) and its expression during hindbrain development. Nucleic Acids Res. *21*, 1087–1095.

Pérez-Martín, M., Cifuentes, M., Grondona, J.M., López-Avalos, M.D., Gómez-Pinedo, U., García-Verdugo, J.M., and Fernández-Llebrez, P. (2010a). IGF-I stimulates neurogenesis in the hypothalamus of adult rats. Eur. J. Neurosci. *31*, 1533–1548.

Pérez-Martín, M., Cifuentes, M., Grondona, J.M., López-Avalos, M.D., Gómez-Pinedo, U., García-Verdugo, J.M., and Fernández-Llebrez, P. (2010b). IGF-I stimulates neurogenesis in the hypothalamus of adult rats. Eur. J. Neurosci. *31*, 1533–1548.

Pierce, A.A., and Xu, A.W. (2010). De novo neurogenesis in adult hypothalamus as a compensatory mechanism to regulate energy balance. J. Neurosci. *30*, 723–730.

Rodríguez, E.M., Blázquez, J.L., Pastor, F.E., Peláez, B., Peña, P., Peruzzo, B., and Amat, P. (2005). Hypothalamic tanycytes: a key component of brain-endocrine interaction. Int. Rev. Cytol. *247*, 89–164.

Seymour, P.A., Bennett, W.R., and Slack, J.M. (2004). Fission of pancreatic islets during postnatal growth of the mouse. J. Anat. *204*, 103–116.

Soriano, P. (1999). Generalized lacZ expression with the ROSA26 Cre reporter strain. Nat. Genet. *21*, 70–71.

Srinivas, S., Watanabe, T., Lin, C.S., William, C.M., Tanabe, Y., Jessell, T.M., and Costantini, F. (2001). Cre reporter strains produced by targeted insertion of EYFP and ECFP into the ROSA26 locus. BMC Dev. Biol. *1*, 4.

Stoick-Cooper, C.L., Weidinger, G., Riehle, K.J., Hubbert, C., Major, M.B., Fausto, N., and Moon, R.T. (2007). Distinct Wnt signaling pathways have opposing roles in appendage regeneration. Development *134*, 479–489.

Tang, M., Villaescusa, J.C., Luo, S.X., Guitarte, C., Lei, S., Miyamoto, Y., Taketo, M.M., Arenas, E., and Huang, E.J. (2010). Interactions of Wnt/beta-catenin signaling and sonic hedgehog regulate the neurogenesis of ventral midbrain dopamine neurons. J. Neurosci. *30*, 9280–9291.

Valdivia, L.E., Young, R.M., Hawkins, T.A., Stickney, H.L., Cavodeassi, F., Schwarz, Q., Pullin, L.M., Villegas, R., Moro, E., Argenton, F., et al. (2011). Lef1-dependent Wnt/β-catenin signalling drives the proliferative engine that maintains tissue homeostasis during lateral line development. Development *138*, 3931–3941.

Wang, X., Lee, J.E., and Dorsky, R.I. (2009). Identification of Wnt-responsive cells in the zebrafish hypothalamus. Zebrafish *6*, 49–58.

Wang, X., Imura, T., Sofroniew, M.V., and Fushiki, S. (2011). Loss of adenomatous polyposis coli in Bergmann glia disrupts their unique architecture and leads to cell nonautonomous neurodegeneration of cerebellar Purkinje neurons. Glia *59*, 857–868.

Weidinger, G., Thorpe, C.J., Wuennenberg-Stapleton, K., Ngai, J., and Moon, R.T. (2005). The Sp1-related transcription factors sp5 and sp5-like act downstream of Wnt/beta-catenin signaling in mesoderm and neuroectoderm patterning. Curr. Biol. *15*, 489–500.

Xu, Y., Tamamaki, N., Noda, T., Kimura, K., Itokazu, Y., Matsumoto, N., Dezawa, M., and Ide, C. (2005). Neurogenesis in the ependymal layer of the adult rat 3rd ventricle. Exp. Neurol. *192*, 251–264.

Yee, C.L., Wang, Y., Anderson, S., Ekker, M., and Rubenstein, J.L. (2009). Arcuate nucleus expression of NKX2.1 and DLX and lineages expressing these transcription factors in neuropeptide Y(+), proopiomelanocortin(+), and tyrosine hydroxylase(+) neurons in neonatal and adult mice. J. Comp. Neurol. *517*, 37–50.

Yuan, T.F., and Arias-Carrión, O. (2011). Adult neurogenesis in the hypothalamus: evidence, functions, and implications. CNS Neurol. Disord. Drug Targets *10*, 433–439.

Zhou, C.J., Zhao, C., and Pleasure, S.J. (2004). Wnt signaling mutants have decreased dentate granule cell production and radial glial scaffolding abnormalities. J. Neurosci. *24*, 121–126.

Developmental Cell, Volume *23*

Supplemental Information

Wnt Signaling Regulates Postembryonic Hypothalamic Progenitor Differentiation

Xu Wang, Daniel Kopinke, Junji Lin, Adam D. McPherson, Robert N. Duncan, Hideo Otsuna, Enrico Moro, Kazuyuki Hoshijima, David J. Grunwald, Francesco Argenton, Chi-Bin Chien, L. Charles Murtaugh, and Richard I. Dorsky

Inventory of Supplemental Information:

Figures:

Figure S1 supports Figure 1 by showing further characterization of long and short half-life Wnt reporters in the hypothalamus. It depicts BrdU labeling at two different timepoints, and shows the responsiveness of both reporters to Wnt inhibition.

Figure S2 supports Table 1 by showing co-staining of the short half-life Wnt reporter and the *dlx5/6:gfp* reporter with cell type specific markers. Quantification of these results is provided in Table 1.

Figure S3 supports Figure 2 by showing the expression of a candidate Wnt ligand and two Tcf transcription factors in the posterior hypothalamus. These data serve to justify the analysis of *lef1* mutants in Figure 2.

Figure S4 supports Figure 3 by showing effects on cell death, Wnt activity, mitosis, and differentiation following conditional activation and inhibition of Wnt signaling. Specific effects of these manipulations on proliferation and differentiation are quantified in Figure 3.

Methods:

Detailed descriptions of fish and mouse strains, as well as antibodies, are listed here.

Supplemental Figures and Legends

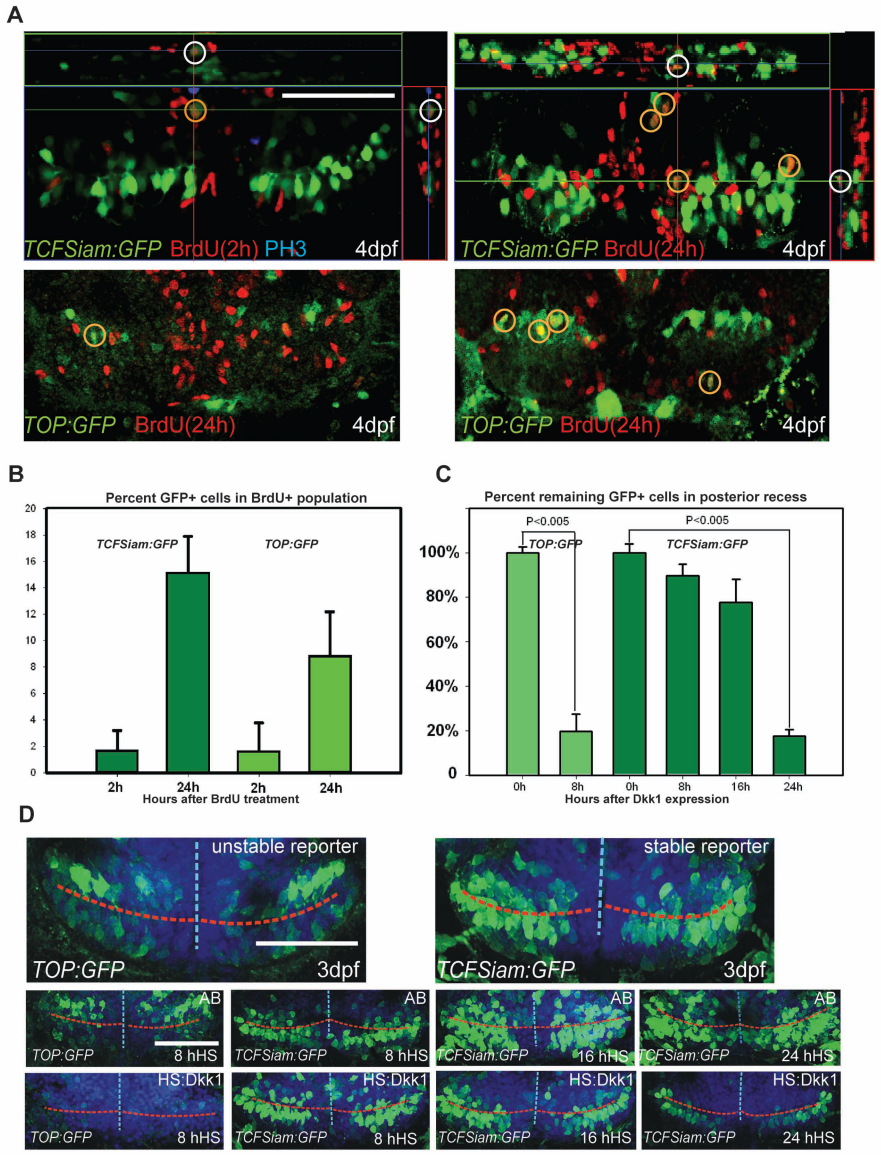

Figure S1 Analysis of Wnt reporter at 4dpf, related to Figure 1. (A) Ventral view of the posterior recess region of *TOP:GFP* and *TCFSiam:GFP* hypothalamus after short (2h) and long term (24h) BrdU labeling; observed with 50μm maximum intensity confocal Z-projections. (B) Quantification of $BrdU^{+}/GFP^{+}$ cells 2 hours or 24 hours after labeling. (C) Relative percentages of GFP^{+} cells following *hs:dkk1* expression at 3dpf, compared to wild-type controls. (D) Ventral view of the posterior recess region of *TOP:GFP* and *TCFSiam:GFP* embryos, 8h, 16h, and 24h after *hs:dkk1* activation at 3dpf. Images are 50μm ventral maximum intensity confocal Z-projections. Scale bars: 80μm. Cell counts were collected from ventral maximum intensity confocal Z-projections through the posterior recess of 3 individual samples for each condition. Error=±SD.

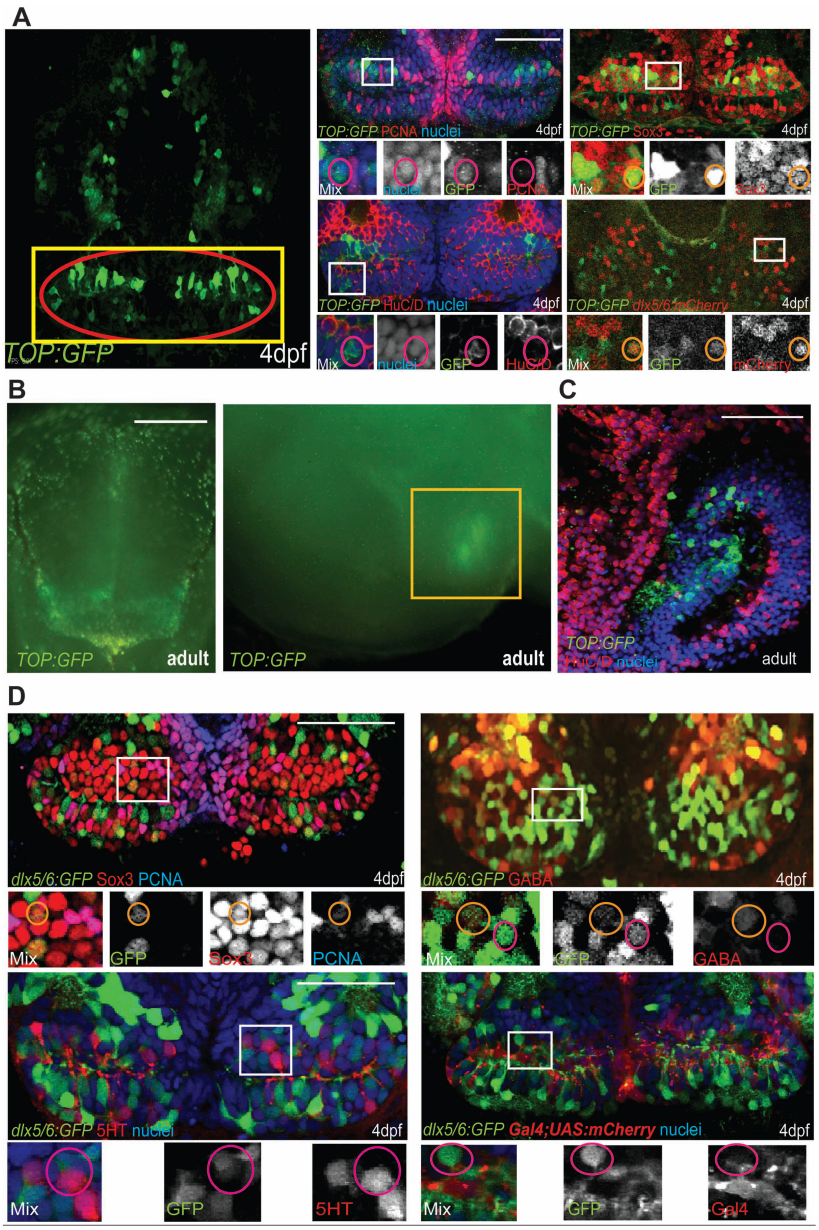
A
TOP:GFP
4dpf
TOP:GFP PCNA nuclei
4dpf
Mix
nuclei
GFP
PCNA
TOP:GFP Sox3
4dpf
Mix
GFP
Sox3
TOP:GFP HuC/D nuclei
4dpf
Mix
nuclei
GFP
HuC/D
TOP:GFP dlx5/6:mCherry
4dpf
Mix
GFP
mCherry
B
TOP:GFP
adult
TOP:GFP
adult
C
TOP:GFP
HuC/D nuclei
adult
D
dlx5/6:GFP Sox3 PCNA
4dpf
Mix
GFP
Sox3
PCNA
dlx5/6:GFP GABA
4dpf
Mix
GFP
GABA
dlx5/6:GFP 5HT nuclei
4dpf
Mix
GFP
5HT
dlx5/6:GFP Gal4;UAS:mCherry nuclei
4dpf
Mix
GFP
Gal4

Figure S2 Identity of reporter-labeled cells, related to Table 1. (A) Maximum-intensity confocal ventral projection of 4dpf *TOP:GFP* hypothalamus on left, yellow box marks the area shown on right and red oval marks the posterior recess. Co-staining of GFP with cell-type specific markers is shown on right. (B) Dissecting microscope images of *TOP:GFP* expression in the adult hypothalamus, from ventral and mid-sagittal views. Yellow box marks the area shown in (C). (C) Co-staining of GFP and HuC/D in the adult hypothalamus. (D) *dlx5/6:GFP* expression overlaps with Sox3, PCNA, and GABA, but not with 5HT or a Gal4 insertion expressed in radial glia (C). White boxes indicate enlarged regions. Small orange circles label cells with colocalization and small magenta circles label cells without colocalization. Single confocal optical sections are shown unless otherwise indicated. Scale bars: Scale bars: (A,C,D) 80μm, (B) 250μm.

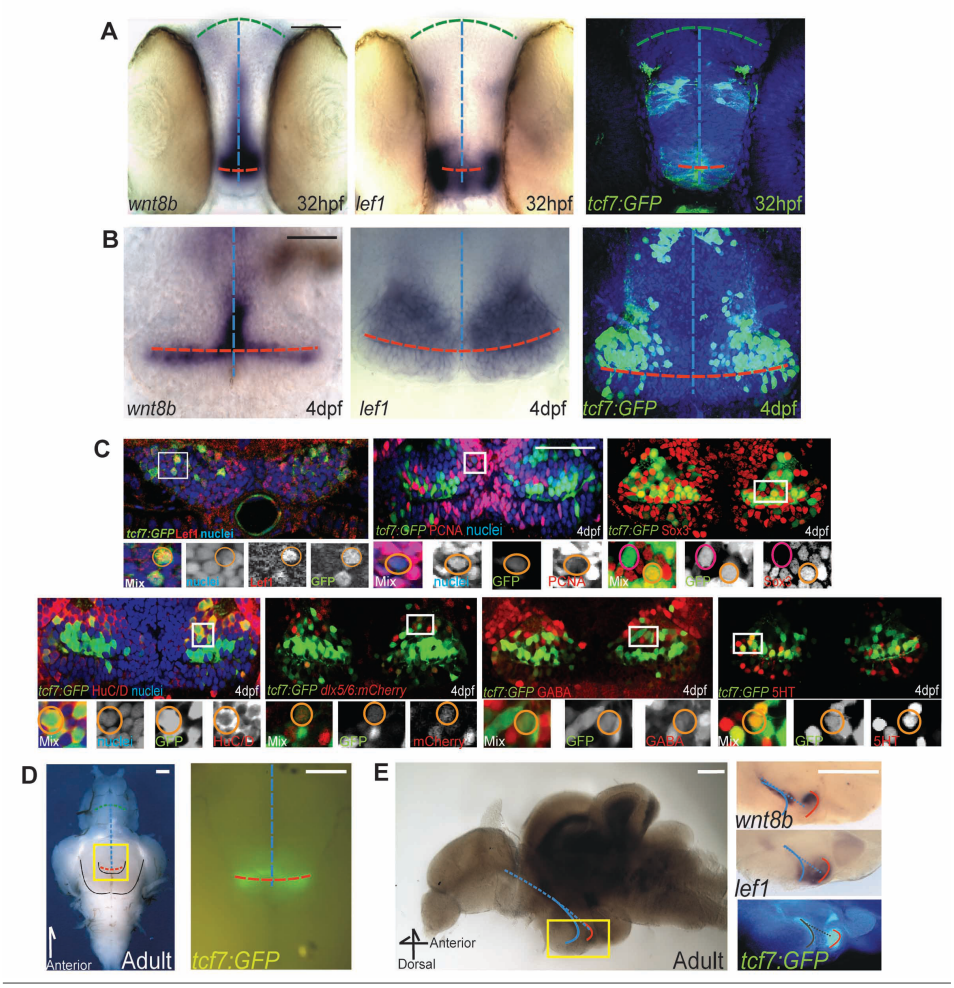
A
wnt8b
32hpf
lef1
32hpf
tcf7:GFP
32hpf
B
wnt8b
4dpf
lef1
4dpf
tcf7:GFP
4dpf
C
tcf7:GFP Lef1 nuclei
tcf7:GFP PCNA nuclei
4dpf
tcf7:GFP Sox3
4dpf
Mix
GFP
PCNA
tcf7:GFP HuC/D nuclei
4dpf
tcf7:GFP dlx5/6:mCherry
4dpf
tcf7:GFP GABA
4dpf
tcf7:GFP 5HT
4dpf
mCherry
D
Anterior
Adult
tcf7:GFP
E
Anterior
Dorsal
Adult
wnt8b
lef1
tcf7:GFP

Figure S3 Expression of Wnt pathway components in zebrafish hypothalamic neural progenitors, related to Figure 2. (A,B) *wnt8b* mRNA, *lef1* mRNA, and *tcf7:GFP* expression at 32hpf (A), and 4dpf (B) in ventral whole-mount views. (C) Co-expression of *tcf7:GFP* in the 4dpf hypothalamus with cell-type specific markers. (D) Bright-field and fluorescent dissecting microscope ventral images of the adult hypothalamus expressing *tcf7:GFP*. Yellow box in the bright field image indicates the region magnified in the fluorescent image. (E) Mid-sagittal view of *wnt8b* mRNA, *lef1* mRNA, and *tcf7:GFP* expression in the adult hypothalamus. Yellow box in the left image indicates the region magnified in the right images. Blue line: 3rd ventricle; Red line: Posterior recess. A 12μm transverse cryosection is shown for Lef1 staining in (C), all other panels show single confocal optical sections from ventral views unless otherwise indicated. Scale bars: (A,B) 50μm, (C) 80μm, (D,E) 250μm.

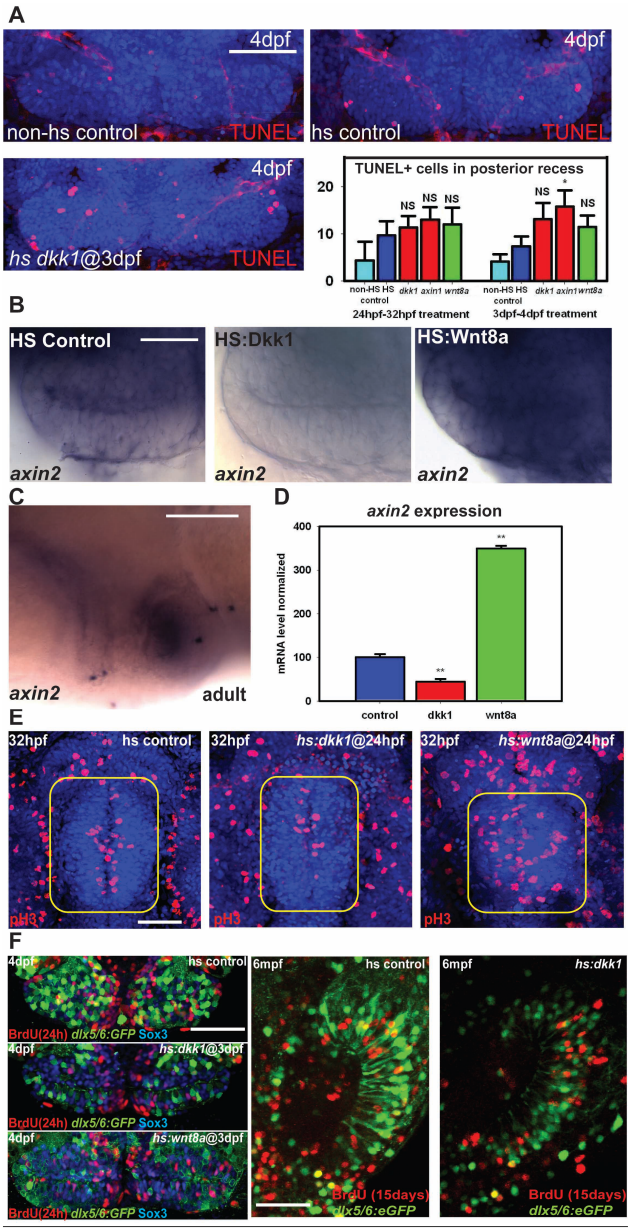
A
4dpf
non-hs control
TUNEL
4dpf
hs control
TUNEL
4dpf
hs dkk1@3dpf
TUNEL
TUNEL+ cells in posterior recess
20
10
0
NS
NS
NS
NS
*
NS
non-HS HS control
dkk1 axin1 wnt8a
24hpf-32hpf treatment
non-HS HS control
dkk1 axin1 wnt8a
3dpf-4dpf treatment
B
HS Control
axin2
HS:Dkk1
axin2
HS:Wnt8a
axin2
C
axin2
adult
D
axin2 expression
mRNA level normalized
400
300
200
100
0
**
**
control
dkk1
wnt8a
E
32hpf
hs control
pH3
32hpf
hs:dkk1@24hpf
pH3
32hpf
hs:wnt8a@24hpf
pH3
F
4dpf
hs control
BrdU(24h) dlx5/6:GFP Sox3
4dpf
hs:dkk1@3dpf
BrdU(24h) dlx5/6:GFP Sox3
4dpf
hs:wnt8a@3dpf
BrdU(24h) dlx5/6:GFP Sox3
6mpf
hs control
BrdU (15days)
dlx5/6:eGFP
6mpf
hs:dkk1
BrdU (15days)
dlx5/6:eGFP

Figure S4 Effects of Wnt signaling on hypothalamic progenitors, related to Figure 3. (A) Ventral confocal optical sections of TUNEL staining at 4dpf, and counts of $TUNEL^{+}$ cells at 32hpf and 4dpf. Only *hs:axin1* expression from 3-4dpf significantly increases cell death compared to heat shock alone. (B) *axin2* in situ hybridization at 4dpf following heat shock at 3dpf. (C) *axin2* in situ hybridization in a mid-sagittal section of the adult hypothalamus. Red oval marks posterior recess. (D) *axin2* mRNA expression levels in the dissected adult hypothalamus following Wnt pathway inhibition or activation for 15 days. (E) Phospho-Histone H3 staining in the 32hpf hypothalamus (yellow squares). (F) Co-localization of BrdU labeling with Sox3 and *dlx5/6:GFP* labeling in the 4dpf and adult posterior recess. Single confocal optical sections are shown in all panels. Scale bars: (A,C,F) 80μm, (B) 25μm, (E) 50μm. Cell counts were collected from ventral maximum intensity confocal Z-projections through 3 individual brains. The entire hypothalamus was counted at 32hpf, and the entire posterior recess was counted at 4dpf. **: $p<0.05$ compared to non-HS control. Error=±SD.

Supplemental Experimental Procedures

Fish strains

The following lines have been described previously: *Tg(TOP:GFP)*^{w25} (Dorsky et al., 2002), *Tg(gfap:GFP)*^{mi2001} (Bernardos and Raymond, 2006), *Tg(hsp701:tcf3-GFP)*^{w26} (Lewis et al., 2004), *Tg(hsp701:wnt8a-GFP)*^{w34} (Weidinger et al., 2005), *Tg(hsp701:dkk1-GFP)*^{w32} (Stoick-Cooper et al., 2007), *Et(T2KHG)*^{nkhg21c} (Nagayoshi et al., 2008), *Tg(1.4dlx5a/-dlx6a:GFP)*^{ot1} (Ghanem et al., 2003), and *Tg(UAS-E1b:NfsB-mCherry)*^{jh17} (Parsons et al., 2009), *Tg(UAS-E1b:Kaede)*^{s1999t} (Scott et al., 2007).

lef1^{zd11} was made by ZFN mutagenesis (described in detail below).

Tg(hsp701:GFP-axin1)^{zd13} was made by inserting a cDNA containing *GFP* fused to zebrafish *axin1* into a pCS2+ backbone vector containing the *hsp70-4* promoter. A stable transgenic line was produced by plasmid injection at the 1-cell stage followed by screening for germline transmission of heat shock-induced GFP expression.

Tg(dlx5/6:mCherry)^{zd14} was made by inserting the *1.4dlx5a/-dlx6a* enhancer/promoter (Ghanem et al., 2003) upstream of an *mCherry* cDNA in a Tol2 destination vector using multisite Gateway cloning (Kwan et al., 2007). A stable transgenic line was produced by plasmid injection with *tol2* mRNA at the 1-cell stage followed by screening for germline transmission of mCherry expression.

Tg(7xTCF-Xla.Siam:GFP)^{ia4} (*TCFSiam:GFP*) was made by inserting the 7xTCF-Siam enhancer/promoter (Maretto et al., 2003) upstream of an *eGFP* cDNA in a Tol2 destination vector using multisite Gateway cloning (Kwan et al., 2007). A stable transgenic line was produced by plasmid

injection with *tol2* mRNA at the 1-cell stage followed by screening for germline transmission of GFP.

The *Et(Gal4VP16; myl7:gfp)*^{zc1066a} enhancer-trap line was generated by plasmid injection with *tol2* mRNA at the 1-cell stage. Potential founders were crossed to *Tg(UAS-E1b:Kaede)*^{s1999t} fish for testing and identified by Kaede expression in embryos. Identified F1 transgenics were crossed to *Tg(UAS-E1b:nfsB-mCherry)*^{jh17} fish and embryos were imaged at 1, 2, and 5 dpf for identification of expression patterns.

Mice

BAT-LacZ (Maretto et al., 2003), *Hes1*^{C2} (Kopinke et al., 2011), *R26R*^{EYFP} (Srinivas et al., 2001), *R26R*^{LacZ} (Soriano, 1999), and *Ctnnb1*$^{lox(ex3)}$ (Harada et al., 1999) mice have been described previously. Floxed and germline β-catenin loss-of-function mice, Ctnnb1^{lox} and Ctnnb1$^{\Delta}$ respectively (Brault et al., 2001), were obtained from Jackson Laboratories. *Hes1*$^{C2/+}$*; R26R*$^{LacZ/+}$ mice were used for lineage tracing experiments. For ß-catenin loss-of-function experiments, *Hes1*$^{C2/+}$*; R26R*$^{EYFP/+}$*; Ctnnb1* $^{lox/\Delta}$ mice (referred to as *Ctnnb1*$^{Hes1\text{-}cKO}$) were compared to control *Hes1*$^{C2/+}$*; R26R*$^{EYFP/+}$*; Ctnnb1* $^{lox/+}$ (*Ctnnb1*$^{Hes1\text{-}het}$) animals. To assess a potential ß-catenin gain-of-function phenotype, crosses were set up to yield *Hes1*$^{C2/+}$*; R26R*$^{EYFP/+}$*; Ctnnb1* $^{lox(ex3)/+}$ (*Ctnnb1*$^{Hes1\text{-}GOF}$) and *Hes1*$^{C2/+}$*; R26R*$^{EYFP/+}$ (*Ctnnb1*$^{Hes1\text{-}ctrl}$) mice. All genotypes included the *R26R*^{EYFP} or *R26R*^{LacZ} reporter allele to follow the fate of recombined cells.

Antibodies

Primary antibodies used were: mouse anti PCNA (Sigma: P8825), rabbit anti Sox3 (Gift from M. Klymkowsky), rabbit anti GFP (Molecular Probes: A11122), mouse anti GFP (Molecular Probes:

A11120), chick anti GFP (Aves Labs: GFP-1020), mouse anti HuC/D (Molecular Probes: A21271), rabbit anti 5HT (ImmunoStar: 541016), rabbit anti GABA (Sigma: A2052), mouse anti BrdU (Sigma: B8434), rat anti BrdU (Abcam: ab6326), rabbit anti BLBP (Abcam: ab32432), mouse anti GFAP (zrf-1; ZIRC [Eugene, OR]), goat anti Sox2 (Santa Cruz: sc-17320), rabbit anti DCX (Abcam: ab18732), rabbit anti Dlx2 (Abcam: ab18188), rabbit anti GFAP (Abcam: ab7260), mouse anti NeuN (Millipore: MAB377), chick anti LacZ (Abcam: ab9361), rabbit anti pH3 (Cell Signaling: 9713), rabbit anti Lef1 (Open Biosystems), rabbit anti LEF1 (Cell Signaling: 2230). Secondary antibodies were obtained from Jackson ImmunoResearch. Hoechst33342 was used to stain cell nuclei.

–

Supplemental References

Bernardos, R.L., and Raymond, P.A. (2006). GFAP transgenic zebrafish. Gene Expr Patterns *6*, 1007-1013.

Ghanem, N., Jarinova, O., Amores, A., Long, Q., Hatch, G., Park, B.K., Rubenstein, J.L., and Ekker, M. (2003). Regulatory roles of conserved intergenic domains in vertebrate Dlx bigene clusters. Genome Res *13*, 533-543.

Kwan, K.M., Fujimoto, E., Grabher, C., Mangum, B.D., Hardy, M.E., Campbell, D.S., Parant, J.M., Yost, H.J., Kanki, J.P., and Chien, C.B. (2007). The Tol2kit: a multisite gateway-based construction kit for Tol2 transposon transgenesis constructs. Dev Dyn *236*, 3088-3099.

Parsons, M.J., Pisharath, H., Yusuff, S., Moore, J.C., Siekmann, A.F., Lawson, N., and Leach, S.D. (2009). Notch-responsive cells initiate the secondary transition in larval zebrafish pancreas. Mech Dev *126*, 898-912.

Scott, E.K., Mason, L., Arrenberg, A.B., Ziv, L., Gosse, N.J., Xiao, T., Chi, N.C., Asakawa, K., Kawakami, K., and Baier, H. (2007). Targeting neural circuitry in zebrafish using GAL4 enhancer trapping. Nat Methods *4*, 323-326.

CHAPTER 3

HIGH-RESOLUTION ANALYSIS OF CENTRAL NERVOUS SYSTEM EXPRESSION PATTERNS IN ZEBRAFISH GAL4 ENHANCER-TRAP LINES

Reprint of: Otsuna, H., Hutcheson, D., Duncan, R., McPherson, A., Scoresby, A., Gaynes, B., Tong, Z., Fujimoto, E., Kwan, K., Chien, C., et al. (2015). High-resolution analysis of CNS expression patterns in zebrafish Gal4 enhancer-trap lines. Developmental Dynamics.

Introduction

As I mentioned in the introduction to Chapter 2, I collaborated with Dr. Hideo Otsuna from Dr. Chi-Bin Chien's lab (Neurobiology and Anatomy Dept.) in order to determine whether any of his Gal4 enhancer trap lines would prove useful in our study of hypothalamic neurogenesis. This did prove fruitful as I came across *Et(Gal4VP16; myl7:gfp)*^{zc1066a}. This line drove expression in tanycytes, a radial glia-like population of cells, in the posterior recess. I was able to characterize, map, and demonstrate the use of their enhancer trap system (Fig. 5), which is why I include this study as Chapter 3. Briefly, in the characterization, I found that this line labeled a population of Wnt-responsive tanycytes. I mapped the insertion to the growth hormone 1 locus. Finally I performed NTR mediated ablations of this line at multiple dosages and time periods to determine its optimal range (data not shown in paper). The work I did helped demonstrate the usefulness of this Gal4/UAS system in their study. It also provided a valuable reagent that became the focus of Rob Duncan's, a fellow graduate student in my lab, thesis research.

DEVELOPMENTAL DYNAMICS 00:00–00, 2015
DOI: 10.1002/DVDY.24260

PATTERNS & PHENOTYPES

High-Resolution Analysis of Central Nervous System Expression Patterns in Zebrafish Gal4 Enhancer-Trap Lines

Hideo Otsuna,[1] David A. Hutcheson,[1] Robert N. Duncan,[1] Adam D. McPherson,[1] Aaron N. Scoresby,[2] Brooke F. Gaynes,[2] Zongzong Tong,[1] Esther Fujimoto,[1] Kristen M. Kwan,[2] Chi-Bin Chien,[1] and Richard I. Dorsky[1]*

[1]Department of Neurobiology and Anatomy, University of Utah, Salt Lake City, Utah
[2]Department of Human Genetics, University of Utah, Salt Lake City, Utah

Background: The application of the Gal4/UAS system to enhancer and gene trapping screens in zebrafish has greatly increased the ability to label and manipulate cell populations in multiple tissues, including the central nervous system (CNS). However the ability to select existing lines for specific applications has been limited by the lack of detailed expression analysis. **Results:** We describe a Gal4 enhancer trap screen in which we used advanced image analysis, including three-dimensional confocal reconstructions and documentation of expression patterns at multiple developmental time points. In all, we have created and annotated 98 lines exhibiting a wide range of expression patterns, most of which include CNS expression. Expression was also observed in nonneural tissues such as muscle, skin epithelium, vasculature, and neural crest derivatives. All lines and data are publicly available from the Zebrafish International Research Center (ZIRC) from the Zebrafish Model Organism Database (ZFIN). **Conclusions:** Our detailed documentation of expression patterns, combined with the public availability of images and fish lines, provides a valuable resource for researchers wishing to study CNS development and function in zebrafish. Our data also suggest that many existing enhancer trap lines may have previously uncharacterized expression in multiple tissues and cell types. *Developmental Dynamics 000:000–000, 2015.* © 2015 Wiley Periodicals, Inc.

Key words: CNS; Gal4; zebrafish; neural circuit; confocal

Submitted 3 December 2014; Accepted 26 January 2015; Published online 00 Month 2015

Introduction

The function of specific neuronal populations forms the basis of most animal behaviors, but in vertebrates many of these populations remain unstudied. Although new resources such as transgenic lines are becoming available (Satou et al., 2013), a detailed analysis of central nervous system (CNS) neuronal and glial identities, morphology, connectivity, and physiological properties has been hampered by a lack of reagents and tools suitable for such approaches. Similarly, developmental studies of CNS cells and nuclei have been limited as many enhancers remain undefined or are not available.

Zebrafish represent an ideal vertebrate system in which to study CNS development and function. Physically small and transparent at larval stages, the entire zebrafish CNS can be imaged at high resolution in whole-mount. A wide range of reporter lines can be used to characterize neuronal shape using fluorescent proteins (Mumm et al., 2006), synaptic connectivity using FP fusions directed to presynaptic or postsynaptic sites (Campbell et al., 2007), or neuronal activity using genetically-encoded calcium indicators such as cameleon (Higashijima et al., 2003) or inverse pericam (Li et al., 2005). One can test whether neurons function in particular behaviors by killing them through conversion of a prodrug to a cytotoxin using nitroreductase (Curado et al., 2007; Pisharath et al., 2007), or by silencing their synaptic output using tetanus toxin light chain (Asakawa et al., 2008). Recently, it has even become possible to activate neurons with light, by expressing the light-gated ionotropic glutamate receptor (Szobota et al., 2007) or the light-activated cation channel, channelrhodopsin-2 (Douglass et al., 2008).

Until recently, only a handful of neuronal populations were accessible to these types of manipulation, either because they could be identified by anatomical position (e.g., retinal cells), or were labeled by one of a few neuron-specific reporter transgenics. In recent years, the use of the Gal4-enhancer trap screens has gained traction in zebrafish. Gal4 is a yeast transcriptional activator that binds to an Upstream Activating Sequence (UAS), leading to transcription of associated genes (Brand and Perrimon, 1993). Used effectively to create neural specific enhancer trap lines in Drosophila (Otsuna and Ito, 2006), the Gal4/UAS system has been adapted to zebrafish (Scheer and Campos-Ortega, 1999; Koster and Fraser, 2001; Scheer et al., 2001; Halpern et al., 2008) using previously identified gene enhancers, or in unbiased

Additional Supporting Information may be found in the online version of this article.
Grant sponsor: NIH; Grant numbers: RO1MH092256 and R01GM098151.
Drs. Otsuna and Hutcheson contributed equally to the work.
*Correspondence to: Richard I. Dorsky, Department of Neurobiology & Anatomy, University of Utah, MREB 401, 20 N 1900 E, Salt Lake City, UT 84112. E-mail: richard.dorsky@neuro.utah.edu

Article is online at: http://onlinelibrary.wiley.com/doi/10.1002/dvdy.24260/abstract

enhancer trap (ET) (Davison et al., 2007; Scott et al., 2007; Asakawa et al., 2008; Ogura et al., 2009) and gene trap (GT) (Asakawa et al., 2008, 2013; Balciuniene and Balciunas, 2013) screens. These screens identified several hundred lines of fish with defined expression patterns, many of which have been made available to the community at large.

As a resource, Gal4 enhancer trap lines still have several shortcomings. First, they represent a small slice of potential expression patterns. Particularly in the CNS, the vast majority of cell populations remain "un-trapped" such that there are no Gal4 or other transgenic lines available with which to manipulate them. Second, in previous screens, several lines have background (nonenhancer driven) expression in heart, muscle, and lens thought to be due to the minimal promoters used in the Gal4 enhancer trap constructs (Scott et al., 2007; Asakawa et al., 2008). This background could obscure neuronal morphology and projections in the retina and spinal cord. Third, and most importantly, the collections that do exist are often difficult to search for desired expression patterns as limited detail in images can omit or obscure signals in specific CNS cell types. It is thus often unclear whether existing enhancer trap lines are truly specific, as higher resolution analysis may uncover cell populations expressing reporter proteins at lower levels.

Using a newly engineered Gal4 enhancer trap construct, we have carried out a screen to address these shortcomings. To maximize the usefulness of our lines, we have greatly expanded the visual documentation such that researchers can more easily find enhancer trap lines with expression patterns of interest. We have produced compound images at several timepoints: 1 day postfertilization (dpf), 2 dpf, and 5–6 dpf, to cover most of the development of the embryonic and larval zebrafish. These compound images are represented as Maximum Intensity Projections where appropriate, so that all structures can be identified in a single image regardless of focal plane. Additionally, we have produced confocal projections through the 5 dpf larval brain and rendered these into three-dimensional (3D) movies (Supplementary Movies S1 and S2, which are available online). Consisting of 98 lines, our screen effectively labels neuronal and glial cells in the CNS, as well as cells and tissues elsewhere in the developing zebrafish. This screen together with our high resolution and 3D data will allow researchers interested in neuronal development and function to identify and use truly appropriate lines, all of which are freely available to the community from ZFIN/ZIRC.

Results and Discussion

Generation of Gal4 constructs for use in enhancer trap screens

For our screen, we engineered new Tol2 based Gal4 enhancer trap constructs (Fig. 1A, Genbank accession #KC800697). The full length Tol2 was replaced with a truncated miniTol2 (Balciunas et al., 2006). To minimize nonspecific background expression, we used a short minimal promoter consisting of an 11 bp fragment containing an adenovirus *E1b* TATA box, followed by a 30 bp fragment spanning the transcriptional start site of the carp *beta-actin* gene (Koster and Fraser, 2001). This promoter produces transient background expression in the notochord of some lines at 24 hpf stage (42 lines), which disappears by day 2 in most lines. Otherwise, our Gal4 lines showed no reproducible background expression patterns. We also used an optimized Gal4-VP16 (413–470) fusion for transcriptional activation (Ogura et al., 2009). Two additional Gal4 enhancer trap constructs were created in which Gal4 was fused to the FF activation sequence (Genbank accession #KC800698 and #KC800699). This activation sequence uses two VP16 transcription activation modules and has previously been used without any reports of toxicity (Asakawa et al., 2008). Ten pilot lines were established using these constructs (*zc1080A, zc1081A, zc1082A, zc1083A, zc1084A, zc1087A, zc1088A, zc1090A, zc1091A, and zc1093A*), but because we did not observe any appreciable advantages relative to our Gal4-VP16 construct in terms of expression level, we did not continue to use it in our screen. All other lines were created with the Gal4-VP16 (413–470) construct.

Finally, using the zebrafish Tol2kit (Kwan et al., 2007), we engineered a cardiac specific *myl7* reporter cassette driving either eGFP or TagRFP (a monomeric red fluorophore with 555 nm excitation maximum, Evrogen). This marker allowed us to rapidly screen for embryos that contained a successful Tol2 integration. One must note, however, that the presence or absence of the *myl7:FP* marker does not indicate the number of integrations in F0 fish. Furthermore, the number of inherited Gal4 expression patterns, indicative of successful enhancer traps, is not equivalent to transgene insertions.

Isolation of 98 Lines, Nearly All With Expression Patterns in the CNS

A screen was performed by mating wild type (TU) fish and injecting F0 embryos at the 1-cell stage with 25 pg of Gal4 enhancer trap construct DNA (Fig. 1a) and 25–50 pg transposase mRNA (Kwan et al., 2007). F0 fish were raised to maturity and mated to *UAS* reporter fish to produce F1 offspring. In most cases, the UAS-reporter fish *Tg(UAS-E1b:NTR-mCherry)*^{c264}, (Davison et al., 2007) was used. Occasionally, either UAS-reporter fish *Tg(UAS-E1b:Kaede)*^{s1999t} (Davison et al., 2007) or *Tg(5xUAS:eGFP)*^{nkuasgfp1a} (Asakawa et al., 2008) was used instead. F1 embryos exhibited one of the following patterns: (1) no expression, most likely indicating lack of germline mTol2 integration; (2) heart expression only, indicating vector integration but no enhancer trap; (3) heart expression and a *UAS*-reporter expression pattern, indicating a successful enhancer trap; or (4) heart expression and multiple *UAS*-reporter expression patterns indicating multiple successful enhancer traps. Importantly, all lines exhibiting tissue-specific *UAS*-reporter expression also had expression of the heart marker, indicating that it represents an effective tool to screen for transgene insertions.

Based on the interests of our laboratory, 86 F1 lines were established that expressed a *UAS*-driven reporter in unique patterns that included the CNS. As seen in Table 1, use of our Gal4 enhancer trap construct resulted in a very high rate of single enhancer traps as defined by expression of a single pattern (67%). Most of the remaining F1 lines had two independent expression patterns, with a small number exhibiting three or four patterns (Table 1). After outcrossing, we generated 120 individual Gal4 enhancer trap lines. Several lines were lost as we were unable to maintain them or obtain sperm for cryopreservation. Thus, we were left with 98 unique lines, almost all of which show expression in CNS tissues under the control of trapped enhancers (Tables 2 and 3).

Imaging of Expression Patterns

Complex expression patterns from successful enhancer traps are often difficult to capture in a single image. Images obtained from

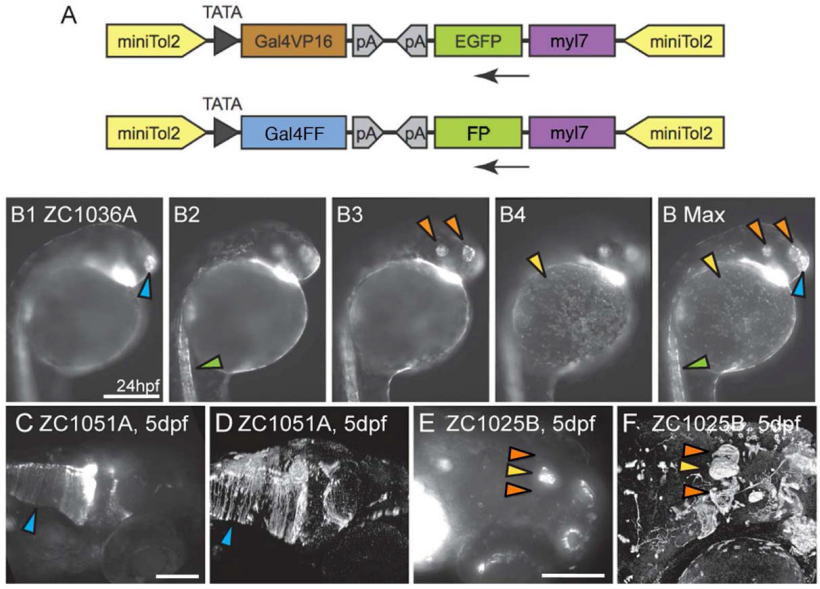

Fig. 1. Gal4 enhancer trap constructs and imaging. **A:** Enhancer trap constructs used to generate all lines. **B1-B Max:** To convey as much information as possible, compound microscopic images were taken at multiple depths (B1–B4) and used to generate Maximum Intensity Projections (B Max) in which signal from multiple focal depths is visible. Arrowheads mark the olfactory placode (blue), spinal neurons (green), otic vesicle and retina (orange) and epithelial cells (yellow). Images B1–B Max are lateral views. **C–F:** Confocal images enhance fine details relative to compound microscopic images. Glial endfeet are clearly visible in the confocal image (D, Arrowhead) but are not clear in the compound scope image (C, Arrowhead). Habenulae are visible in confocal (F, Orange arrowheads) but not compound (E, Orange arrowheads) image. (E,F) Pineal gland marked by yellow arrowhead. Images C–F are dorsolateral views. Scale bars = 250 μm in B1–B MAX; 250 μm in C,D; 100 μm in E,F.

a stereomicroscope lack resolution while images obtained from a compound microscope lack the necessary focal depth for a vertebrate organism. We attempted to address these problems by acquiring compound serial images at different focal depths, and then merging them into maximum intensity projections. As seen in Figure 1 (B1-Bmax), we were able to create a single image that captures all the expression elements from a wide range of focal planes. Thus, more data can be presented in fewer images, facilitating the search for desired lines and expression patterns.

While intensely labeled structures are clearly identifiable in both compound and confocal images (Fig. 1C–F), compound images often fail to capture less intense expression typical of individual cells and axons, particularly in live embryos (Fig. 1C–F, arrowheads). Thus, while the compound image in Figure 1C shows expression in hindbrain cells, the confocal images allow clear identification of glial expression as indicated by mCherry+ glial end feet (Fig. 1D). Similarly, other structures only weakly labeled are often missing in the live-embryo compound image. In Figure 1E and 1F, the epiphysis (yellow arrowhead) is clearly visible. The habenula, located laterally on both sides of the epiphysis (orange arrowheads) is only visible in the antibody stained confocal image (Fig. 1F).

Lines Exhibit a Wide Range of Temporal and Spatial Expression Patterns

As with prior Gal4 enhancer trap screens, we observed expression in a wide variety of tissues. Our focus being on generation of lines that are useful for analysis of CNS development and function, a majority of the lines that we isolated and maintained exhibit expression in this tissue (89/98), including all divisions of the brain and spinal cord. Sensory elements of the peripheral nervous system (PNS; neuromasts, olfactory epithelium) were also trapped. Many of the lines also showed expression in non-neural tissues including the skin epithelium, vasculature, and musculature (Table 2). Additionally, we were surprised to find many lines with expression in at least a subset of radial glial cells. For instance, 11 lines showed expression in retinal Müller glial cells, 15 lines had expression in other CNS radial glia, and 11 lines showed expression in both cell populations (Table 2). Whether this represents a natural bias toward glial gene expression in the zebrafish genome, an inherent bias in our Gal4 construct, or a reflection of the expertise of our laboratory in identifying this cell type is unclear. Regardless, the presence of so many radial glial-targeted lines opens up exciting possibilities to

TABLE 1. Rates of Multiple Expression Patterns Derived From Enhancer Trap Screen Using mTol2 Enhancer Trap Construct[a]

Expression patterns derived from Gal4 ET screen		
	Initial F1	Outcrossed F3
Single pattern	58 (67%)	58
Double pattern	23 (27%)	46
Triple pattern	4 (5%)	12
Quadruple pattern	1 (1%)	4
Totals	86	120

[a]Number and frequency of single, double, triple, and quadruple patterns in F1 lines exhibiting reporter expression, and resulting number of unique enhancer trap lines after outcrossing to F3 generation.

TABLE 2. Tissue-Specific Expression Patterns Derived From Gal4 Enhancer Trap Screen

Expression by tissue			
CNS	No. of lines	Other	No. of lines
Amacrine cell	3	Blood vessel	2
Anterior commissure	2	Epidermal cells	30
Epiphysis	8	Extraocular muscle	10
Forebrain	28	Fin	4
Glia	26	Hatching gland	1
Habenula	5	Lateral line	8
Hindbrain	39	Lens	1
Hypothalamus	13	Muscle	35
MHB	7	Notochord	42
Midbrain	43	Pancreas	2
Muller glia	22	Pronephros	1
Olfactory placode/bulb	31	Tail	3
Otic vesicle	12	Vasculature	8
Pituitary	1		
Retina	43		
RGC	4		
Rohon-Beard cells	3		
Spinal neuron	29		
Tectum	22		
Trigeminal ganglion	4		

study glia and glial-neuronal interactions in the developing, functioning, or regenerating vertebrate CNS.

Because expression patterns are often spatially complex and can be transient in development, individual images at single developmental timepoints are not always informative. To make our screen more useful to the community, we chose to obtain images at three different developmental timepoints: 24 hpf, 48 hpf, and 5 or 6 dpf. We found many examples of expression patterns in which a tissue was labeled throughout development. For example line *1037B* shows expression in spinal neurons at all three timepoints (Fig. 2A–C). In contrast, other lines show expression that is absent at earlier timepoints but initiates or expands at later stages. *zc1009A* shows labeling of neuromasts starting at 48 hpf and expanded expression by 5 dpf when additional neuromasts have been deposited (Fig. 2D–F). Additionally, some lines such as *zc1030A* show strong expression at 24 and 48 hpf but greatly reduced expression by 5 dpf (Fig. 2G–I), while others such as *zc1032A* show transient expression only at a single timepoint (Fig. 2J–L). By analyzing reporter expression at multiple timepoints, we were thus able to more accurately capture dynamic Gal4 expression profiles, something that is particularly useful for developmental studies.

Even within an individual Gal4 enhancer trap line, we observed variable expression patterns. By crossing *zc1016B* to a line simultaneously expressing both *Tg(5xUAS:eGFP)*^{nf82} and *Tg(UAS-E1b:NTR-mCherry)*^{c264}, we can show this variability in a single animal (Fig. 2M–O). Both reporters were expressed in skin epithelial cells, but the majority of cells were labeled for only one reporter, clearly illustrating the variegation associated with *UAS* reporters (Davison et al., 2007; Scott, 2009; Akitake et al., 2011). Thus, in cases where the cells targeted by a specific enhancer trap need to be precisely defined, it is critical that either the Gal4 line be crossed to several different *UAS* reporters or the location of the insertion be mapped to better define the trapped enhancer. Importantly though, despite this background of variegation, we did not observe variability in the tissues or cell types expressing Gal4-driven reporters between individual embryos or multiple generations of a given line. We therefore believe that our Gal4 insertions are stable and reproducible.

3D Confocal Imaging Shows Detailed Neural Expression

Although maximum intensity projections greatly increase the amount of information one can display in a single image, for complex three-dimensional structures such as the CNS these images are often still insufficient. Single-plane images do not convey three-dimensional information, nor do they allow the viewer to isolate and follow neuronal projections. To overcome this problem and make our screen more useful for study of the CNS, we have used confocal imaging together with the 3D rendering program FluoRender (Wan et al., 2009). The 5 dpf embryos were stained with antibodies to the respective UAS reporter (generally mCherry), and ToPro3 to label nuclei and provide a counterstain for better anatomical localization of the expression region. Rendered 3D reconstructions show highly detailed expression patterns in the CNS including the habenula, telencephalon, and ventral tectum (Fig. 3A–C). In the retina, our screen has isolated lines with expression in a wide range of cell types including bipolar cells, photoreceptors, amacrine cells, Müller glia, and ganglion cells (Fig. 3D–H). In the brainstem, examples of lines we have isolated show expression in radial glia, ventral motor neurons, and the rostral cerebellum (Fig. 3I–K). In many cases, the morphology of substructures such as glial end feet, arborizations of individual cells, and axonal projections is clearly visible.

To fully take advantage of our data, rotatable 3D reconstructions were created and saved in MPEG file format. This allows us to convey with even greater clarity the types of cells labeled, their position in the CNS, and their axonal projections. For instance, in

TABLE 3. Full List of Enhancer Trap Lines Deposited With ZIRC/ZFINa

Line	CNS	Other
1000A	retina, MHB	Notochord, epidermal cells
1002A	olfactory placode/bulb	Lens, muscle
1003A	forebrain, midbrain, habenula retina, olfactory placode/bulb	Notochord, epidermal cells Extraocular muscle, fin
1004A	Amacrine cells, hindbrain retina, midbrain	Epidermal cells, notochord Trigeminal ganglion, muscle
1006A	hindbrain, retina, otic vesicle	Muscle
1007A	spinal neurons, hindbrain	Muscle
1008A	Amacrine cells, hypothalamus midbrain, otic vesicle, retina	Epidermal cells Muscle, lateral line
1009A	midbrain, hindbrain olfactory placode/bulb	Lateral line, muscle, epidermal cells Blood vessels, pancreas, fin
1010A	olfactory placode/bulb, pituitary	Epidermal cells, notochord, hatching gland
1011A		Epidermal cells
1012A	midbrain, tectum, otic vesicle hindbrain, glia, Muller glia	Epidermal cells Notochord, blood vessel
1013A	otic vesicle amacrine cell, retina	Muscle, trigeminal ganglion Epidermal cells
1015A	Muller glia, retina, otic vesicle	Muscle, epidermal cells
1016A	retina, RGC, Muller glia Rohon-Beard cells, otic vesicle olfactory placode/bulb	Fin
1016C	olfactory placode/bulb, glia, midbrain spinal neuron, hypothalamus, tectum hindbrain, forebrain, Muller glia	Notochord Muscle Vasculature
1016D	Muller glia, glia	Epidermal cells, notochord, hatching gland extraocular muscle
1017A	spinal motor neuron, midbrain	Epidermal cells
1018A	retina, forebrain, hindbrain	Notochord, epidermal cells, extraocular muscle olfactory placode/bulb, glia
1019A	forebrain, retina, RGC midbrain, tectum, hindbrain	Lateral line
1019B	spinal neuron, Muller glia	
1020A	spinal neuron	Muscle, trigeminal ganglion Notochord
1020B	forebrain, Muller glia, retina midbrain, hindbrain, glia	
1021A	otic vesicle, hindbrain	Epidermal cells, vasculature
1022A	olfactory placode/bulb	Notochord
1022B	midbrain, hypothalamus anterior commissure, MHB olfactory placode/bulb	
1023A	midbrain, forebrain, retina, Muller glia	Epidermal cells, muscle
1023B	midbrain, tectum, retina, forebrain, olfactory placode/bulb, hindbrain, MHB	Muscle
1023D		Notochord, vasculature, epidermal cells, fin
1024A	midbrain, retina, bipolar cells	
1025A	hypothalamus, retina, glia, hindbrain tectum, midbrain, forebrain	Notochord
1025B	anterior commissure, retina, habenula olfactory placode/bulb, epiphysis	Epidermal cells Muscle
1025D	olfactory placode/bulb	Epidermal cells, notochord
1026A	epiphysis, midbrain, hypothalamus glia, olfactory placode/bulb, forebrain	
1029E	glia, tectum, hypothalamus	
1030A	Muller glia, spinal neuron olfactory placode/bulb, retina	Notochord
1031A	Muller glia, glia, spinal neurons tectum, midbrain, forebrain, hindbrain	
1032A	glia, olfactory placode/bulb midbrain, forebrain, spinal neurons	Muscle Epidermal cells

TABLE 3. *Continued*

Line	CNS	Other
1033A	glia, midbrain, MHB, RGC, hindbrain	Pronephros, lateral line
1034A	forebrain, hindbrain, midbrain	Notochord
	spinal neuron, habenula	Extraocular muscle
1035A	olfactory placode/bulb, retina	Vasculature, epidermal cells
1036A	olfactory placode/bulb	Epidermal cells, muscle, notochord
1037A		Extraocular muscle, muscle, notochord
1037B	spinal neuron, Rohon-Beard cells	Trigeminal ganglion
1037C	glia, midbrain, Muller glia, retina hindbrain, tectum, forebrain	Muscle
1038A	glia, olfactory placode/bulb	Epidermal cells
	retina, Muller glia	Pancreas
1039A	Forebrain, midbrain, retina, hindbrain, Muller glia, hindbrain, glia Spinal neurons, hypothalamus	Notochord
1039B	Hypothalamus, spinal neurons, retina, tectum, midbrain, hindbrain, forebrain	
1040A	Spinal neuron	Muscle, notochord
1040B	Spinal neurons, retina,	Vasculature
	Rohon-Beard cells	Notochord
1041A	Olfactory placode/bulb	Muscle, notochord
1042A	Forebrain, midbrain, retina, hindbrain, hypothalamus, spinal neurons	
1044A	Glia, midbrain, hindbrain, hypothalamus, spinal neurons	
1046A	Spinal neuron	Vasculature
1047A	Olfactory placode/bulb,	Epidermal cells
	epiphysis, hindbrain, otic vesicle,	Muscle
	spinal neurons, forebrain	Notochord
1048A	Retina, Muller glia,	Lateral line,
	olfactory placode/bulb	extraocular muscle
1049A	Otic vesicle	
1050A	Spinal neurons, midbrain, retina, glia, tectum, olfactory placode/bulb	Notochord
1051A	Midbrain, glia MHB, hindbrain	
1052A	Tectum, midbrain	
1052B	Forebrain, midbrain	Muscle, notochord
1053A	Glia, Muller glia, midbrain, forebrain, spinal neurons, hindbrain, otic vesicle	Notochord
1054A	Midbrain, spinal neurons, tectum	
1055A	Forebrain, midbrain, tectum, hindbrain, spinal neurons, retina, RGC	
1055B	Otic vesicle, Muller glia, retina, glia	Extraocular muscle, epidermal cells
1056A	Epiphysis, hindbrain, spinal neurons	Extraocular muscle, notochord
1057A	Retina, olfactory placode/bulb tectum, midbrain, spinal neuron	Nnotochord
1060A	Olfactory placode/bulb, glia	Lateral line, notochord, muscle
1062A		Lateral line, notochord
1062B	Forebrain, midbrain, hindbrain, spinal neuron, glia	
1063A	Forebrain, hypothalamus, hindbrain,	Notochord
	Muller glia, retina, epiphysis, midbrain	Muscle
1063B	Olfactory placode/bulb	
1065A	Tectum, midbrain, hindbrain, forebrain,	Muscle
	olfactory placode/bulb, glia	Notochord
1066A	Olfactory placode/bulb, hypothalamus, forebrain, midbrain, tectum	
1067A	Olfactory placode/bulb	Notochord, tail, extraocular muscle
1068A	Dorsal retina, Muller glia, midbrain, forebrain, otic vesicle, habenula	Notochord
1069A	Retina, Muller glia	Muscle, extraocular muscle

TABLE 3. *Continued*

Line	CNS	Other
1070A	Midbrain, spinal neurons, tectum, glia	Notochord
1071A	Midbrain, hindbrain	Muscle
1072A		Vasculature, notochord, epidermal cells
1074B	Retina, Muller glia	Vasculature, epidermal cells
1075A	Glia, tectum, midbrain	Notochord
1076A	Forebrain, retina, hindbrain	Notochord, muscle, tail
1077A	Retina, hindbrain, MHB	Notochord, muscle
1078A	Tectum	
1080A	Hindbrain, tectum, glia	
1081A	Retina, Muller glia	Muscle
1082A	Hindbrain	Muscle
1083A	Retina, Muller glia	
1084A	Retina, hindbrain	Epidermal cells
1085A	Epiphysis	Epidermal cells
1086A	Olfactory placode/bulb	Muscle, epidermal cells
1087A	Glia	Tail, muscle
1088A	Retina, epiphysis, hindbrain Olfactory placode/ bulb, hypothalamus	Muscle
1090A	Hindbrain	
1091A		Notochord
1093A		Notochord
1094A	Forebrain, midbrain Hindbrain, spinal neuron	

Figure 4, line *zc1022B* shows clear expression in the hypothalamus. When viewing an MPEG of the 3D reconstruction of confocal images for this line, it becomes clear that the expressing cells are located in the ventral portion of the hypothalamus, with axonal projections that extend between a more dorsal level of the hypothalamus and a small cluster of cells located in the telencephalon (Supplementary Movie S1, MPEG of *zc1022B*). Line *zc1016C* shows expression clearly in neurons of the telencephalon and tectum, while expression in the hypothalamus is obscured by hindbrain expression in the dorsal view (Fig. 3B). When viewed in MPEG format, the 3D rendering shows reporter-expressing cells are in the ventral tectum, and they project axons to the ventrolateral border of the neuropil layer (Supplementary Movie S2, MPEG of *zc1016C*). Likewise, the labeled telencephalon neurons whose cell bodies lay along the dorsal midline extend axons toward the lateral border of the telencephalon. By rotating the 3D reconstruction, the hypothalamic expression in the ventral CNS is also clearly seen as two clusters of cells visible at the very bottom of the image (Supplementary Movie S2). Analysis of images in 3D thus greatly enhances the ability to determine exactly where in the CNS a given set of cells resides and projects.

Use of Lines to Define and Manipulate CNS Cells

Within the CNS, many structures contain a complex assortment of cell types and functions. For instance, the hypothalamus contains neurons that respond to several different neurotransmitters, and both receive and send information to a wide range of targets. Investigating the development and circuitry of the hypothalamus requires genetic tools that are specific to functional and anatomical subsets of neurons. In this screen, we have identified *zc1022B*, *zc1016C*, and 7 other lines that express the UAS reporter in the hypothalamus under the control of trapped enhancers (Fig. 4). Expression patterns range from just a few individual neurons to large regional subsets of the hypothalamus. The *zc1066A* allele shows expression in the posterior recess of the hypothalamus. We have found that this enhancer trap marks radial glia based on coexpression with BLBP and Glutamine synthetase (Wang et al., 2012). We have also used this allele to perform cell ablations, by crossing to fish expressing *Tg(UAS-E1b:NTR-mCherry)*^{c264}. Following treatment with the pro-drug metrodinazole (Mtz), almost all labeled radial glia in the hypothalamus were ablated (Fig. 5A,B), illustrating the efficacy of this line as a genetic driver. Because of the relatively limited expression pattern of the allele (Fig. 5C), the enhancer trap can thus be used to selectively manipulate hypothalamic radial glia. Using an inverse-polymerase chain reaction (PCR) strategy we mapped the insertion to only one position, approximately 800 bp upstream of the *growth hormone 1* (*gh1*) gene start site (Fig. 5D, red box). Of interest, the resulting enhancer trap does not recapitulate the *gh1* expression pattern, which is limited to the pituitary. This serves as a cautionary note that enhancer-trap lines may not necessarily reflect the expression of even closely neighboring genes.

Expression in Nonneural Tissues

Although the focus of our work is centered on the CNS, the unbiased nature of enhancer trap screens is such that other expression patterns are also trapped. Among tissues in which we have observed expression are somatic muscle, including slow ocular muscles (*zc1037A*, Fig. 6A,B), vasculature of the head and trunk (Fig. 6C,D), developing pronephric tubules (Fig. 6E), and glia of the lateral line (Fig. 6F). For some, this nonneural expression will be useful. Recently, *zc1044A* was used for experimental

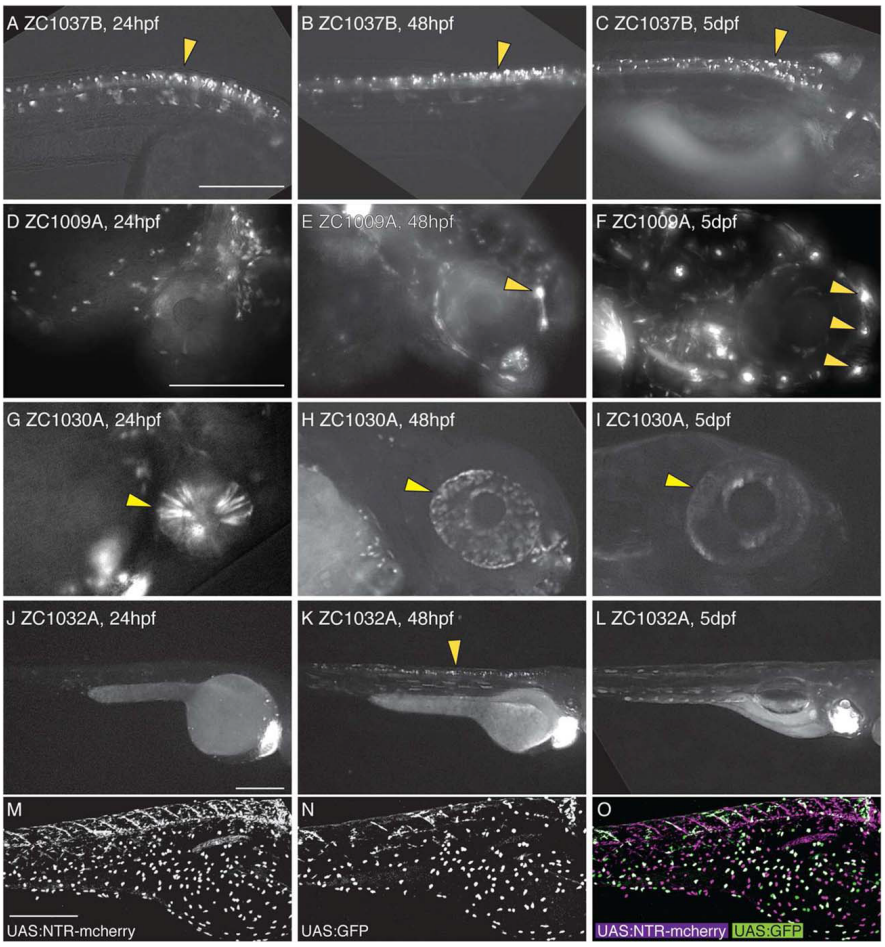

Fig. 2. Dynamic temporal expression patterns in enhancer trap screen. Compound images taken at 24 hpf (**A,D,G,J**), 48 hpf (**B,E,H,K**), or 5 dpf (**C,F,I,L**) show examples of neural expression that is maintained at all ages (A–C), is activated over time (D–F), is inactivated over time (G–I), or is only present at one timepoint (J–L). Arrowheads mark spinal neurons (A–C, K), lateral line neuromasts (E,F), and the eye (G–I). UAS reporters exhibit transgene-specific variegation, leading to partially overlapping but distinct expression patterns in a single animal (**M–O**). All images are lateral views. Scale bar = 250 μm for A–C; 250 μm in D–I, 250 μm in J–L; 300 μm in M–O.

analysis of defects in epidermal cell extrusion (Eisenhoffer et al., 2012).

Conclusions

Our enhancer trap screen has produced 98 lines with unique expression patterns, many of which encompass portions of the nervous system. Maximum intensity projections at multiple developmental stages and high resolution 3D image rendering were used to create a database of unparalleled detail, greatly enhancing the usefulness of this database to the community. However, with the ability to visualize enhancer trap expression at increased resolution comes the observation that many patterns are not specific to a single cell population even within a given

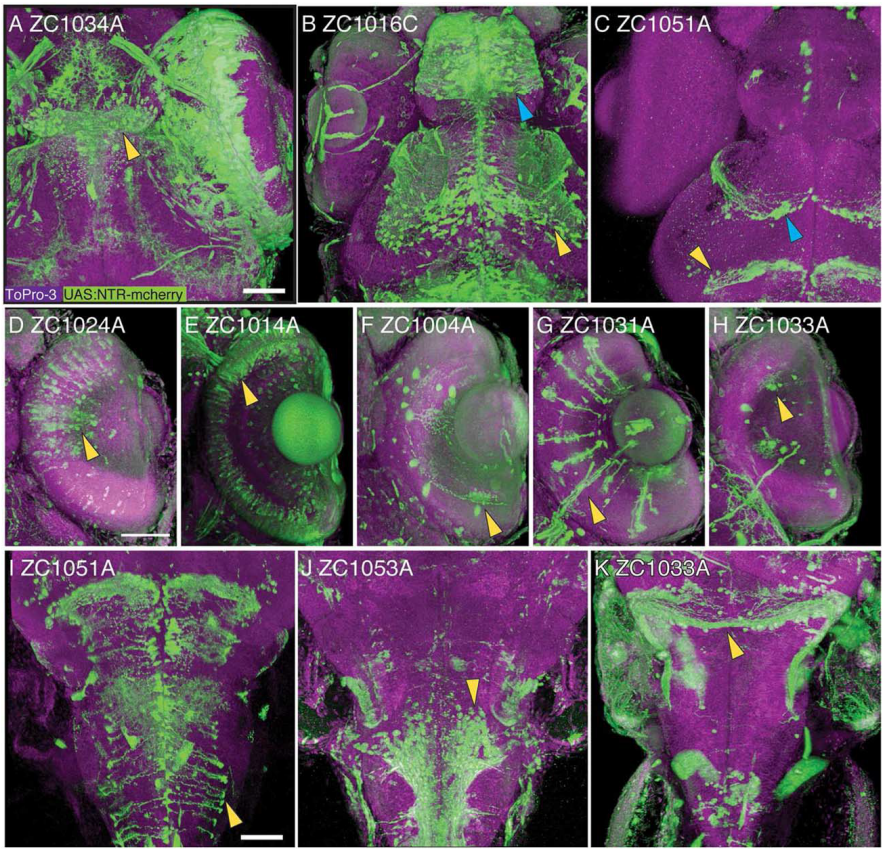

Fig. 3. Confocal 3-D reconstruction images of 5 dpf embryos. Rostral CNS expression patterns are visible in the habenula (**A**, arrowhead), the telencephalon (**B**, blue arrowhead) and ventral tectum (B, yellow arrowhead), glial cells in the tectum (**C**, blue arrowhead) and midbrain–hindbrain boundary (C, yellow arrowhead). Expression is visible in major classes of retinal neurons including bipolar cells (**D**), photoreceptors (**E**), amacrine cells (**F**), Mueller glia (**G**), and ganglion cells (**H**). In the brainstem, expression is visible in radial glia (**I**), ventral neurons (**J**), and the rostral cerebellum (**K**). All images show UAS reporter (green), ToPro3 nuclear stain (magenta), and show dorsal view, with D–H showing a section through the retina. Scale bar = 50 μm.

tissue. This finding leads to the cautionary speculation that many previously characterized enhancer trap lines may also exhibit broad low-level expression in additional tissues and cells. Thus, care should be taken to confirm the specificity of expression, tools should be used to limit the function of Gal4-driven effector molecules where possible, and experimental results should be interpreted with this consideration.

All lines listed in Table 3 will be stored as sperm stocks at ZIRC, and the entire database of images available at ZFIN (http://zfin.org/action/figure/all-figure-view/ZDB-PUB-130724-1). These lines, together with past screens and ongoing enhancer trap efforts will produce an increasingly large number of useful lines. As the number of documented Gal4 lines available to the scientific community increases, it will become increasingly possible to investigate previously intractable questions in vertebrates.

Experimental Procedures

Cloning of Transgenic Constructs

Gal4 enhancer trap constructs were created using multisite Gateway cloning to insert 5′, middle, and 3′ clones into mTol2 backbones. For *ET(E1bTATA;Gal4VP16;mTol2CG3)*(Genbank accession #KC800697), the 5′ clone encoded a TATA basal promoter, the

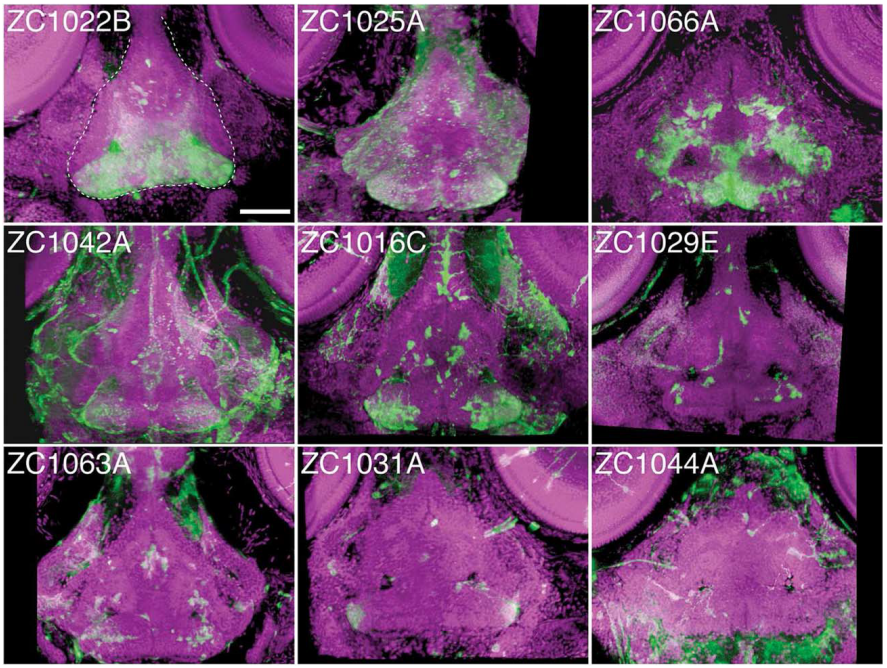

Fig. 4. Individual enhancer traps drive various hypothalamic expression patterns. The 3D reconstructed confocal images, dorsal view, of 5 dpf whole-mount embryos stained for UAS reporter (green) and counterstained with ToPro-3 for nuclei (magenta). Partial 3D reconstruction of these images has been limited to ventral confocal planes to highlight hypothalamic expression while removing more dorsal expressing cells. Dashed white line in panel zc1022B outlines the hypothalamus. Scale bar = 50 μm.

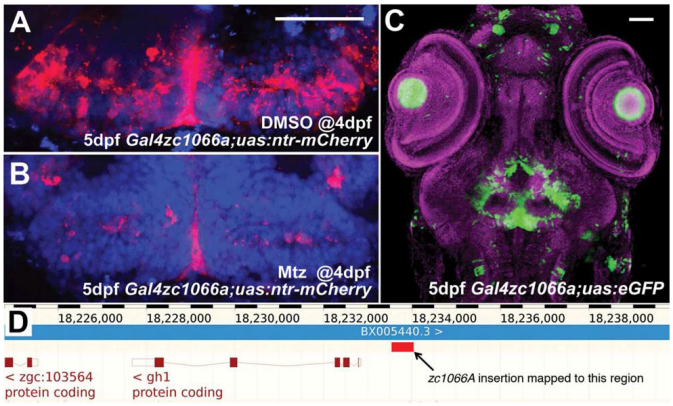

Fig. 5. Use and characterization of a single enhancer trap line. **A:** Line *zc1066a* drives expression of NTR-mCherry in hypothalamic radial glia. **B:** Following incubation in metronidazole for 24 h, most mCherry+ cells are ablated and only debris remains. **C:** A confocal projection through the entire head of a *zc1066a* embryo at 5 dpf shows the specificity of this enhancer trap expression pattern. **D:** Using inverse-PCR, we have mapped the insertion to a genomic region immediately upstream of the *gh1* mRNA. Scale bars = 50 μm.

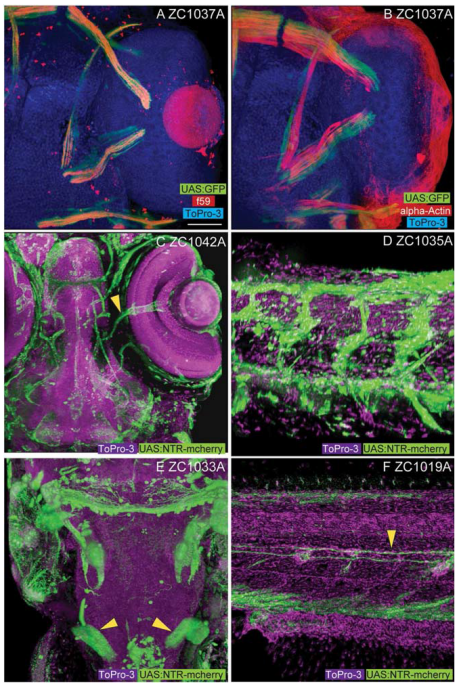

Fig. 6. Non-CNS enhancer trap expression patterns. Among the non-CNS tissues represented in our screen, line *zc1037A* shows expression in slow (**A**, f59 positive) but not fast (**B**, alpha-actin) extraocular myofibers. Vascular expression is visible in both the head (**C**, arrowhead marks central retinal vessels, *zc1042A*) and body (**D**, *zc1035A*). **E:** Labeling of the developing pronephros (arrowheads) is visible in line *zc1033A*. **F:** Labeling of lateral line glial fibers (arrowhead) is visible in line *zc1019A*. Images A, B, C, and E show dorsal views. Images D and F show lateral views. Scale bar = 50 μm in A–F.

middle clone encoded the Gal4VP16(413–470) fusion, and the 3′ clone encoded the polyadenylation sequence. Gateway LR recombination was performed to insert these clones into the pDestmTol2CG3 vector that contains a *myl7* promoter/enhancer driving eGFP in reverse orientation (Kwan et al., 2007). *ET(E1bTATA:Gal4FF;mTol2CG3)* (Genbank accession #KC800698) and *ET(E1bTATA:Gal4FF;mTol2CR3)* (Genbank accession #KC800699) were created in a similar manner except that a Gal4FF fusion was used, and the pDestmTol2CR3 vector contains a TagRFP reporter driven by the *myl7* promoter/enhancer, placed on the opposite strand.

Injections and Establishment of Lines

All fish were used and handled in accordance with University of Utah IACUC guidelines. Wild type TU strain fish were crossed to generate embryos. Injections were performed at the 1-cell stage by injecting 25 pg of enhancer trap DNA with 50 pg of Transposase mRNA. Injected F0 embryos were raised until maturity and then crossed to UAS-reporter lines. F1 embryos were scored for the presence or absence of both the heart specific *myl7* reporter of transgenic integration as well as novel UAS-reporter expression patterns. F1 embryos positive for UAS-reporter expression were raised and outcrossed to the F3 generation to isolate individual expression patterns in cases where multiple productive enhancer trap integrations occurred in the same fish. Individual enhancer trap lines were given allele designations *zc1000 – zc1094*. At the end of each allele, an A, B, C, or D was appended to indicate that a specific line was the 1st, 2nd, 3rd, or 4th line obtained from a given F0 founder after outcrossing. Thus, both *zc1062A* and *zc1062B* were derived from the same F0 founder, but were isolated through outcrossing as separate insertions/enhancer traps. Outcrossed Gal4 lines were propagated with crosses to *Tg(5xUAS:eGFP)*^{zf82} (Asakawa et al., 2008) and *Tg(UAS-E1b:NTR-mCherry)*^{c264} (Davison et al., 2007).

Imaging and Analysis

Stable enhancer trap lines were analyzed first on an Olympus SZX16 fluorescent dissecting microscope to validate successful outcrossing/isolation of single enhancer traps. Live embryos were imaged at 4× to 20× magnification on an Olympus BX51WI fluorescent compound microscope at 1 dpf, 2 dpf, and 5 dpf to document expression patterns over a developmental timecourse. Embryos were embedded in FEP tubes (Cole-Parmer #EW-06406-60) and sealed with water to optically clear the tube. Confocal imaging was performed using an Olympus FV1000 confocal microscope with a 30× silicon oil objective (UPLSAP030xS NA1.05). Antibody stained samples were embedded in 100% glycerol. The 3D reconstructions were performed with FluoRender using 3-degree increments throughout a full 360-degree rotation. Serial images were imported into ImageJ and exported as non-compressed AVI movies. Movies were compressed by using TMPGEnc 4.0 Xpress (Pegasys).

Immunostaining

For confocal imaging, 5–6 dpf embryos were fixed for 2 hours at room temperature (4% paraformaldehyde), washed with phosphate buffered saline (PBS)/Triton (0.5% Triton), permeabilized with 0.5 U Dispase (Gibco #17105-041) for 45 min, then blocked with goat serum for 30 min. Next, embryos were incubated in primary antibodies: f59 (Developmental Studies Hybridoma Bank), 1:10; DsRed Polyclonal Antibody (#632496 - Clontech, 1:300; alpha-actin – Sigma #A2547), 1:100; in block for 3 days at 4°C. Embryos were washed in PBS/Triton for 5 hours, then incubated in secondary antibodies and counterstain: Cy3-AffiniPure Goat Anti-Rabbit IgG (H+L) (111–165–003, Jackson) 1:300; Alexa Fluor® 488 Goat Anti-Mouse IgG (H+L) (A-1100, Life Technologies). 1:300; and TO-PRO®-3 Iodide (642/661) (T3605, Life Technologies), 1:300, for 3 days at 4°C. Following staining, embryos were washed for 5 hr in PBS/Triton, cleared in 50:50 glycerol/PBS for 2 hr at 4°C, and cleared in 80:20 glycerol/water overnight. At this point, embryos were stored at −20°C until imaging.

Cell Ablation

For cell ablations, 4 dpf fish were placed in media containing 1 mM Metronidazole (1 M stock in dimethyl sulfoxide [DMSO]; Sigma) for 24 hr. Control fish were placed in media containing an

equivalent concentration of DMSO. After fixation, dissected whole brains were imaged for native mCherry expression using confocal microscopy.

Insertion Mapping

Mapping by inverse PCR was carried out by phenol:chloroform extraction of genomic DNA from F3 generation embryos. Initial PCR used primers Tol2INV5A (5′-CTTGAGTATTAAGGAAG-TAAAAGT-3′) and Tol2INV5B (5′-TTACTCAAGTAAGATTC-TAGCC-3′) and was followed by a nested PCR with primers Tol2INV6A (5′-AAGCAAGAAAGAAAACTAGAG-3′) and Tol2-INV6B (5′-TGAGTAAAATTTTCCCTAAGT-3′). PCR products were sequenced and BLASTN against Zebrafish Zv8 build was performed.

Acknowledgments

We thank Maurine Hobbs and Sharon Johnson of the University of Utah's Centralized Zebrafish Animal Resource center.

References

Akitake CM, Macurak M, Halpern ME, Goll MG. 2011. Transgenerational analysis of transcriptional silencing in zebrafish. Dev Biol 352:191–201.

Asakawa K, Abe G, Kawakami K. 2013. Cellular dissection of the spinal cord motor column by BAC transgenesis and gene trapping in zebrafish. Front Neural Circuits 7:100.

Asakawa K, Suster ML, Mizusawa K, Nagayoshi S, Kotani T, Urasaki A, Kishimoto Y, Hibi M, Kawakami K. 2008. Genetic dissection of neural circuits by Tol2 transposon-mediated Gal4 gene and enhancer trapping in zebrafish. Proc Natl Acad Sci U S A 105:1255–1260.

Balciunas D, Wangensteen KJ, Wilber A, Bell J, Geurts A, Sivasubbu S, Wang X, Hackett PB, Largaespada DA, McIvor RS, Ekker SC. 2006. Harnessing a high cargo-capacity transposon for genetic applications in vertebrates. PLoS Genet 2:e169.

Balciuniene J, Balciunas D. 2013. Gene trapping using gal4 in zebrafish. J Vis Exp :e50113.

Brand AH, Perrimon N. 1993. Targeted gene expression as a means of altering cell fates and generating dominant phenotypes. Development 118:401–415.

Campbell DS, Stringham SA, Timm A, Xiao T, Law MY, Baier H, Nonet ML, Chien CB. 2007. Slit1a inhibits retinal ganglion cell arborization and synaptogenesis via Robo2-dependent and -independent pathways. Neuron 55:231–245.

Curado S, Anderson RM, Jungblut B, Mumm J, Schroeter E, Stainier DY. 2007. Conditional targeted cell ablation in zebrafish: a new tool for regeneration studies. Dev Dyn 236:1025–1035.

Davison JM, Akitake CM, Goll MG, Rhee JM, Gosse N, Baier H, Halpern ME, Leach SD, Parsons MJ. 2007. Transactivation from Gal4-VP16 transgenic insertions for tissue-specific cell labeling and ablation in zebrafish. Dev Biol 304:811–824.

Douglass AD, Kraves S, Deisseroth K, Schier AF, Engert F. 2008. Escape behavior elicited by single, channelrhodopsin-2-evoked spikes in zebrafish somatosensory neurons. Curr Biol 18:1133–1137.

Eisenhoffer GT, Loftus PD, Yoshigi M, Otsuna H, Chien CB, Morcos PA, Rosenblatt J. 2012. Crowding induces live cell extrusion to maintain homeostatic cell numbers in epithelia. Nature 484:546–549.

Halpern ME, Rhee J, Goll MG, Akitake CM, Parsons M, Leach SD. 2008. Gal4/UAS transgenic tools and their application to zebrafish. Zebrafish 5:97–110.

Higashijima S, Masino MA, Mandel G, Fetcho JR. 2003. Imaging neuronal activity during zebrafish behavior with a genetically encoded calcium indicator. J Neurophysiol 90:3986–3997.

Koster RW, Fraser SE. 2001. Tracing transgene expression in living zebrafish embryos. Dev Biol 233:329–346.

Kwan KM, Fujimoto E, Grabher C, Mangum BD, Hardy ME, Campbell DS, Parant JM, Yost HJ, Kanki JP, Chien CB. 2007. The Tol2kit: a multisite gateway-based construction kit for Tol2 transposon transgenesis constructs. Dev Dyn 236:3088–3099.

Li J, Mack JA, Souren M, Yaksi E, Higashijima S, Mione M, Fetcho JR, Friedrich RW. 2005. Early development of functional spatial maps in the zebrafish olfactory bulb. J Neurosci 25:5784–5795.

Mumm JS, Williams PR, Godinho L, Koerber A, Pittman AJ, Roeser T, Chien CB, Baier H, Wong RO. 2006. In vivo imaging reveals dendritic targeting of laminated afferents by zebrafish retinal ganglion cells. Neuron 52:609–621.

Ogura E, Okuda Y, Kondoh H, Kamachi Y. 2009. Adaptation of GAL4 activators for GAL4 enhancer trapping in zebrafish. Dev Dyn 238:641–655.

Otsuna H, Ito K. 2006. Systematic analysis of the visual projection neurons of Drosophila melanogaster. I. Lobula-specific pathways. J Comp Neurol 497:928–958.

Pisharath H, Rhee JM, Swanson MA, Leach SD, Parsons MJ. 2007. Targeted ablation of beta cells in the embryonic zebrafish pancreas using E. coli nitroreductase. Mech Dev 124:218–229.

Satou C, Kimura Y, Hirata H, Suster ML, Kawakami K, Higashijima S. 2013. Transgenic tools to characterize neuronal properties of discrete populations of zebrafish neurons. Development 140:3927–3931.

Scheer N, Campos-Ortega JA. 1999. Use of the Gal4-UAS technique for targeted gene expression in the zebrafish. Mech Dev 80:153–158.

Scheer N, Groth A, Hans S, Campos-Ortega JA. 2001. An instructive function for Notch in promoting gliogenesis in the zebrafish retina. Development 128:1099–1107.

Scott EK. 2009. The Gal4/UAS toolbox in zebrafish: new approaches for defining behavioral circuits. J Neurochem 110:441–456.

Scott EK, Mason L, Arrenberg AB, Ziv L, Gosse NJ, Xiao T, Chi NC, Asakawa K, Kawakami K, Baier H. 2007. Targeting neural circuitry in zebrafish using GAL4 enhancer trapping. Nat Methods 4:323–326.

Szobota S, Gorostiza P, Del Bene F, Wyart C, Fortin DL, Kolstad KD, Tulyathan O, Volgraf M, Numano R, Aaron HL, Scott EK, Kramer RH, Flannery J, Baier H, Trauner D, Isacoff EY. 2007. Remote control of neuronal activity with a light-gated glutamate receptor. Neuron 54:535–545.

Wan Y, Otsuna H, Chien CB, Hansen C. 2009. An interactive visualization tool for multi-channel confocal microscopy data in neurobiology research. IEEE Trans Vis Comput Graph 15:1489–1496.

Wang X, Kopinke D, Lin J, McPherson AD, Duncan RN, Otsuna H, Moro E, Hoshijima K, Grunwald DJ, Argenton F, Chien CB, Murtaugh LC, Dorsky RI. 2012. Wnt signaling regulates postembryonic hypothalamic progenitor differentiation. Dev Cell 23:624–636.

CHAPTER 4

CONTINUOUS GENERATION OF DOPAMINERGIC NEURONS IN THE ZEBRAFISH HYPOTHALAMUS MEDIATES RECOVERY OF MOTOR BEHAVIOR

Introduction

Postembryonic neurogenesis has been observed in several regions of the vertebrate brain, including the dentate gyrus and rostral migratory stream in mammals, and is required for normal behavior (Aimone et al., 2014; Gould, 2007; Imayoshi et al., 2008). Recently, the hypothalamus has also been shown to undergo continuous neurogenesis as a way to mediate energy balance (Bolborea and Dale, 2013; Cheng, 2013; Lee and Blackshaw, 2012; Li et al., 2012; Maia V. Kokoeva, 2005; Pierce and Xu, 2010; Sousa-Ferreira et al., 2014). As the hypothalamus regulates multiple functional outputs, it is likely that additional behaviors may be affected by postembryonic neurogenesis in this brain structure. Here, we have identified a progenitor population in the zebrafish hypothalamus that continuously generates neurons that express *tyrosine hydroxylase* 2 (*th2*). We develop and use novel transgenic tools to characterize the lineage of *th2*+ cells and demonstrate that they are dopaminergic. Through genetic ablation and optogenetic activation, we then show that *th2*+ neurons modulate the initiation of swimming behavior in zebrafish larvae. Finally, we find that the generation of new *th2*+ neurons following ablation correlates with restoration of normal behavior. This work thus identifies for the first time a population of dopaminergic neurons that regulates motor behavior and is capable of functional recovery.

Results and discussion

th2+ neurons are dopaminergic and arise from dlx5/6-expressing precursors

In the mammalian hypothalamus, the embryonic neural precursor lineage expressing *Dlx* genes produces dopaminergic neurons (Yee et al., 2009). From previous studies in our laboratory, we found that neural precursors expressing a *dlx5/6* enhancer were continuously present in the zebrafish hypothalamus (Wang et al., 2012). However, we failed to observe expression of Tyrosine Hydroxylase (TH), a marker of dopaminergic neurons, in this lineage using available antibodies. Because zebrafish and other nonmammalian vertebrates express a second *tyrosine hydroxylase* gene, *th2* (Yamamoto et al., 2010, 2011), we examined the expression of a transgenic reporter using 9.6 kb of *th2* upstream regulatory sequence driving *GFP-Aequorin* (Fig. 4.1A). This construct was used to establish a stable transgenic zebrafish line [*Tg(th2:GFP-Aequorin)*^{zd201}, hereafter referred to as *th2:GFP,* Fig. 4.1A,B], and double labeling with a *th2* mRNA probe showed extensive overlap with GFP throughout the hypothalamic posterior recess (Fig. 4.1C). Next, we crossed the *th2:GFP* reporter line to fish expressing a *dlx5/6:mCherry* reporter, which is expressed in neural precursors (Wang et al., 2012), and analyzed coexpression in the hypothalamic posterior recess at 7 dpf. We found that 83.9% +/- 3.9% (SEM, n=5 brains) of GFP+ cells also expressed mCherry protein that persisted through terminal differentiation (Fig. 4.1D), indicating that TH2+ neurons arise from this lineage. While a previous study concluded that *th2*+ cells are serotonergic (Ren et al., 2013), we

instead found that 92.8% +/- 6.9% (SEM, n=5 brains) of *th2:GFP*+ cells at 7 dpf were double labeled with a dopamine antibody (Fig. 4.1E). In contrast, only 5.4 +/- 4.2% (SEM, n=5 brains) of *th2:GFP*+ cells were labeled with a serotonin antibody (Fig. 4.1F). In agreement with a recent analysis using a Th2 antibody (Semenova, 2014), we therefore conclude that *th2*+ cells are dopaminergic, and like other dopaminergic populations in mammals, are generated by *Dlx*+ neural precursors.

th2+ cells are continuously generated throughout life

Because we have previously shown that hypothalamic *dlx5/6*+ precursors are present through adult stages [12], we reasoned that *th2*+ cells arising from these precursors might also be generated postembryonically. To test this hypothesis, we administered 10 mM BrdU to *th2:GFP* transgenic larvae and adults for 24 hours, and following a chase period, we found newly born GFP+ cells at 9 days post-fertilization (dpf), 25 dpf, and 6 months post-fertilization (mpf) (Fig. 4.2A-C). Consistent with a higher rate of neurogenesis in younger animals, the BrdU labeling index was 10.4% with only 3 days of chase in early larvae (9 dpf), 5.9% with 2 weeks of chase in late larvae (25 dpf), and 1.1% with 2 weeks of chase in adults (Fig. 4.2D). We observed a higher BrdU labeling index in the *dlx5/6*+ precursor population at all stages (data not shown), suggesting that the birth of *th2*+ neurons may be more tightly regulated, perhaps in response to environmental signals. Overall, our data indicate that zebrafish constantly generate dopaminergic neurons in the hypothalamus throughout their lifespan.

Ablation of th2+ neurons reduces swimming frequency

While a function for hypothalamic *th2*+ neurons in the modulation of motor function has been previously suggested (Mu et al., 2012), a definitive behavioral analysis of this population has not been performed due to the lack of specific genetic tools. We therefore took a genetic approach to ablate *th2*+ cells and examine the resulting effects on behavior. We generated a *th2:Gal4* transgenic line [*Tg(th2:Gal-VP16)*^{zd202}] which was crossed to *Tg(UAS-E1b:NTR-mCherry)*^{c264} fish (Otsuna et al., 2015) to drive Nitroreductase (NTR) expression in *th2*+ neurons (Fig. 4.3A, Fig. 4.4A, Fig. 4.5A) and enable chemical ablation (Curado et al., 2007; Curado et al., 2008). While the hypothalamic posterior recess of untreated brains had an average of 128.7 ± 20.6 mCherry+ cells (S.E.M., n=7 brains), after addition of 5 mM metronidazole (MTZ) to double transgenic embryos from 5-7 dpf, we observed a reduction to 18.1 ± 2.4 cells/brain (S.E.M., n=10 brains), a decrease of 86% (Fig. 4.3A-B). The effects of ablation on spontaneous swimming were then measured in single 8 dpf larvae over a 10-minute recording period, during which the animals were allowed to move freely within a dish. Ablation of *th2*+ neurons significantly reduced both the bout frequency and total amount of time spent swimming, but not the amplitude of individual swimming bouts (Fig. 4.3C-E, Fig. 4.5C, Supplemental Movies 1-2, p=0.009 for swim frequency; p=0.020 for swim time by 2-way ANOVA). In contrast, treating nontransgenic siblings with MTZ (Fig. 4.3C-E), and ablation of hypothalamic radial glia using a separate transgenic line (Otsuna et al., 2015) (Fig. 4.5D-E), did not affect swimming behavior. Decreased frequency of

swimming was also observed following MTZ treatment of an independent transgenic line, expressing NTR-GFP directly under the control of the *th2* enhancer (Fig. 4.3F-I and Fig. 4.5B). Our data thus suggest that *th2*+ neurons regulate the initiation of movement.

Activation of th2+ neurons drives swimming

To test the sufficiency of *th2*+ neurons for the initiation of swimming, we expressed Channelrhodopsin-2 (ChR2) in these cells by crossing *Tg(UAS:ChR2-YFP)*^{a144} (Lacoste et al., 2015) and *Tg(th2:Gal-VP16)*^{zd202} fish (Fig. 4.5E) Expression of the ChR2-YFP fusion protein specifically in posterior recess neurons allowed us to examine their axon trajectory and targets using whole-brain confocal imaging (Fig. 4.3J; Supplemental Movie 3). We found that a majority of axons appear to terminate a short distance from the posterior recess, likely in the posterior tuberculum. This projection pattern differentiates the *th2*+ neurons from *th1*-expressing cells in the posterior recess, which primarily innervate local hypothalamic targets (Tay et al., 2011).

Freely moving larvae in a dish were then stimulated with 5-second pulses of blue light delivered once per minute over a 10-minute period, causing activation of the cells as indicated by *cfos* expression (Fig. 4.5G). During the blue light pulse, larvae from ChR2+ crosses showed increased frequency of swimming compared to controls (Fig. 4.3K, Fig. 4.5H, Supplemental Movies 4-5). Automated tracking revealed that increased bout frequency during the stimulus resulted in a significant increase in the animal's cumulative displacement compared to baseline (Fig. 4.5I-J). Together with the ablation experiments, these

data indicate that *th2*+ neurons may function either in the direct activation of motor behavior, or as suggested previously, in modulating the threshold of a motor response to sensory-evoked stimuli (Mu et al., 2012).

th2+ neurons are restored after ablation

Based on our observations that *th2*+ neurons are continuously generated, we hypothesized that the cell population may have the ability to recover following ablation. We therefore performed ablations from 5-7 dpf and behavioral analysis at 8 dpf as described above, then treated larvae with 10 mM BrdU for 2 days, and allowed them to recover for 2 weeks before receiving an acute treatment of 5 mM MTZ or 0.5% DMSO. Following immunohistochemistry with mCherry and BrdU antibodies, ablated animals showed a striking recovery in the overall mCherry+ population (Fig. 4.4A,B,E). While these data do not allow us to distinguish true regeneration from the normal process of cell addition during the experiment, we observed a significant increase in the fraction of newly born mCherry+ cells compared to unablated controls, consistent with an injury response (Fig. 4.4F). The actual level of neurogenesis was likely even higher, due to the fact that progenitors becoming postmitotic before 8 dpf were not labeled with BrdU. Regardless, these data show that *th2*+ neurons are capable of recovery after injury, similar to dopaminergic neurons in the mammalian olfactory bulb (Schwob, 2002). Interestingly, those neurons arise from progenitors expressing a similar series of developmental transcription factors as we have observed in the zebrafish hypothalamus (Lee et al., 2006; Wang et al., 2012).

Replacement of th2 neurons results in recovery of swimming deficits

Because adult-born *th2*+ cells extend both short radial processes into the ventricle and long projections (Fig. 4.2C), we hypothesized that cells born after ablation may be capable of re-integrating into existing circuits. We therefore tested whether *th2*+ cell replacement led to functional recovery of the swimming deficits resulting from their ablation. Following a 2-week recovery period, MTZ-treated and control fish received another treatment with MTZ or DMSO (Fig. 4.4A-E), and behavioral analysis was performed on groups of 3 larvae. Fish in which the *th2*+ neurons had been ablated at 7 dpf displayed swimming behavior indistinguishable from that of unablated siblings ($p=0.60$ for swim frequency; $p=0.80$ for swim time by 2-way ANOVA), while fish receiving an ablation at 25 dpf displayed a significant decrease in swimming bout frequency and time spent swimming (Fig. 4.4G-H, Fig. 4.6, $p=0.034$ for swim frequency; $p=0.032$ for swim time by 2-way ANOVA). Together, these data indicate a strong correlation between the replacement of *th2*+ cells and functional recovery of the behavior they regulate. While proof of functional integration into circuitry will require further analysis of physiological activity, our results are consistent with this possibility.

Conclusions

This study provides the first genetic analysis of the *th2*+ neuronal population in the zebrafish hypothalamus. We have shown that *th2*+ neurons are dopaminergic and arise from *dlx5/6*+ precursors, similar to dopaminergic neurons in the mammalian hypothalamus and olfactory bulb. In addition, we find that *th2*+ neurons regulate the frequency of spontaneous swimming, providing the first

genetically validated link between these neurons and a behavioral function. Most intriguingly, our data indicate *th2*+ neurons are replaced within 2 weeks after ablation, coinciding with a recovery of normal swimming behavior. Together, our findings suggest that even in nonregenerative mammalian systems, replacement of dopaminergic neurons that modulate motor function after loss from disease or injury could potentially support the recovery of normal behavior

Experimental procedures

Use of zebrafish

Larvae were raised in E3 medium at 28.5°C until 5-7 dpf at which point they were fed daily until analysis. Larval and adult brains were obtained by dissection from animals fixed in 4% paraformaldehyde + 5% sucrose in PBS. Ablations were performed by immersion in E3 media containing 5 mM MTZ in 0.5% DMSO for 2 days in the dark. BrdU labeling of larvae was performed by immersion in E3 medium with 10 mM BrdU in the dark. Adult fish were injected interperitoneally with 10 mM BrdU in 110 mM NaCl. All procedures were approved by the IACUC committee at the University of Utah.

Generation of transgenic lines

For *th2:GFP-Aequorin*, *th2:Gal4-VP16,* and *th2:ChR2-tRFP* transgenes, a 9.6 kb regulatory sequence flanking the 5' end of the *th2* open reading frame was cloned by gap repair recombineering (http://ncifrederick.cancer.gov/research/brb/recombineeringInformation.aspx) from BAC clone CH211-260P3 into a Gateway donor vector to make *pENTR:th2(9.6kb)*. This vector was used for LR cloning into destination vectors

containing *GFP-Aequorin, Gal4-VP16*, or *ChR2-tRFP* coding sequence flanked by Tol2 transposon sites. The *th2:NTR-EGFP* transgene was generated by replacement of the *ChR2-tRFP* coding sequence with an *NTR-eGFP* coding sequence (Lambert et al., 2012) in the destination vector using restriction digestion and ligation.

To generate stable transgenic lines for *th2:GFP-Aequorin* and *th2:Gal4-VP16*, 10-50 pg of DNA was injected into fertilized, single-cell zebrafish embryos along with 20-30 pg Tol2 mRNA to enable genomic integration. Founder animals were identified by outcrossing and screening progeny for fluorescence, or by PCR detection of the transgene. Individual lines were established after two successive generations of outcrossing to WT animals. Allele designations for stable lines are *Tg(th2:GFP-Aequorin)*^{zd201} and *Tg(th2:Gal-VP16)*^{zd202}.

In situ hybridization and immunohistochemistry

In situ hybridization was performed as previously described in (Thisse and Thisse, 2008). Antisense probe for *th2* was generated by PCR amplification using the primers below, followed by transcription with T7 RNA Polymerase. *th2* primers: 5'- CGGAGACAGCTTCGTGTT, 3'- GCTCATTAGAAAGGGCATA. *cfos* probe was made as previously described (von Trotha et al., 2014)

Immunohistochemistry was performed as previously described in (Otsuna et al., 2015), with the addition of treatment with 2 N HCl for 30-60 minutes for BrdU detection.

The following primary antibodies were used: Rabbit anti-DA (purchased from H.W.M. Steinbusch), Rabbit anti-5HT (Sigma, S5545), Mouse anti-GFP

(Invitrogen, A11120), Rabbit anti-GFP (Invitrogen, A11122), Chicken anti-GFP (Aves, GFP-1020), Rabbit anti-dsRed (Clontech, 632496), Mouse anti-BrdU (DSHB, G3G4-BrdU), Chicken anti-BrdU (Aves, CBDU-65A-Z)

The following secondary antibodies were used: Goat anti-Mouse Alexa Fluor 448 (Invitrogen, A11001), Goat anti-Rabbit Alexa Fluor 488 (Invitrogen, A11008), Donkey anti-Chicken Alexa Fluor 488 (Jackson ImmunoResearch, 703-545-155), Goat anti-Chicken Alexa Fluor 568 (Invitrogen, A11041), Goat anti-Mouse Alexa Fluor 633 (Invitrogen, A21050), Goat anti-Chicken Alexa Fluor 633 (Invitrogen, A21103), Goat anti-Mouse Alexa Fluor 647 (Invitrogen, A21235), Goat anti-Rabbit Alexa Fluor 647 ((Invitrogen, A21244), Goat anti-Chicken Alexa Fluor 647 (Invitrogen, A21449)

Microscopy

Whole larval brains were imaged ventrally through the entire hypothalamus, determined by the anatomy of the 3rd ventricle and posterior recess. Adult brains were bisected midsagittally and imaged laterally from the midsagittal surface. Images were collected on an Olympus FV1000 confocal microscope, an Olympus BX51WI compound fluorescence microscope, and an Olympus SZX16 fluorescence dissecting microscope. Image quantification was performed with ImageJ software, and images were processed for figures using Adobe Photoshop.

Behavior

All behavioral measurements were made on a custom-built apparatus in which the movements of free-swimming animals were monitored using a Pike CCD camera (Allied Vision Tech, Stadtroda, Germany) controlled by custom LabView software (National Instruments, Austin, TX). For optogenetics experiments, animals were stimulated with 470 nm light from a high-power LED at 0.6 mW/mm^2, distributed uniformly across the arena with a condenser lens and photographic diffuser paper. Movement was analyzed online using a running frame subtraction, in which the maximal pixel intensity change in each difference image was computed and then saved. Frames in which the fish moved were apparent as transient spikes in this vector. Subsequent analysis in MATLAB identified swim bouts using a spike-finding algorithm and computed the amplitude and frequency of these events as a measure of locomotor activity. Automated tracking analyses were performed by applying custom MATLAB scripts to movies of the behavior acquired at 404 frames/s, then measuring each animal's instantaneous velocities and cumulative displacement during the stimulus and baseline periods.

Statistical analyses

Single variable pairwise comparisons were analyzed using a Student t-test. Multivariable datasets were analyzed using ANOVA, followed by Bonferroni Multiple Comparisons test to produce multiplicity-adjusted p values for pairwise comparisons. Significance was defined as a p value of 0.05 or smaller. Outliers were excluded at $p<0.01$, using Grubbs' test.

Authors and contributions

Adam D. McPherson, Joshua P. Barrios, Sasha J. Luks-Morgan, John P. Manfredi, Joshua L. Bonkowsky, Adam D. Douglass, and Richard I. Dorsky

All experiments were performed by A.D.M., except for *th2 in situs* (J.P.B.). S.J.L-M. and A.D.D. performed computational analysis for ChR2 experiments. Transgenic lines were made by A.D.D. [*Tg(th2:GFP-Aequorin)*^{zd201}], and by J.L.B. [*Tg(th2:Gal-VP16)*^{zd202}]. J.P.M. performed statistical analyses. A.D.D. and R.I.D. supervised all the experiments and edited the manuscript.

Acknowledgements

We thank the University of Utah Centralized Zebrafish Animal Resource (CZAR) for assistance with animal care and the Cell Imaging Core for assistance with confocal microscopy. We thank Shiela Samson for making the *th2 in situ* probe.

A.D.D. was funded by a Sloan Foundation Research Fellowship, R.I.D was funded by NIH R01 NS082645, and. J.L.B. was funded by NIH DP2 MH100008. A.D.M. was funded by NIH 5T32 HD07491 and A.D.M. and S.J.L.-M. were both funded by NIDCD 5T32 DC008553.

References

Aimone, J.B., Li, Y., Lee, S.W., Clemenson, G.D., Deng, W., and Gage, F.H. (2014). Regulation and function of adult neurogenesis: from genes to cognition. Physiological Reviews *94*, 991-1026.

Bolborea, M., and Dale, N. (2013). Hypothalamic tanycytes: potential roles in the control of feeding and energy balance. Trends in Neurosciences *36*, 91-100.

Cheng, M.F. (2013). Hypothalamic neurogenesis in the adult brain. Frontiers in Neuroendocrinology *34*, 167-178.

Curado, S., Anderson, R.M., Jungblut, B., Mumm, J., Schroeter, E., and Stainier, D.Y. (2007). Conditional targeted cell ablation in zebrafish: a new tool for regeneration studies. Developmental Dynamics *236*, 1025-1035.

Curado, S., Stainier, D.Y., and Anderson, R.M. (2008). Nitroreductase-mediated cell/tissue ablation in zebrafish: a spatially and temporally controlled ablation method with applications in developmental and regeneration studies. Nature Protocols *3*, 948-954.

Gould, E. (2007). How widespread is adult neurogenesis in mammals? Nature Reviews Neuroscience *8*, 481-488.

Imayoshi, I., Sakamoto, M., Ohtsuka, T., Takao, K., Miyakawa, T., Yamaguchi, M., Mori, K., Ikeda, T., Itohara, S., and Kageyama, R. (2008). Roles of continuous neurogenesis in the structural and functional integrity of the adult forebrain. Nature Neuroscience *11*, 1153-1161.

Lacoste, A.M., Schoppik, D., Robson, D.N., Haesemeyer, M., Portugues, R., Li, J.M., Randlett, O., Wee, C.L., Engert, F., and Schier, A.F. (2015). A convergent and essential interneuron pathway for Mauthner-cell-mediated escapes. Current Biology *25*, 1526-1534.

Lambert, A.M., Bonkowsky, J.L., and Masino, M.A. (2012). The conserved dopaminergic diencephalospinal tract mediates vertebrate locomotor development in zebrafish larvae. The Journal of Neuroscience *32*, 13488-13500.

Lee, D.A., and Blackshaw, S. (2012). Functional implications of hypothalamic neurogenesis in the adult mammalian brain. International Journal of Developmental Neuroscience *30*, 615-621.

Lee, J.E., Wu, S.F., Goering, L.M., and Dorsky, R.I. (2006). Canonical Wnt signaling through Lef1 is required for hypothalamic neurogenesis. Development *133*, 4451-4461.

Li, J., Tang, Y., and Cai, D. (2012). IKKbeta/NF-kappaB disrupts adult hypothalamic neural stem cells to mediate a neurodegenerative mechanism of dietary obesity and pre-diabetes. Nature Cell Biology *14*, 999-1012.

Maia V. Kokoeva, H.Y., Jeffrey S. Flier (2005). Neurogenesis in the hypothalamus of adult mice: potential role in energy balance. Science *310*, 679-683.

Mu, Y., Li, X.Q., Zhang, B., and Du, J.L. (2012). Visual input modulates audiomotor function via hypothalamic dopaminergic neurons through a cooperative mechanism. Neuron *75*, 688-699.

Otsuna, H., Hutcheson, D., Duncan, R., McPherson, A., Scoresby, A., Gaynes, B., Tong, Z., Fujimoto, E., Kwan, K., Chien, C*., et al.* (2015). High-resolution analysis of CNS expression patterns in zebrafish Gal4 enhancer-trap lines. Developmental Dynamics *244*, 785-796.

Pierce, A.A., and Xu, A.W. (2010). De novo neurogenesis in adult hypothalamus as a compensatory mechanism to regulate energy balance. The Journal of Neuroscience *30*, 723-730.

Ren, G., Li, S., Zhong, H., and Lin, S. (2013). Zebrafish tyrosine hydroxylase 2 gene encodes tryptophan hydroxylase. The Journal of Biological Chemistry *288*, 22451-22459.

Schwob, J.E. (2002). Neural regeneration and the peripheral olfactory system. The Anatomical Record *269*, 33-49.

Semenova, S.A.C., Y.C.; Zhao, X.; Rauvala, H.; Panula, P. (2014). The tyrosine hydroxylase 2 (TH2) system in zebrafish brain and stress activation of hypothalamic cells. Histochemical Cell Biology *142*, 619-633.

Sousa-Ferreira, L., de Almeida, L.P., and Cavadas, C. (2014). Role of hypothalamic neurogenesis in feeding regulation. Trends in Endocrinology and Metabolism *25*, 80-88.

Tay, T.L., Ronneberger, O., Ryu, S., Nitschke, R., and Driever, W. (2011). Comprehensive catecholaminergic projectome analysis reveals single-neuron integration of zebrafish ascending and descending dopaminergic systems. Nature Communications *2*, 171.

Thisse, C., and Thisse, B. (2008). High-resolution in situ hybridization to whole-mount zebrafish embryos. Nature Protocols *3*, 59-69.

von Trotha, J.W., Vernier, P., and Bally-Cuif, L. (2014). Emotions and motivated behavior converge on an amygdala-like structure in the zebrafish. The European Journal of Neuroscience *40*, 3302-3315.

Wang, X., Kopinke, D., Lin, J., McPherson, A.D., Duncan, R.N., Otsuna, H., Moro, E., Hoshijima, K., Grunwald, D.J., Argenton, F.*, et al.* (2012). Wnt signaling regulates postembryonic hypothalamic progenitor differentiation. Developmental Cell *23*, 624-636.

Yamamoto, K., Ruuskanen, J.O., Wullimann, M.F., and Vernier, P. (2010). Two tyrosine hydroxylase genes in vertebrates: new dopaminergic territories revealed in the zebrafish brain. Molecular and Cellular Neurosciences *43*, 394-402.

Yamamoto, K., Ruuskanen, J.O., Wullimann, M.F., and Vernier, P. (2011). Differential expression of dopaminergic cell markers in the adult zebrafish forebrain. The Journal of Comparative Neurology *519*, 576-598.

Yee, C.L., Wang, Y., Anderson, S., Ekker, M., and Rubenstein, J.L. (2009). Arcuate nucleus expression of NKX2.1 and DLX and lineages expressing these transcription factors in neuropeptide Y(+), proopiomelanocortin(+), and tyrosine hydroxylase(+) neurons in neonatal and adult mice. The Journal of Comparative Neurology *517*, 37-50.

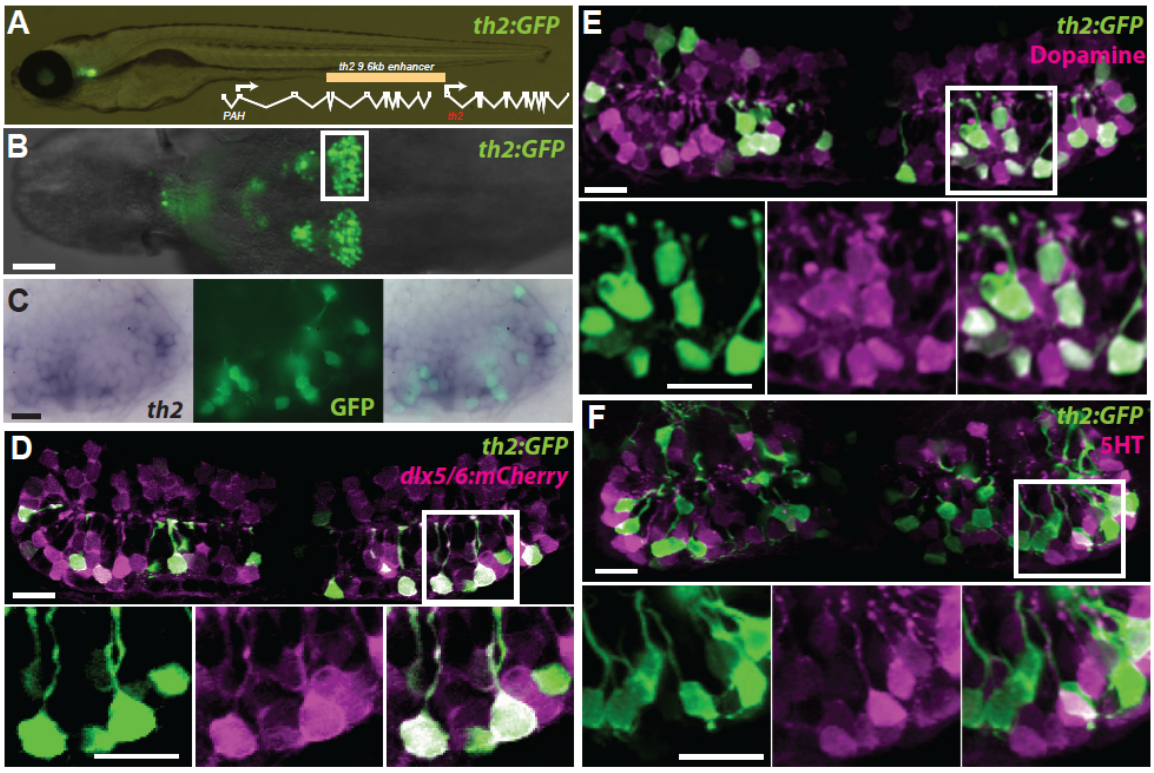

Figure 4.1: A *th2:GFP* transgene labels dopaminergic neurons derived from a dlx5/6+ precursor lineage. (A) Live zebrafish 7 dpf larva expressing *th2:GFP* with schematic of *th2* enhancer/promoter region used for transgenes. (B) Ventral whole-mount view of *th2:GFP* expression in a dissected 7 dpf brain, box indicates area of posterior recess shown in (C-F). (C) Simultaneous *in situ* hybridization for *th2* mRNA (left) and anti-GFP immunohistochemistry (middle) shows transcript expression in all *th2:GFP*+ cells (right). Ventral whole-mount view of a dissected 7 dpf brain is shown. (D) Co-expression analysis shows that most *th2*:*GFP*+ cells (green) express *dlx5/6:mCherry* (magenta), indicating their origin from *dlx5/6*+ precursors. (E) Co-expression analysis shows that most *th2*:*GFP*+ cells (green) express dopamine (magenta). (F) Co-expression analysis shows that few *th2*:*GFP*+ cells (green) express serotonin (magenta). All images in (D-F) are ventral maximum intensity confocal Z-projections of the hypothalamic posterior recess from dissected 7 dpf brains. Individual and merged channels of boxed regions are shown in lower panels. Scale bar in (B) = 50μm, all other scale bars = 10μM.

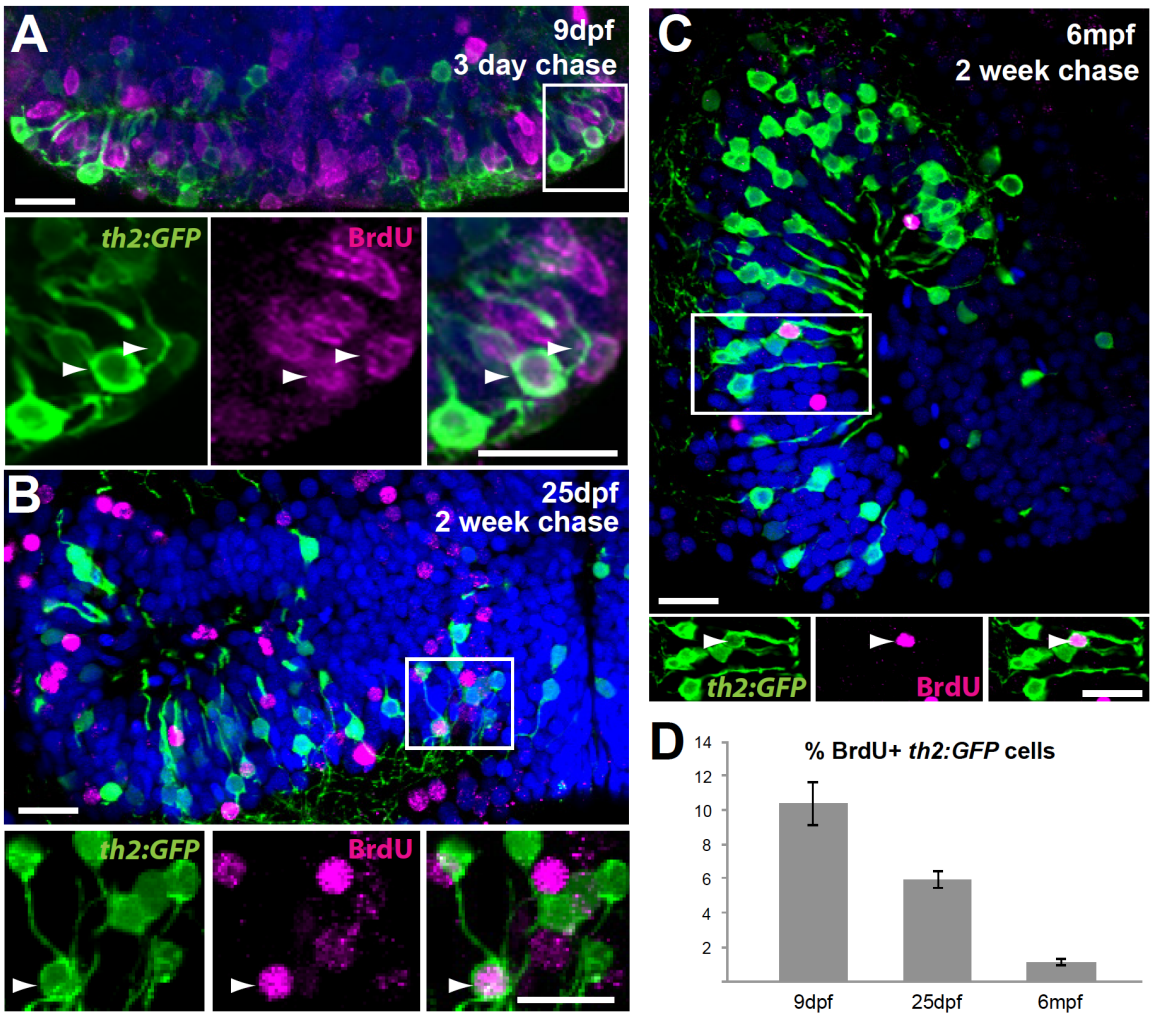

Figure 4.2: *th2* + cells are continuously generated throughout life. (A) 5 dpf larvae were treated with BrdU for 24 hours and analyzed at 9 dpf. Numerous *th2:GFP*+ cells (green) are labeled with BrdU (magenta) in the hypothalamic posterior recess. Arrowheads indicate double-labeled cells. (B) 12 dpf larvae were treated with BrdU for 24 hours and analyzed at 25 dpf. *th2:GFP*+ cells (green) labeled with BrdU (magenta) can be found in medial regions of the hypothalamic posterior recess. Arrowheads indicate double-labeled cells. (C) 6 mpf fish were injected interperitoneally with BrdU and analyzed 2 weeks later. *th2:GFP*+ cells (green) labeled with BrdU (magenta) can be found in a midsagittal view of the hypothalamic posterior recess. Arrowheads indicate double-labeled cells. (D) Percent of BrdU+ cells in the *th2:GFP*+ population throughout the entire posterior recess. Error bars=SEM, n=5 brains. Images in (A-B) are ventral maximum intensity confocal Z-projections of the hypothalamic posterior recess. Images in (C) are maximum intensity confocal Z-projections from midsagittal views of the hypothalamic posterior recess. Individual and merged channels of boxed region are shown in lower panels. Scale bars=10μM.

Figure 4.3: *th2*+ cells modulate the initiation of swimming behavior. (A-B) Representative brains of 8 dpf *th2:Gal4-VP16; UAS:NTR-mCherry* larvae treated with 0.5% DMSO (A) or 5mM MTZ (B) from 5-7 dpf. (C-E) Effects of ablation on behavior in 8 dpf larvae as measured by swimming frequency, (C) time spent swimming (D), and swim amplitude (E) Error bars=SEM, n=6 larvae for each condition except NTR+ fish treated with MTZ, wherein n=5 due to exclusion of an outlier ($p<0.01$, Grubbs' test). Two-way ANOVA indicates a significant interaction between genotype and treatment for swim initiations ($p=0.009$ for swim frequency; $p=0.020$ for swim time), but not for swim amplitude. Adjusted p values shown for pairwise comparisons are based on Bonferroni Multiple Comparison test. (F-G) Representative brains from 8 dpf *th2:NTR-EGFP* larvae treated with 0.5% DMSO (F) or 5mM MTZ (G) from 5-7 dpf. (G-H) Effects of ablation on swimming behavior in 8 dpf larvae as measured by swimming frequency (H) and time spent swimming (I). Error bars=SEM, n=8 individual larvae for each condition. p values based on Student t-test. (J) Representative brain of *th2:Gal4: UAS:ChR2-YFP* larva, showing that most axons appear to terminate nearby in the posterior tuberculum. (K) Average swim bouts/sec before and during blue light pulse for individual larvae. Error bars=SEM, n=4 (wild-type), n=5 (ChR2). Two-way ANOVA demonstrates significant interaction between genotype and light exposure ($p=0.0025$). Adjusted p values shown for pairwise comparisons are based on Bonferroni Multiple Comparison test. Images in (A-B,F-G,J) are ventral maximum intensity confocal Z-projections of the brain. Scale bar = 10μM.

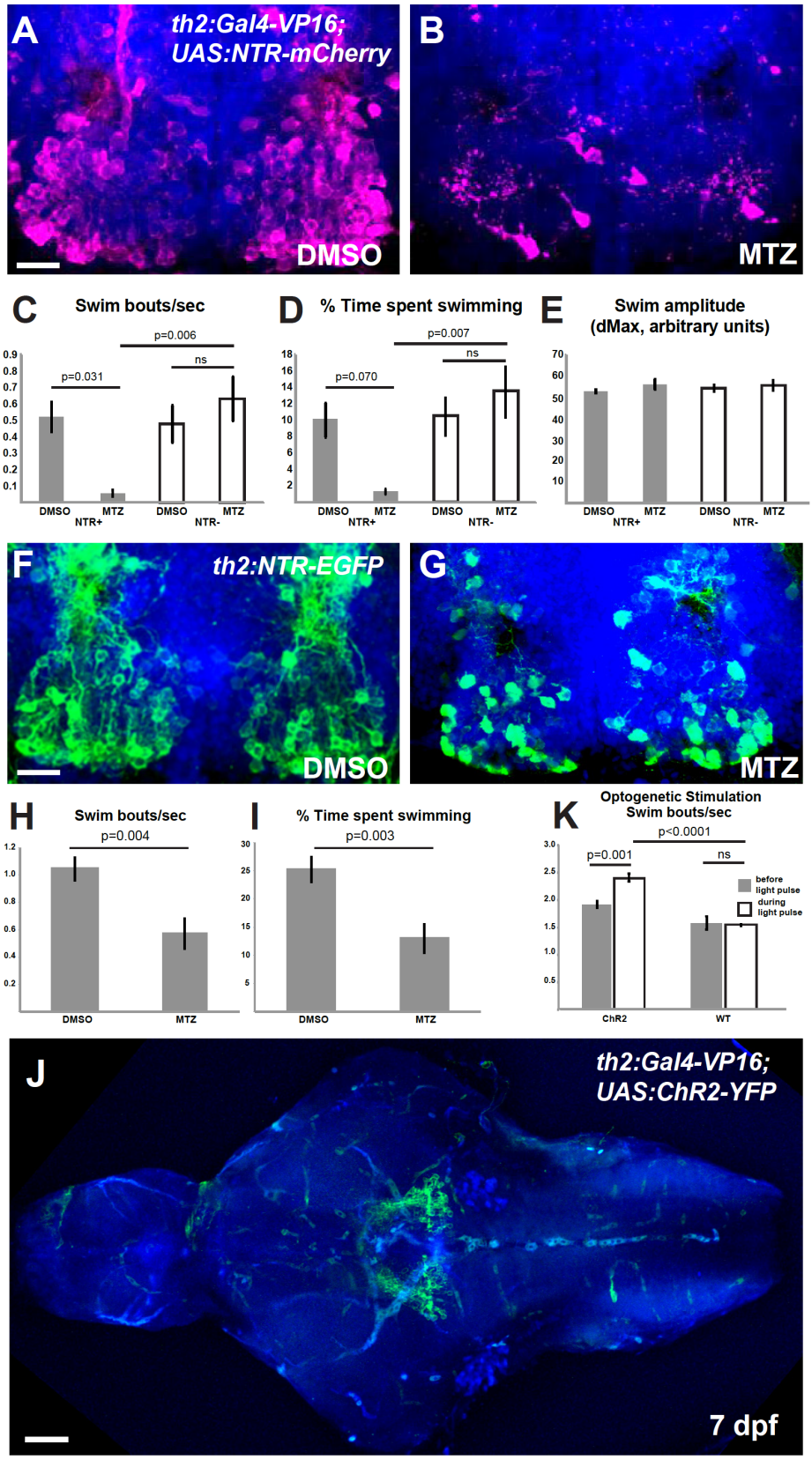
A
th2:Gal4-VP16;
UAS:NTR-mCherry
DMSO
B
MTZ
C
Swim bouts/sec
p=0.006
ns
p=0.031
DMSO
MTZ
DMSO
MTZ
NTR+
NTR-
D
% Time spent swimming
p=0.007
ns
p=0.070
DMSO
MTZ
DMSO
MTZ
NTR+
NTR-
E
Swim amplitude
(dMax, arbitrary units)
DMSO
MTZ
DMSO
MTZ
NTR+
NTR-
F
th2:NTR-EGFP
DMSO
G
MTZ
H
Swim bouts/sec
p=0.004
DMSO
MTZ
I
% Time spent swimming
p=0.003
DMSO
MTZ
K
Optogenetic Stimulation
Swim bouts/sec
p<0.0001
p=0.001
ns
before light pulse
during light pulse
ChR2
WT
J
th2:Gal4-VP16;
UAS:ChR2-YFP
7 dpf

Figure 4.4: *th2*+ cells are replaced after ablation and mediate functional recovery of swimming behavior. (A-D) Representative brains from th2:Gal4-VP16; UAS:NTR-mCherry larvae that were treated with 0.5% DMSO or 5mM MTZ from 5-7 dpf, followed by 10 mM BrdU from 8-10 dpf and allowed to recover for 2 weeks (10-25 dpf) before acute treatments with 0.5% DMSO or 5mM MTZ. (E) Recovery of th2+ cells measured by total cell number. Analysis of the 4 groups by 2-way ANOVA indicates that the 25 dpf treatment has a significant effect on the number of th2:mCherry cells at 28 dpf ($p=0.0001$), while the 7 dpf treatment does not ($p=0.082$); nor is there a significant interaction between two successive treatments ($p=0.20$). Adjusted p values shown for pairwise comparisons are based on Bonferroni Multiple Comparison test. n=3 brains for larvae untreated at 7 dpf, n=4 brains for larvae treated with MTZ at 7 dpf. (F) Percent labeled by BrdU at 8 dpf . Error bars=SEM, n=5 brains. p value based on Student t-test. (G-H) Recovery of behavior 3 weeks after ablation as measured by swimming frequency (G) and time spent swimming (H), n=5 groups for each condition except n=4 for wild-type larvae treated with MTZ+DMSO after exclusion of an outlier ($p<0.001$, Grubbs' test). Statistical analyses were performed separately for the wild-type and NTR+ larvae. Two-way ANOVA of wild-type larvae shows no significant effect of either the 7 dpf treatment ($p=0.95$ for swim frequency; $p=0.89$ for swim time) or the 25 dpf treatment ($p=0.13$ for swim frequency; $p=0.37$ for swim time) at 28 dpf, and there is no significant interaction between the successive treatments ($p=0.66$ for swim frequency; $p=0.76$ for swim time). For NTR+ larvae, 2-way ANOVA indicates that the 7 dpf treatment does not affect swimming behavior at 28 dpf ($p=0.60$ for swim frequency; $p=0.80$ for swim time), while the 25 dpf treatment has a significant effect ($p=0.034$ for swim frequency; $p=0.032$ for swim time). There was no significant interaction between the successive treatments ($p=0.55$ for swim frequency; $p=0.64$ for swim time). Adjusted p values shown for pairwise comparisons are based on Bonferroni Multiple Comparison test. Images in (A-D) are ventral maximum intensity confocal Z-projections of the hypothalamic posterior recess. Scale bar = 10μM.

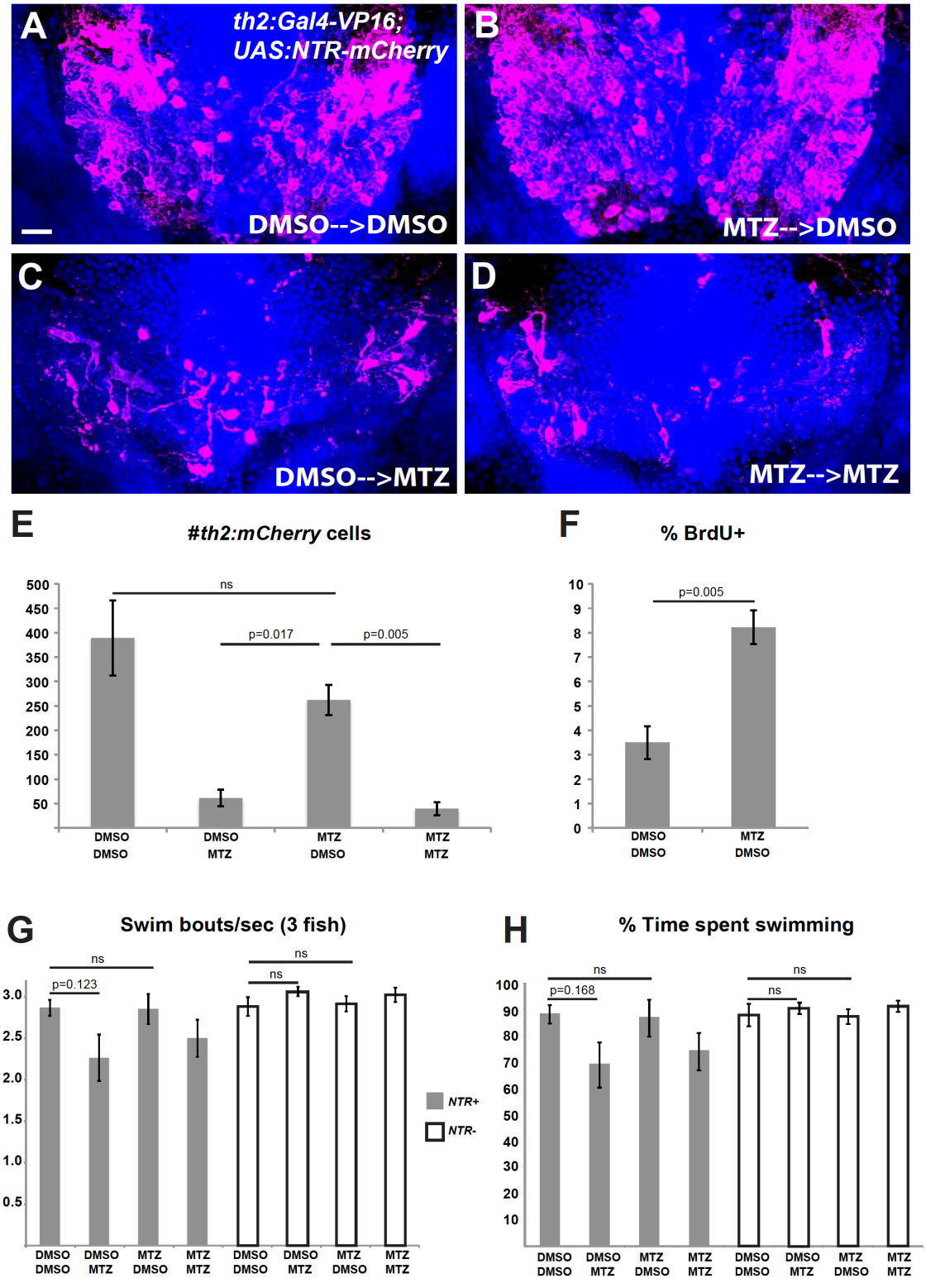
A
th2:Gal4-VP16;
UAS:NTR-mCherry
DMSO-->DMSO
B
MTZ-->DMSO
C
DMSO-->MTZ
D
MTZ-->MTZ
E
#th2:mCherry cells
500
450
400
350
300
250
200
150
100
50
ns
p=0.017
p=0.005
DMSO DMSO
DMSO MTZ
MTZ DMSO
MTZ MTZ
F
% BrdU+
10
9
8
7
6
5
4
3
2
1
0
p=0.005
DMSO DMSO
MTZ DMSO
G
Swim bouts/sec (3 fish)
3.0
2.5
2.0
1.5
1.0
0.5
ns
p=0.123
ns
ns
NTR+
NTR-
DMSO DMSO
DMSO MTZ
MTZ DMSO
MTZ MTZ
DMSO DMSO
DMSO MTZ
MTZ DMSO
MTZ MTZ
H
% Time spent swimming
100
90
80
70
60
50
40
30
20
10
ns
p=0.168
ns
ns
DMSO DMSO
DMSO MTZ
MTZ DMSO
MTZ MTZ
DMSO DMSO
DMSO MTZ
MTZ DMSO
MTZ MTZ

Figure 4.5: *th2*+ cells modulate the initiation of swimming behavior. (A-B) Live 7 dpf larvae expressing *th2:Gal4-VP16;UAS;NTR-mCherry* (A) and *th2:NTR-EGFP* (B). (C) Representative behavioral plots of single 8 dpf larvae from same cohort analyzed in Figure 4.3. Each red arrowhead indicates a swim bout, defined as a superthreshold spike in the running frame subtraction trace, which is plotted as a black line. Y-axis indicates the maximum pixel displacement for each frame, in arbitrary units. (D-E) Effects of ablation of hypothalamic radial glia on behavior in 8 dpf larvae. Larvae expressing *Et(Gal4-VP16)^{zc1066a}; UAS;NTR-mCherry* were treated with 0.5% DMSO or 5mM MTZ from 5-7 dpf as described for *th2*+ cell ablations. Error bars=SEM, n=6 larvae for each condition. (F) Live 7 dpf larva expressing *th2:Gal4-VP16;UAS;ChR2-YFP.* (G) Expression of *cfos* in the posterior recess of 7 dpf larvae that were unstimulated, or stimulated for 30 seconds with 470nm light once per minute for 10 minutes. (H) Raster plots and cumulative counts of swim bouts before, during (blue shading), and after light pulse summing all trials for one dish of 10 larvae quantified in Figure 4.3K. Histogram bins are 200 ms wide. All fish exhibited a visually mediated transient reduction in swimming at light offset. (I) Tracking analysis reveals that fish expressing ChR2 exhibit an increased cumulative displacement during the 3s of optogenetic stimulation versus the 3s baseline condition. Error bars=SEM, n=24 control larvae, n=25 Chr2+ larvae. (J) Increased displacement reflects an increase in swim bout frequency. In the left panels, swim trajectories are color-coded to indicate the baseline (red) and stimulus (blue) periods. Right panels depict the instantaneous velocities vs. time for each trial.

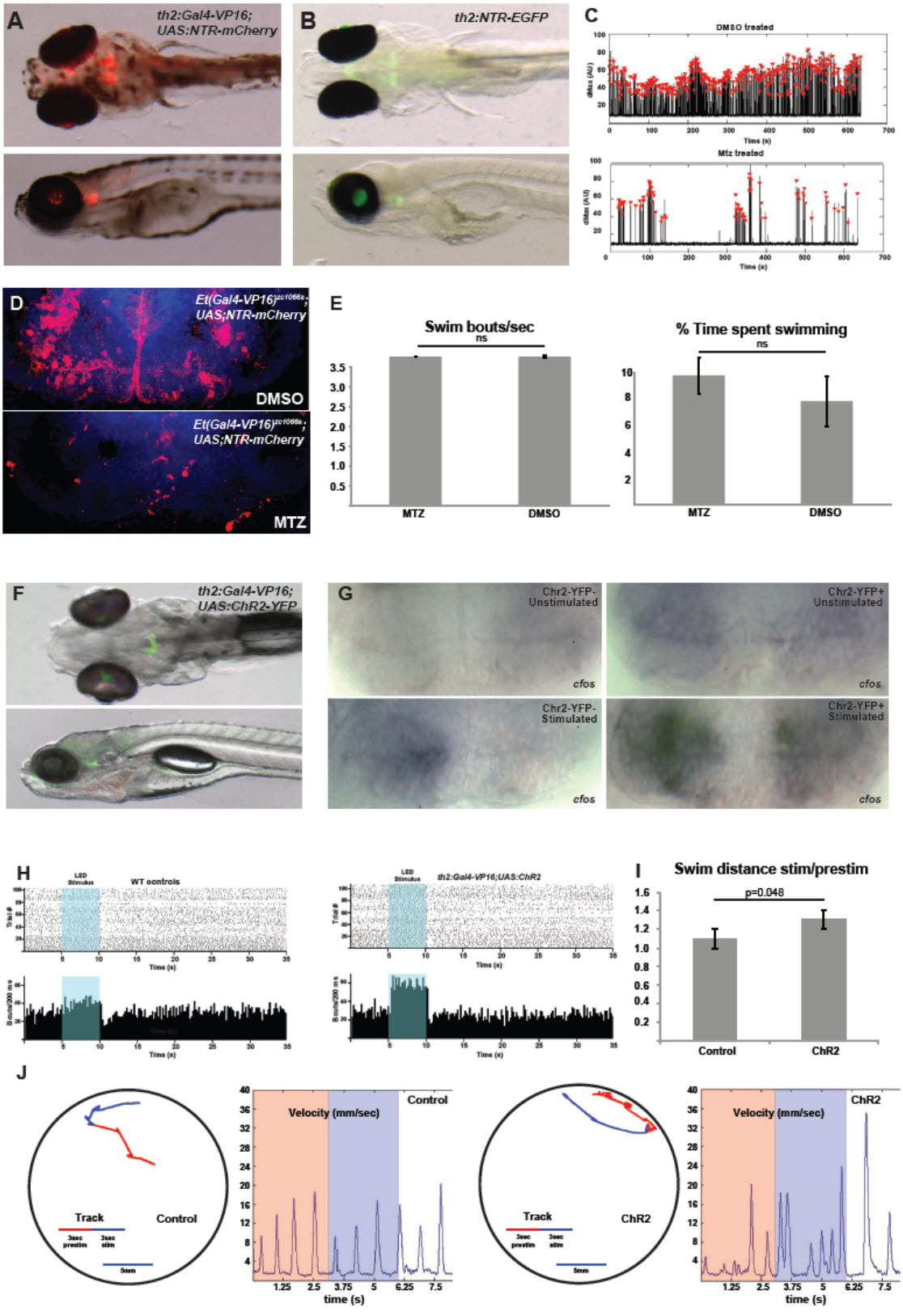
A
th2:Gal4-VP16;
UAS:NTR-mCherry
B
th2:NTR-EGFP
C
DMSO treated
Mtz treated
Time (s)
D
Et(Gal4-VP16)zc1066a;
UAS;NTR-mCherry
DMSO
MTZ
E
Swim bouts/sec
ns
MTZ
DMSO
% Time spent swimming
ns
MTZ
DMSO
F
th2:Gal4-VP16;
UAS:ChR2-YFP
G
Chr2-YFP-
Unstimulated
Chr2-YFP+
Unstimulated
Chr2-YFP-
Stimulated
Chr2-YFP+
Stimulated
cfos
H
WT controls
th2:Gal4-VP16;UAS:ChR2
LED Stimulus
Time (s)
I
Swim distance stim/prestim
p=0.048
Control
ChR2
J
Track
Control
ChR2
Velocity (mm/sec)
time (s)

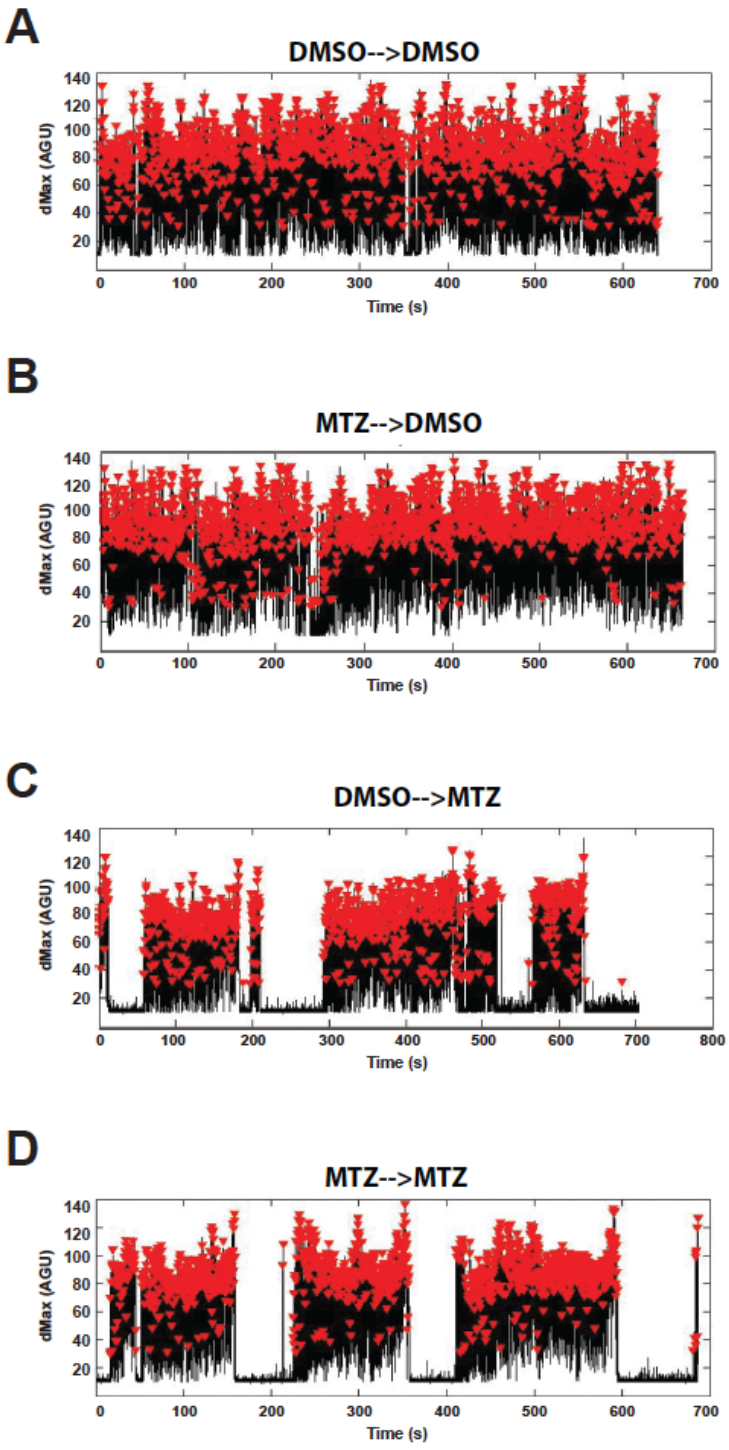

Figure 4.6: *th2*+ cells are replaced after ablation and mediate functional recovery of swimming behavior. (A-D) Representative spike plots of a group of three juvenile fish from same cohort analyzed in Figure 4.4. Each red arrowhead indicates a swim bout, defined as a superthreshold spike in the running frame subtraction trace, which is plotted as a black line.

Supplemental Movies 1 and 2: Representative movies of *th2:Gal-VP16; UAS-E1b:NTR-mCherry* larvae treated with DMSO (Movie 1) or MTZ (Movie 2) from 5-7 dpf, showing spontaneous and evoked swimming.

Supplemental Movie 3: 3D confocal projection of the *th2:Gal4: UAS:ChR2-YFP* brain shown in Fig. 3J.

Supplemental Movies 4 and 5: Representative movies of th2:GFP (Movie 4) and *th2:Gal4-VP16;UAS:ChR2-YFP* (Movie 5) larvae during blue light pulse. Blue arrow in top left corner indicates when blue light is on.

CHAPTER 5

CONCLUSIONS, SIGNIFICANCE, AND FUTURE DIRECTIONS

In this dissertation, I have presented my contributions toward advancing the understanding of hypothalamic neurogenesis in the zebrafish. When I began this work, little was known about the identity and function of neural precursors in the zebrafish caudal hypothalamus. Through a variety of methods, I have answered these questions and improved upon our knowledge of this system.

Analyzing neurogenesis in *dlx5/6* neural precursors

One of the limits to studying neurogenesis in the zebrafish hypothalamus is a lack of tools to label and manipulate the proliferative cells. When I began my work, we did not have techniques to directly investigate the neural precursors in the hypothalamus. Therefore, I developed tools and optimized techniques for investigating these cells. The *Tg(dlx5/6:mCherry)*^{zd14} line that I designed and made proved to be very valuable in the study presented in Chapter 2. This line helped us to determine that *dlx5/6*-positive neural precursors were Wnt responsive. Both of our Wnt reporter lines expressed GFP, as did our *dlx5/6* reporter line. Therefore, we could not perform coexpression analysis. *Tg(dlx5/6:mCherry)*^{zd14} provided us with a way to accomplish this task. This line was a critical tool to further our understanding of postembryonic neurogenesis in the hypothalamus. However, this line is not simply a reporter line, it also has cell ablation capability. The full transgene is *dlx5/6:loxP-mCherry-loxP-NTR*, which in the presence of Cre recombinase will excise mCherry and allow for expression of Nitroreductase (NTR). This would enable us to specifically ablate immature neural precursors at any time point by the subsequent addition of metronidazole (MTZ). The goal here was to allow normal development to occur and then ablate

only newly born cells and ask what was the affect of arresting postembryonic neurogenesis in the hypothalamus. Unfortunately, we were unable to develop or find a Cre line that expressed specifically in the hypothalamus. However, Dave Hutchinson, in our lab, just recently cloned the *Nkx2.1* promoter, which is specifically expressed in the hypothalamus. Therefore, development of *Nkx2.1:Cre* and *Nkx2.1:CreERT* transgenic lines and subsequent crossing to my Cre-responsive line will allow us to selectively ablate *dlx5/6* neural precursors at any time point and ask whether continual neurogenesis is necessary for normal physiology and behavior.

Analyzing a proliferative population of tanycytes in the hypothalamus

I was able to identify and characterize a Gal4 enhancer trap line that drove expression in tanycytes in the posterior recess of the zebrafish hypothalamus (*Et(Gal4VP16; myl7:gfp)*^{zc1066a}). Tanycytes are a proliferative, radial glia-like cell population. I initially believed that this line might prove useful for my investigation of *dlx5/6* neural precursors. However, I determined that *dlx5/6:GFP* expression did not overlap with the Gal4 expression. However, my work on this line lent significant data to the studies in Chapters 2 and 3. In Chapter 2, I found that Gal4 was expressed in Wnt-responsive cells early in development, but these cell populations diverged by postembryonic stages and few Wnt-responsive cells exhibited Gal4 expression. Though we did determine that this tanycyte population was regulated by Wnt signaling. We showed that Wnt pathway inhibition and activation increased and decreased the total cell population, respectively.

In Chapter 3, I used this line to display the utility of the tools developed in this enhancer trap study. This helped us show the power this screen has to find novel drivers that drive Gal4 expression in new cell populations. Also my work helped illustrate the ability to immediately manipulate these cells genetically by crossing them to transgenic lines that express UAS constructs that can drive expression of numerous genes of interest, such as the Nitroreductase (NTR) gene.

In terms of future directions, this reagent has already proven useful in our labs investigations of hypothalamic neurogenesis. Rob Duncan, a fellow graduate student in our lab, has already performed an extensive investigation to further characterize these tanycytes and determine how Wnt signaling regulates their proliferation. In the future, it will be interesting to determine whether these cells respond to any other signals and how these signals are relayed to the cells. These cells also have short processes into the ventricle so it would be interesting to determine whether they are receiving cues from the cerebral spinal fluid (CSF) as well. Also considering this morphology, it would be interesting to determine whether they are capable of signaling to other cells and what physiology they might regulate. One method to address this question would be to cross the *Et(Gal4VP16; myl7:gfp)*^{zc1066a} line to UAS transgenic lines that drive expression of neural activity reporters, like GCamP5, and determine what experimental manipulations may lead to altered activity from baseline.

Regenerative th2 cells are dopaminergic and modulate motor behavior

The majority of my work has focused on determining the cellular identity and function of *dlx5/6*-expressing neural precursors. In Chapter 4, I present a study that I performed that definitively showed for the first time that tyrosine hydroxylase 2 (*th2*) cells are derived from the *dlx5/6* lineage and are dopaminergic but not serotonergic. First, this answered a long-standing question in the field as to the molecular identity of the *th2* neurons. It also provided evidence that these cells may be analogous to the *Dlx* lineage in the mammalian hypothalamus. Recall that in Chapter 2 we show that *dlx5/6* cells are GABAergic; however, we had not observed Tyrosine Hydroxylase expression in these cells. Therefore, this is the first evidence that similar to mammals *dlx5/6* cells in the zebrafish hypothalamus produce GABAergic and dopaminergic neurons.

I also showed that *th2* cells were capable of being continually generated throughout adulthood. This was a significant finding because to our knowledge, there was no evidence of this in the hypothalamus of any species. Therefore, the zebrafish is a unique model organism for studying postembryonic neurogenesis in the hypothalamus.

My study also provides the first direct evidence that *th2* neurons can regulate motor behavior. One previous study suggested that *th2* neurons in the caudal hypothalamus project to the Mauthner neurons of the reticulospinal network to modulate a cross modal startle response (Mu et al., 2012). My findings show that ablation of *th2* neurons results in a reduction in swimming frequency while optogenetic activation is sufficient to drive swimming. This fits

with the previous model of *th2* neurons modulating the animal's startle response to environmental cues, but also suggests *th2* neurons may be capable of directly controlling locomotion. Future studies could possibly determine this by making use of genetically encoded calcium indicators (GECIs), such as GCaMP5 (Akerboom et al., 2012). These GECIs allow for the detection of neuronal activity *in vivo*. The Douglass lab that collaborated on the study in Chapter 4 have been developing multiple transgenic lines that drive expression of GCaMP5 in single cell populations, like *th2* neurons, as well as pan-neuronally. Adam Douglass' lab is also developing methods to express and utilize genetically encoded voltage indicators, like Arch3 (Kralj et al., 2012). In future studies utilizing these neuronal activity reporters in combination with the transgenic lines I developed to drive NTR and ChR2 in *th2* neurons from Chapter 4, it is possible that we could further deduce how the *th2* neurons modulate the locomotor circuit by ablating and activating these neurons and determining what changes take place in neuronal activity within the locomoter circuit. An additional strategy to further determine how *th2* cells modulate behavior would be to express designer receptors exclusively activated by designer drugs (DREADD) receptors. DREADD receptors are synthetic G-protein coupled receptors that allow the experimenter to use pharmacologically inert compounds to activate or inactivate neuronal activity in a dose-dependent fashion (Dong, 2010; Rogan and Roth, 2011). Thus, this technology would allow us an additional level of control over the *th2* neuron population and could allow us to determine subtleties in their signaling that may lead to further understanding of their role in behavior and physiology.

As I mentioned above in the introduction, an intriguing idea is that the increased size and cell diversity observed in the zebrafish hypothalamus compared to that of “higher vertebrates” may be due to the fact that some of these cell populations are the evolutionary origin of highly specialized brain structures present in mammals. I report that a majority of *th2* neurons send anterior projections that terminate nearby in the posterior tuberculum. In the mammalian brain, the ventral tegmental area (VTA) and substantia nigra (SN) are two dopamine-rich midbrain structures that also send anterior projections to the nucleus accumbens (NAc) and striatum, respectively, where they release dopamine in order to modulate many behaviors such as motivation and locomotion, respectively (Alcaro et al., 2007). These structures reside just caudal to the hypothalamus in the mammalian brain and do not appear to have homologues in the zebrafish brain. However, it has been suggested that dopaminergic neurons of the zebrafish diencephalic ascending system represent the VTA/SNc counterpart in zebrafish (Filippi et al., 2012). However, these diencephalic ascending dopaminergic neurons are described by their expression of the transcription factor otp, which does not overlap with *th2* expression in the diencephalon. Therefore, the *th2* population in the zebrafish hypothalamus does not appear to be neuroanatomically analogous to the VTA and SN but rather represents a separate population dopaminergic neurons that may have input into that circuit, perhaps to modulate stress or arousal responses.

Finally, my findings that *th2* cells can recover after ablation and this restores normal swimming function has major significance. This work has been

important in establishing hypothalamic *th2* cells as a bona fide model of postembryonic neurogenesis with regenerative capacity. More importantly, I have demonstrated for the first time that a population of dopaminergic cells can modulate locomotor function and are capable of functional recovery in the vertebrate brain. This could provide valuable inroads toward neurodegenerative research, such as Parkinson's disease. Parkinson's disease (PD) is characterized by a progressive deterioration of midbrain dopaminergic neuron function and subsequent cell death. Current PD treatments have shown some success in compensating for these losses by increasing systemic dopamine from the remaining cell population (Hickey and Stacy, 2011). However, no treatment has been found to arrest or prevent the progressive cell death and patients eventually succumb to the disease. Efforts to develop such treatments would benefit enormously from knowledge of any system in which dopaminergic neurons are known to exhibit postembryonic neurogenesis and regeneration. As I mentioned in the introduction in Chapter 1, many factors influence hypothalamic neurogenesis. Therefore, I believe that future studies into what regulates *th2* neuron proliferation could have great therapeutic relevance. For example, it would be useful to determine whether environmental cues affect the number of *th2* cells, in the hypothalamus. By determining what cues initiate neurogenesis of *th2* cells we could gain insight into what signaling pathways may be regulating this process. It is also possible that that neuronal activity of the *th2* cells may affect proliferation. It has been reported that local neural activity can influence neural stem cell proliferation and differentiation (Malmersjo et al., 2013). Altered

neural activity in disease states can also affect the rates of neural stem cell proliferation (Nochi et al., 2013). Utilizing the genetically encoded neural activity reporters mentioned above could provide insight toward determining whether *th2* neuronal activity coincides with altered levels of proliferation in the hypothalamus. Further, use of DREADD receptors or optogenetic methods would allow us to selectively activate the th2 cells and ask whether chronic activation leads to altered levels of dopaminergic neuron proliferation in the hypothalamus. Determining what makes the zebrafish brain permissive to new dopamine neuron growth as well as how these cells signal within the brain to control movement may prove a valuable resource toward development of therapeutics for Parkinson's disease.

Summary

I believe that the work I present in this dissertation provides significant advances in our understanding of postembryonic hypothalamic neurogenesis. This work has shed new understanding on the factors regulating *dlx5/6+* neural precursor differentiation in the hypothalamus. I report *th2* neurons as a newly identified cell type arising from the *dlx5/6* lineage. I show that these neurons are dopaminergic, continually generated throughout adulthood, control locomotion, and are capable of functional recovery. This, to our knowledge, is the first reported case of vertebrate dopaminergic neurons that control locomotion being capable of functional recovery. My work may also provide the framework toward future studies into postembryonic neurogenesis and neurodegenerative disease therapy.

References

Akerboom, J., Chen, T.W., Wardill, T.J., Tian, L., Marvin, J.S., Mutlu, S., Calderon, N.C., Esposti, F., Borghuis, B.G., Sun, X.R.*, et al.* (2012). Optimization of a GCaMP calcium indicator for neural activity imaging. The Journal of Neuroscience *32*, 13819-13840.

Alcaro, A., Huber, R., and Panksepp, J. (2007). Behavioral functions of the mesolimbic dopaminergic system-an affective neuroethological perspective. Brain Research Review *56*, 283-321.

Dong, S.A., J.A.; Farrell, M.; Roth, B.L. (2010). A chemical-genetic approach for precise spatio-temporal control of cellular signaling. Molecular Biosystems *6*, 1376-1380.

Filippi, A., Jainok, C., and Driever, W. (2012). Analysis of transcriptional codes for zebrafish dopaminergic neurons reveals essential functions of Arx and Isl1 in prethalamic dopaminergic neuron development. Developmental Biology *369*, 133-149.

Hickey, P., and Stacy, M. (2011). Available and emerging treatments for Parkinson's disease: a review. Drug Design, Development and Therapy *5*, 241-254.

Kralj, J.M., Douglass, A.D., Hochbaum, D.R., Maclaurin, D., and Cohen, A.E. (2012). Optical recording of action potentials in mammalian neurons using a microbial rhodopsin. Nature Methods *9*, 90-95.

Malmersjo, S., Rebellato, P., Smedler, E., Planert, H., Kanatani, S., Liste, I., Nanou, E., Sunner, H., Abdelhady, S., Zhang, S.*, et al.* (2013). Neural progenitors organize in small-world networks to promote cell proliferation. Proceedings of the National Academy of Sciences of the United States of America *110*, E1524-1532.

Mu, Y., Li, X.Q., Zhang, B., and Du, J.L. (2012). Visual input modulates audiomotor function via hypothalamic dopaminergic neurons through a cooperative mechanism. Neuron *75*, 688-699.

Nochi, R., Kaneko, J., Okada, N., Terazono, Y., Matani, A., and Hisatsune, T. (2013). Diazepam treatment blocks the elevation of hippocampal activity and the accelerated proliferation of hippocampal neural stem cells after focal cerebral ischemia in mice. Journal of Neuroscience Research *91*, 1429-1439.

Rogan, S.C., and Roth, B.L. (2011). Remote control of neuronal signaling. Pharmacological Reviews *63*, 291-315.

APPENDIX

FURTHER OBSERVATIONS OF NEUROGENESIS IN ADULT ZEBRAFISH

Introduction

In the course of studying hypothalamic neurogenesis, I became interested in whether I could develop assays to investigate the relation between neurogenesis and behavior in adult zebrafish. I present some of these data in Chapters 2 and 5 of this dissertation. Specifically, in the study presented in Chapter 2, it was shown that *dlx5/6:gfp* expression colocalizes with BrdU labeling after a 15-day chase in the adult hypothalamus. Furthermore, in the study in Chapter 5, we show that *th2:gfp* expression also colocalizes with BrdU labeling after 15 days in the adult hypothalamus. In this appendix, I present a few more observations that I have made in the adult zebrafish hypothalamus. Unfortunately, our lab did not possess the proper equipment for further investigation of behavior at adult stages during the time of my studies and time and scope of further analysis was not feasible for my dissertation. However, I believe these findings may provide valuable insight for future studies in the lab, especially if collaboration with the Douglass lab continues, as they are now developing new techniques for behavioral analyses.

Feeding and fasting affect cell proliferation in the hypothalamus

As mentioned in the Chapter 1 introduction, several studies in the mouse have determined that manipulating normal levels of neurogenesis affects feeding behavior and energy metabolism (Kokoeva, 2005; Lee et al., 2012) and conversely, diet can affect rates of proliferation in the hypothalamus (Li et al., 2012). Considering that there are high rates of neurogenesis in the zebrafish hypothalamus that are analogous to the feeding centers in the mouse brain, I

was curious whether feeding and fasting paradigms could affect neurogenesis in the fish. Indeed, my preliminary results show that following BrdU treatment, fasting resulted in an increase in BrdU label-retaining cells in the hypothalamus compared to normally fed controls (Fig. A.1A). Conversely, if BrdU is administered following a fast, there is a decrease in the number of BrdU labeled cells, indicating a reduction in proliferation (Fig. A.1B). Taken together, these data suggest that there is either a transition to a slow cell cycle state or cell cycle exit in response to fasting.

Obviously, further analysis of this phenomenon is necessary. In future studies, a thorough time course should be established to determine how quickly this change in proliferation state occurs. To accomplish this, a multistep birth dating analysis (Llorens-Martin and Trejo, 2011) would be beneficial to definitively show that a transition has occurred in cell proliferation. Here, different thymidine analogs, like BrdU, EdU, CldU, and IdU, are pulsed at different time points, allowing one to separately label neurons born at different times. The identity of the cells that are affected by diet also needs to be determined. I thought it would be interesting to determine whether proliferation in response to fasting affects *dlx5/6:gfp*- and *th2:gfp*-expressing cells since these tools were available in the lab. I began a small pilot study where I pulsed adult transgenic fish with BrdU and then fed or fasted them at our zebrafish facility. Not all the brains have been processed yet. However, qualitatively, it appears that fasting increases BrdU labeling in *dlx5/6*+ cells compared to fed controls (Fig 2A), but the number of *th2*+ cells containing BrdU label does not appear to be altered

(Fig. 2B). This preliminary result is promising, though many experimental conditions and levels of quantification remain to be determined. This fits with the model that the cell cycle is affected by fasting because *dlx5/6* is expressed in immature neural precursors whereas *th2* is a marker of mature neurons. Alternatively, it is possible that *th2* cells are not responsive to dietary conditions, and therefore, it would be prudent to test the affects on other mature neuronal populations in this region, such as GABA, serotonin, and histamine. It would also be interesting to determine whether different types of diet affect neurogenesis in a similar way, such as high-fat or low-calorie diets. Overall, I believe that these data merit further investigation into how diet can affect neurogenesis in the hypothalamus.

***th2*+ cells can be ablated in adults just as in larvae**

In Chapter 4, NTR-mediated ablation of *th2*+ cells utilizing *Tg(th2:Gal-VP16)*^{zd202}; *Tg(UAS-E1b:NTR-mCherry)*^{c264} transgenic fish was performed on larvae and juvenile fish and resulted in decreases in locomotion. I was curious whether it was possible to ablate the *th2*+ cells in adults and perform behavioral analyses as well. First, it was necessary to determine if bath application of MTZ was possible in the adult because, to our knowledge, no study has shown that it is possible to ablate neurons in the adult brain with this strategy. Indeed, I show that this is possible and at the same 5 mM dose I previously used in larvae and juveniles (Fig. A.3). In the future, it would also be good to do a dose response curve and quantify the efficiency of *th2* cell death as we did with larvae in Chapter 4.

***th2*+ cell recovery is possible in adults**

Though we were not set up to run adult behavior in our lab, I was still interested in determining whether *th2*+ cells could regenerate in the adult as I reported they did in larvae and juveniles in Chapter 4. In a pilot study, I treated *Tg(th2:Gal-VP16)*^{zd202}; *Tg(UAS-E1b:NTR-mCherry)*^{c264} transgenic fish with either 0.5% DMSO or 5 mM MTZ and allowed them to recover. I found that *th2*+ cells are capable regenerating in the adult as determined by the reemergence of mCherry expression to qualitatively similar levels as controls within 4 weeks, though the amount of mCherry expression was quite variable in both DMSO and MTZ groups (Fig. A.3); therefore, further analysis is necessary. I was also using these brains to determine whether whole mount ventral imaging is better for quantifying the th2 cell population in the posterior recess compared to mid-sagittal imaging. This was not the case. Mid-sagittal imaging appears to be far better for resolving this cell population. The *Tg(th2:NTR-eGFP)* line that I developed (Chapter 4) may be more useful for this study as GFP expression in this line appears to display less variegation than the *Tg(th2:Gal-VP16)*^{zd202}; *Tg(UAS-E1b:NTR-mCherry)*^{c264} transgenics. Despite these mixed results, I think that a more thorough study of regeneration in the adult is warranted. Perhaps 5 mM MTZ is too strong of a treatment at adult stages given that in Chapter 4, I show that *th2*+ cells proliferate at a much lower rate. Therefore, they may not be able to recover from a complete ablation late in life. Partial ablations could be performed with lower doses and shorter pulses to determine if regeneration is more reliable under these conditions. Also, I used older fish for this study (1+

years-old). Future studies could test multiple ages from early to late adulthood, for example 1, 3, 6, 9, and 12 months, to determine whether aging affects the ability of recovery.

Summary

My hope is that the observations presented in this appendix provide the framework for future studies that further our understanding of postembryonic neurogenesis in the adult hypothalamus.

References

Kokoeva, M.V.Y., H.; Flier, J.S. (2005). Neurogenesis in the hypothalamus of adult mice-potential role in energy balance. Science *310*, 679-683.

Lee, D.A., Bedont, J.L., Pak, T., Wang, H., Song, J., Miranda-Angulo, A., Takiar, V., Charubhumi, V., Balordi, F., Takebayashi, H.*, et al.* (2012). Tanycytes of the hypothalamic median eminence form a diet-responsive neurogenic niche. Nature Neuroscience *15*, 700-702.

Li, J., Tang, Y., and Cai, D. (2012). IKKbeta/NF-kappaB disrupts adult hypothalamic neural stem cells to mediate a neurodegenerative mechanism of dietary obesity and pre-diabetes. Nature Cell Biology *14*, 999-1012.

Llorens-Martin, M., and Trejo, J.L. (2011). Multiple birthdating analyses in adult neurogenesis: a line-up of the usual suspects. Frontiers in Neuroscience *5*, 76.

Figure A.1: Fasting affects proliferation in adult zebrafish. (A-B) Representative mid-sagittal views of adult zebrafish brains. BrdU labeling is in magenta and nuclear staining is in blue. (A) Fish were pulsed with 10 mM BrdU by IP injection then fed or fasted for 12 days before sacrifice and immunohistochemistry for BrdU (magenta), and nuclei (blue). (B) Fish were fed or fasted for 7 days then pulsed with 10 mM BrdU by IP injection 4 hours before sacrifice and immunohistochemistry for BrdU (magenta), and nuclei (blue). (shorter feed/fast period used to increase survival when IP injection performed). Dotted lines indicate the ventricle of the posterior recess.

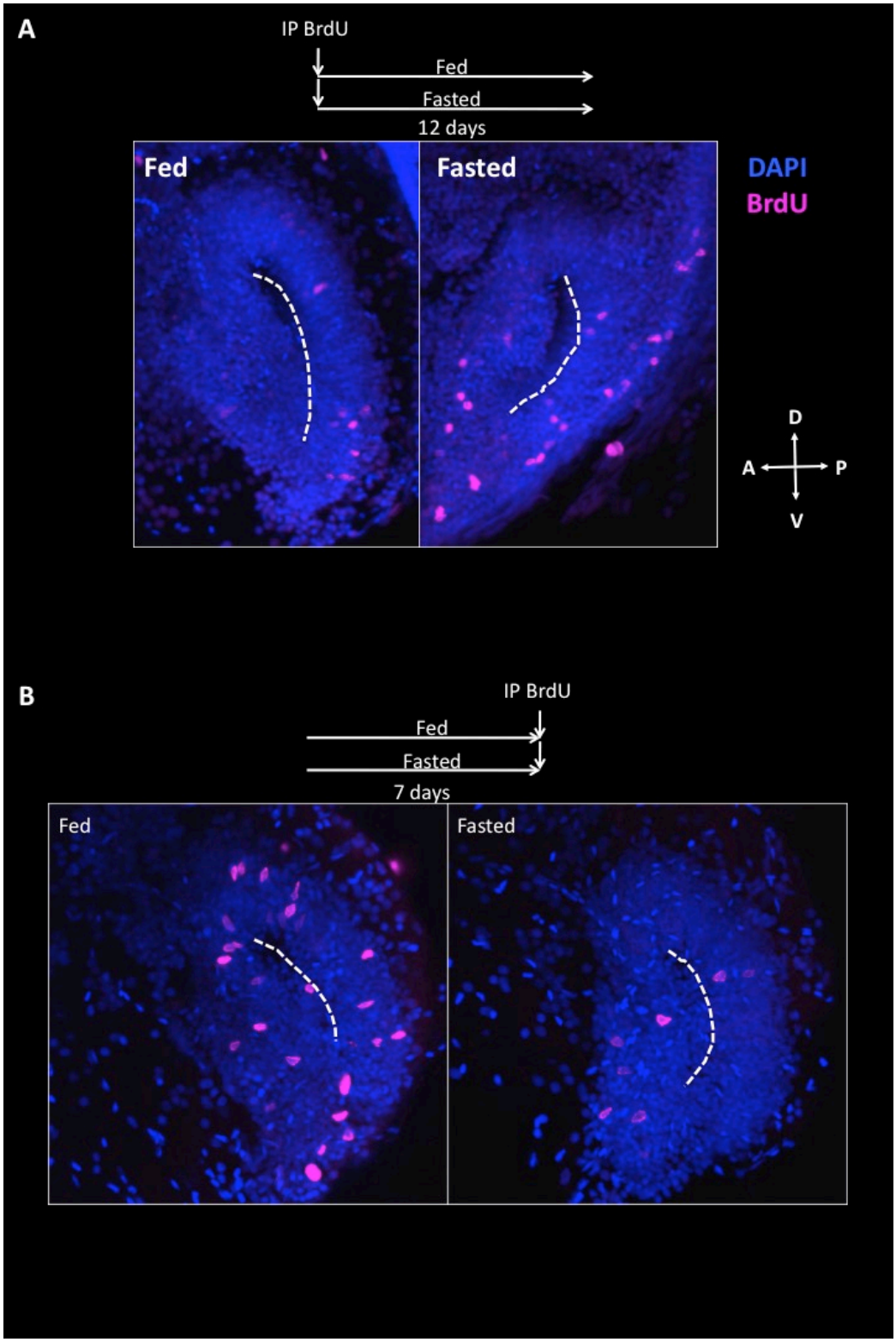
A
IP BrdU
Fed
Fasted
12 days
Fed
Fasted
DAPI
BrdU
D
A
P
V
B
IP BrdU
Fed
Fasted
7 days
Fed
Fasted

Figure A.2: Fasting increases BrdU labeling in dlx5/6+ cells, but not th2+ neurons. (A-B) Representative mid-sagittal views of adult zebrafish brains expressing dlx5/6:gfp (A) or th2:gfp (B). Fish were pulsed with 10 mM BrdU by IP injection then fed or fasted for 15 days before sacrifice and immunohistochemistry for GFP (green), BrdU (magenta), and nuclei (blue). Dotted lines indicate the ventricles. Red arrows indicate cells double positive for GFP and BrdU.

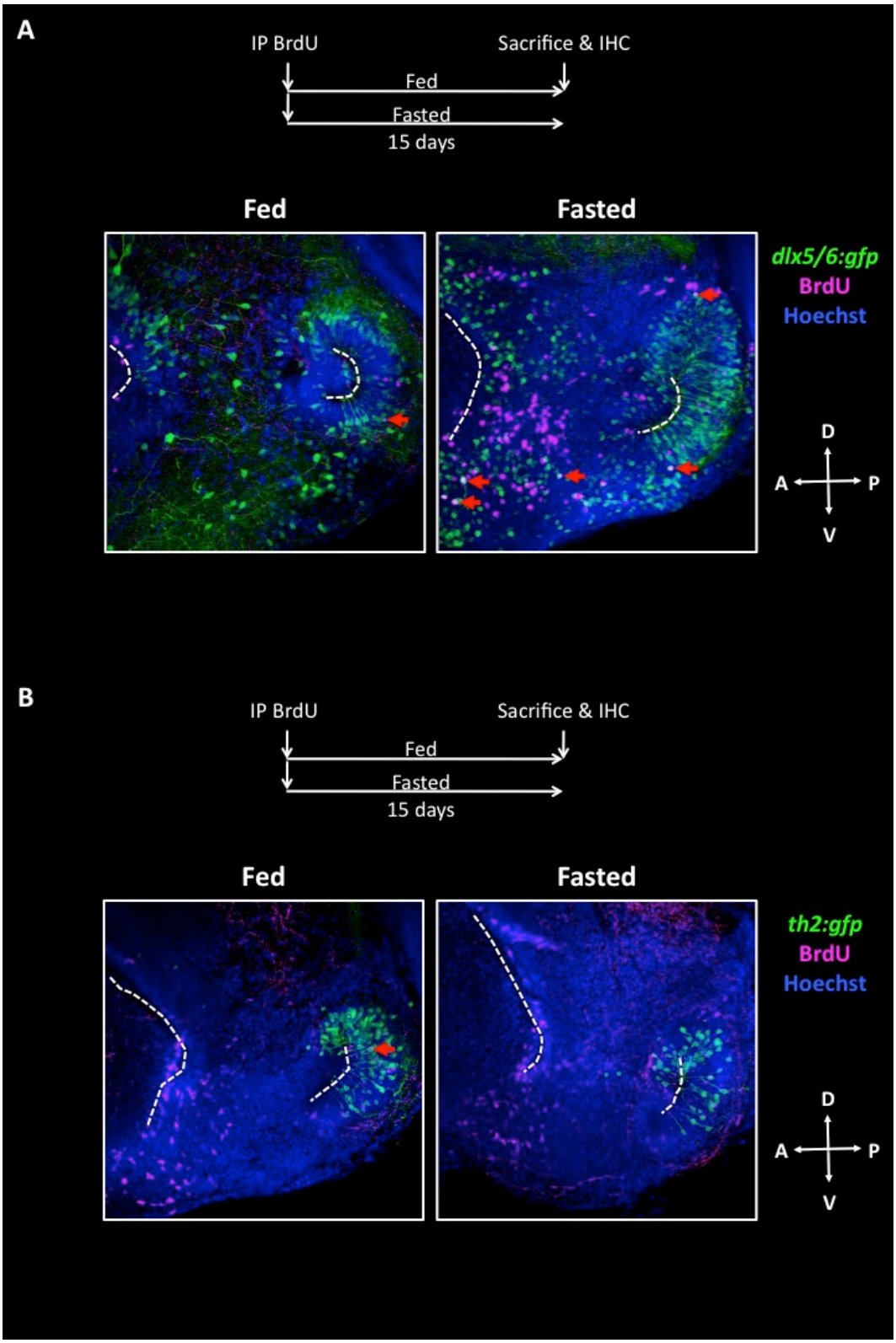
A
IP BrdU
Sacrifice & IHC
Fed
Fasted
15 days
Fed
Fasted
dlx5/6:gfp
BrdU
Hoechst
D
A
P
V
B
IP BrdU
Sacrifice & IHC
Fed
Fasted
15 days
Fed
Fasted
th2:gfp
BrdU
Hoechst
D
A
P
V

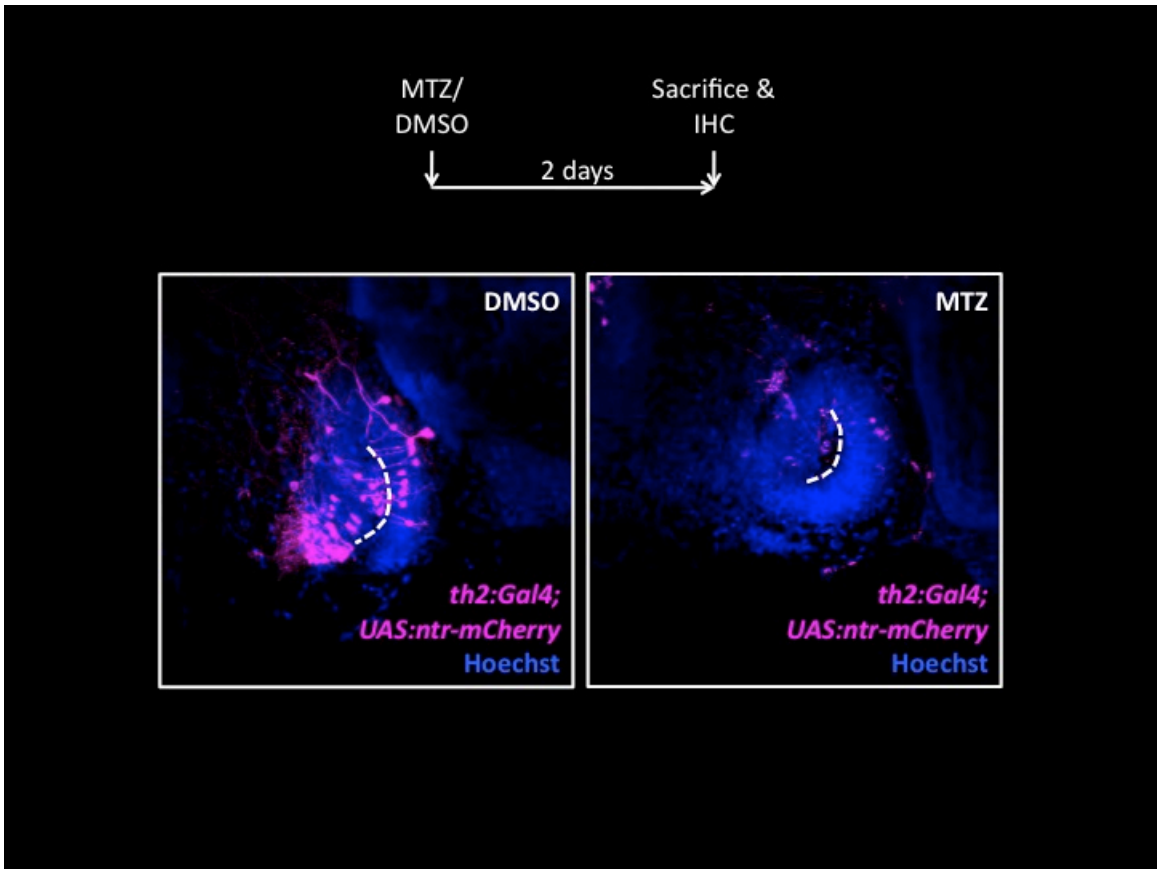

Figure A.3: NTR-mediated ablation of th2+ cells can be performed by bath application of MTZ. Representative mid-sagittal views of adult Tg(*th2:Gal-VP16)^{zd202}; Tg(UAS-E1b:NTR-mCherry)^{c264}* transgenic zebrafish brains treated with either 0.5% DMSO or 5 mM MTZ in fish system water for 2 days. MTZ treated brain exhibit far less mCherry+ cells. Dotted lines indicate the ventricle of the posterior recess.

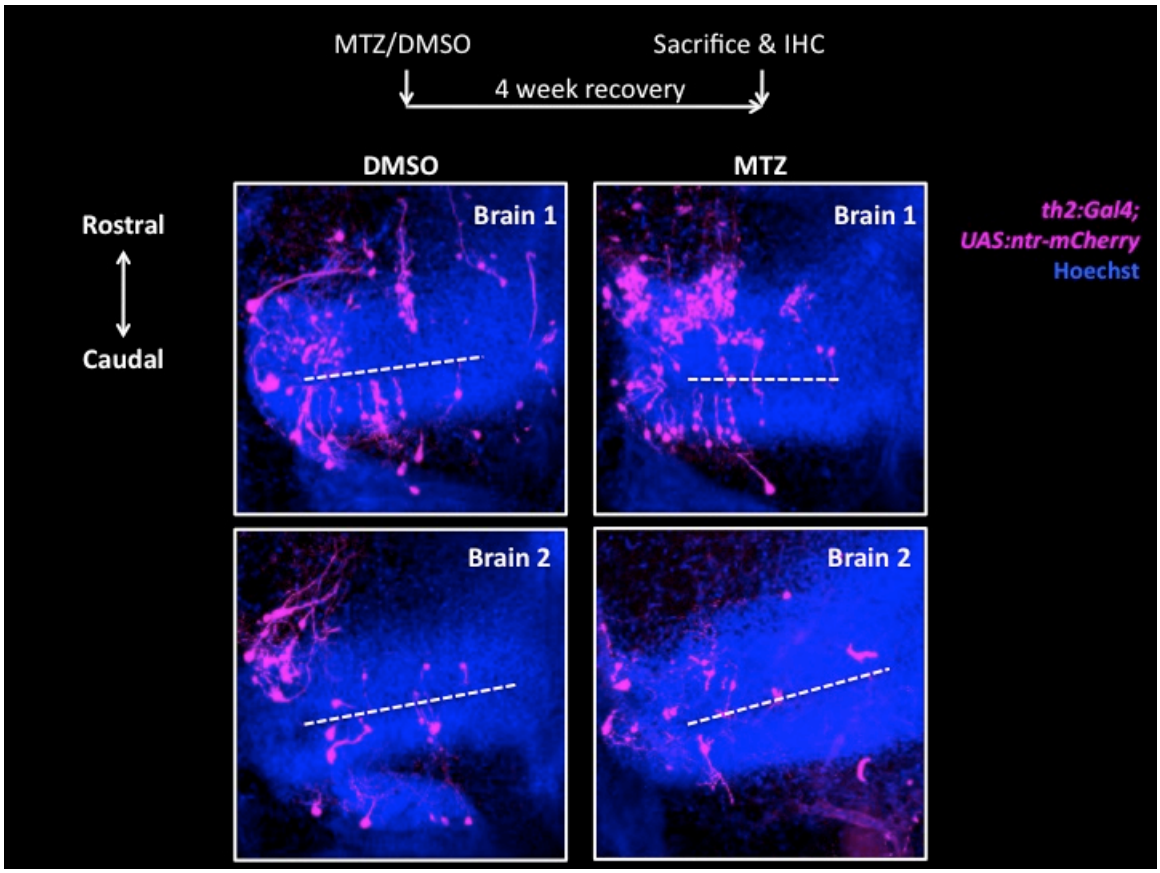

Figure A.4: th2 regeneration is possible in adult zebrafish. Representative ventral views of adult *Tg(th2:Gal-VP16)*^{zd202}*; Tg(UAS-E1b:NTR-mCherry)*^{c264} transgenic zebrafish brains treated with either 0.5% DMSO or 5 mM MTZ in fish system water for 2 days then allowed to recover for 4 weeks (2 brains shown for each condition). Dotted lines indicate the ventricle of the posterior recess.